3GPP TR 36.814 V9.0.0 (2010-03)

Technical Report

3rd Generation Partnership Project; Technical Specification Group Radio Access Network; Evolved Universal Terrestrial Radio Access (E-UTRA); Further advancements for E-UTRA physical layer aspects (Release 9)

Keywords
UMTS, Radio

3GPP

Postal address

3GPP support office address
650 Route des Lucioles - Sophia Antipolis
Valbonne - FRANCE
Tel.: +33 4 92 94 42 00 Fax: +33 4 93 65 47 16

Internet
http://www.3gpp.org

Contents

Foreword

This Technical Report has been produced by the 3rd Generation Partnership Project (3GPP).

The contents of the present document are subject to continuing work within the TSG and may change following formal TSG approval. Should the TSG modify the contents of the present document, it will be re-released by the TSG with an identifying change of release date and an increase in version number as follows:

Version x.y.z

where:

- x the first digit:
  - 1 presented to TSG for information;
  - 2 presented to TSG for approval;
  - 3 or greater indicates TSG approved document under change control.
- y the second digit is incremented for all changes of substance, i.e. technical enhancements, corrections, updates, etc.
- z the third digit is incremented when editorial only changes have been incorporated in the document.

1 Scope

This document is related to the technical report for physical layer aspect of the study item "Further advancements for E-UTRA" [1]. The purpose of this TR is to help TSG RAN WG1 to define and describe the potential physical layer evolution under consideration and compare the benefits of each evolution techniques, along with the complexity evaluation of each technique.

This activity involves the Radio Access work area of the 3GPP studies and has impacts both on the Mobile Equipment and Access Network of the 3GPP systems.

This document is intended to gather all information in order to compare the solutions and gains vs. complexity, and draw a conclusion on way forward.

This document is a 'living' document, i.e. it is permanently updated and presented to TSG-RAN meetings.

2 References

The following documents contain provisions which, through reference in this text, constitute provisions of the present document.

- References are either specific (identified by date of publication, edition number, version number, etc.) or non-specific.
- For a specific reference, subsequent revisions do not apply.
- For a non-specific reference, the latest version applies. In the case of a reference to a 3GPP document (including a GSM document), a non-specific reference implicitly refers to the latest version of that document *in the same Release as the present document*.

[1] 3GPP TD RP-080137: "Proposed SID on LTE-Advanced".

[2] 3GPP TR 21.905: "Vocabulary for 3GPP Specifications".

[3] 3GPP TR 36.913: "Requirements for Evolved UTRA (E-UTRA) and Evolved UTRAN (E-UTRAN)

[4] ITU-R Report M.2135, Guidelines for evaluation of radio interface technologies for IMT-Advanced, 2008-11, http://www.itu.int/publ/R-REP-M.2135-2008/en

[5] 3GPP TS 36.213: "Evolved Universal Terrestrial Radio Access (E-UTRA); Physical layer procedures (Release 8)"

[6] 3GPP TSG RAN1 R1-094954: "Annex A4 Self-evaluation results for TR36.814".

3 Definitions, symbols and abbreviations

3.1 Definitions

Void

3.2 Symbols

Void

3.3 Abbreviations

For the purposes of the present document, the abbreviations defined in 3GPP TS 21.905 [2] and the following apply:

4 Introduction

At the 3GPP TSG RAN #39 meeting, the Study Item description on "Further Advancements for E-UTRA (LTE-Advanced)" was approved [1]. The study item covers technology components to be considered for the evolution of E-UTRA, e.g. to fulfil the requirements on IMT-Advanced. This technical report covers the physical-layer aspects of these technology components.

5 Support of wider bandwidth

C*arrier aggregation*, where two or more *component carriers* are aggregated, is supported by LTE-Advanced in order to support wider transmission bandwidths e.g. up to 100MHz and for spectrum aggregation..

A terminal may simultaneously receive or transmit one or multiple component carriers depending on its capabilities:

- An LTE-Advanced terminal with reception and/or transmission capabilities for carrier aggregation can simultaneously receive and/or transmit on multiple component carriers.
- An LTE Rel-8 terminal can receive and transmit on a single component carrier only, provided that the structure of the component carrier follows the Rel-8 specifications.
    - It shall be possible to configure all component carriers LTE Release 8 compatible, at least when the aggregated numbers of component carriers in the UL and the DL are same. Consideration of non-backward-compatible configurations of LTE-A component carriers is not precluded

The L1 specification shall support carrier aggregation for both contiguous and non-contiguous component carriers with each component carrier limited to a maximum of 110 Resource Blocks using the Release 8 numerology

- For contiguous carrier aggregation, the needed frequency spacing between the contiguous component carriers will be studied by RAN WG4. This study should include the supported number of RBs per component carrier and the needed guard bands between and at the edges for a certain aggregation case.
- If possible, the same solution should be used in the L1 specifications for contiguous and non-contiguous aggregation.

It will be possible to configure a UE to aggregate a different number of component carriers of possibly different bandwidths in the UL and the DL. In typical TDD deployments, the number of component carriers and the bandwidth of each component carrier in UL and DL will be the same. RAN WG4 will study the supported combinations of aggregated component carrier and bandwidths.

5.1 MAC-PHY interface

From a UE perspective, there is one transport block (in absence of spatial multiplexing) and one hybrid-ARQ entity per scheduled component carrier. Each transport block is mapped to a single component carrier only. A UE may be scheduled over multiple component carriers simultaneously.

5.2 DL control signalling

The design principles for downlink control signalling of control region size, uplink and downlink resource assignments, and downlink HARQ ACK/NACK indication are described below.

- Independent control region size is applied for each component carrier. On any carrier with a control region, Rel-8 design (modulation, coding, mapping to resource elements) for PCFICH is reused.

- For signalling of resource assignments for downlink (PDSCH) and uplink (PUSCH) transmission, following mechanisms are supported,
  - PDCCH on a component carrier assigns PDSCH resources on the same component carrier and PUSCH resources on a single linked UL component carrier. Rel-8 PDCCH structure (same coding, same CCE-based resource mapping) and DCI formats are used on each component carrier.
  - PDCCH on a component carrier can assign PDSCH or PUSCH resources in one of multiple component carriers using the carrier indicator field(CIF), where
    - Configuration for the presence of CIF is semi-static and UE specific (i.e. not system-specific or cell-specific)
    - CIF is a fixed 3-bit field, and Rel-8 PDCCH structure (same coding, same CCE-based resource mapping) is reused.
    - CIF location is fixed irrespective of DCI format size
    - Cross-carrier assignments can be configured both when the DCI formats have the same or different sizes
    - Explicit CIF at least for the case of same DCI format size
    - There will be an upper limit on the total number of blind decodes
- For signalling of downlink HARQ ACK/NACK indication, following principles are applied.
  - PHICH physical transmission aspects from Rel-8 (orthogonal code design, modulation, scrambling sequence, mapping to resource elements) are reused.
  - PHICH is transmitted only on the downlink component carrier that was used to transmit the UL grant
  - At least in case that the number of downlink component carriers are more than or equal to that of uplink component carriers and no carrier indicator field is used, the Rel-8 PHICH resource mapping rule is reused.

5.3 UL control signalling

The design principles for uplink control signalling of HARQ ACK/NACK, scheduling request and channel state information (CSI) on PUCCH are described below.

- The Rel-10 PUCCH design supports up to five DL component carriers.
- For signalling of HARQ ACK/NACK on PUCCH for downlink (PDSCH) transmission, following mechanisms are supported:
  - All HARQ ACK/NACK for a UE can be transmitted on PUCCH in absence of PUSCH transmission.
    - In general, transmission of one ACK/NACK for each DL component carrier transport block is supported.
    - In case of power limitation, limited transmission of ACK/NACK for the DL component carrier transport blocks is supported.
    - The design of the ACK/NACK resource allocation should consider performance and power control aspects, while not aiming to optimise for the case of large number of UEs being simultaneously scheduled on multiple DL component carriers.
- The scheduling request is transmitted on PUCCH and is semi-statically mapped onto one UE specific UL component carrier.
- Periodic CSI reporting on PUCCH is supported for up to five DL component carriers. The CSI is semi-statically mapped onto one UE specific UL component carrier and the design follows the Rel-8 principles for CQI/PMI/RI, considering ways to reduce reporting overhead or to extend CSI payload.

6 Uplink transmission scheme

6.1 Uplink spatial multiplexing

Uplink spatial multiplexing of up to four layers is supported by LTE-Advanced.

In the uplink single user spatial multiplexing, up to two transport blocks can be transmitted from a scheduled UE in a subframe per uplink component carrier. Each transport block has its own MCS level. Depending on the number of transmission layers, the modulation symbols associated with each of the transport blocks are mapped onto one or two layers according to the same principle as in Rel-8 E-UTRA downlink spatial multiplexing. The transmission rank can be adapted dynamically. It is possible to configure the uplink single user spatial multiplexing transmission with or without the layer shifting. In case of the layer shifting, shifting in time domain is supported.

If layer shifting is configured, the HARQ-ACKs for all transport blocks are bundled into a single HARQ-ACK. One-bit ACK is transmitted to the UE if all transport blocks are successfully decoded by the eNodeB. Otherwise, one-bit NACK is transmitted to the UE.

If layer shifting is not configured, each transport block has its own HARQ-ACK feedback signalling.

For FDD and TDD, precoding is performed according to a predefined codebook. If layer shifting is not configured, precoding is applied after the layer mapping. If layer shifting is configured, precoding is applied after the layer shifting operation. Application of a single precoding matrix per uplink component carrier is supported. In case of full-rank transmission, only identity precoding matrix is supported. For uplink spatial multiplexing with two transmit antennas, 3-bit precoding codebook as defined in Table 6.1-1 is used.

Table 6.1-1: 3-bit precoding codebook for uplink spatial multiplexing with two transmit antennas

Codebook index	Number of layers υ	
	1	2
0	$\frac{1}{\sqrt{2}}\begin{bmatrix}1\\1\end{bmatrix}$	$\frac{1}{\sqrt{2}}\begin{bmatrix}1 & 0\\0 & 1\end{bmatrix}$
1	$\frac{1}{\sqrt{2}}\begin{bmatrix}1\\-1\end{bmatrix}$	
2	$\frac{1}{\sqrt{2}}\begin{bmatrix}1\\j\end{bmatrix}$	
3	$\frac{1}{\sqrt{2}}\begin{bmatrix}1\\-j\end{bmatrix}$	-
4	$\frac{1}{\sqrt{2}}\begin{bmatrix}1\\0\end{bmatrix}$	
5	$\frac{1}{\sqrt{2}}\begin{bmatrix}0\\1\end{bmatrix}$	

For uplink spatial multiplexing with four transmit antennas, a 6-bit precoding codebook is used. The subset of the precoding codebook used for 1-layer transmission is defined in Table 6.1-2. The baseline for the subset of the precoding codebook used for 2-layer transmission is defined in Table 6.1-3. For 3-layer transmission, the number of precoding matrices is 20, and only BPSK or QPSK alphabets are used for non-zero elements in precoding matrices.

Table 6.1-2: 6-bit precoding codebook for uplink spatial multiplexing with four transmit antennas: precoding matrices for 1-layer transmission.

	Codebook

Index 0 to 7	$\frac{1}{2}\begin{bmatrix}1\\1\\1\\-1\end{bmatrix}$	$\frac{1}{2}\begin{bmatrix}1\\1\\j\\j\end{bmatrix}$	$\frac{1}{2}\begin{bmatrix}1\\1\\-1\\1\end{bmatrix}$	$\frac{1}{2}\begin{bmatrix}1\\1\\-j\\-j\end{bmatrix}$	$\frac{1}{2}\begin{bmatrix}1\\j\\1\\j\end{bmatrix}$	$\frac{1}{2}\begin{bmatrix}1\\j\\j\\1\end{bmatrix}$	$\frac{1}{2}\begin{bmatrix}1\\j\\-1\\-j\end{bmatrix}$	$\frac{1}{2}\begin{bmatrix}1\\j\\-j\\-1\end{bmatrix}$
Index 8 to 15	$\frac{1}{2}\begin{bmatrix}1\\-1\\1\\1\end{bmatrix}$	$\frac{1}{2}\begin{bmatrix}1\\-1\\j\\-j\end{bmatrix}$	$\frac{1}{2}\begin{bmatrix}1\\-1\\-1\\-1\end{bmatrix}$	$\frac{1}{2}\begin{bmatrix}1\\-1\\-j\\j\end{bmatrix}$	$\frac{1}{2}\begin{bmatrix}1\\-j\\1\\-j\end{bmatrix}$	$\frac{1}{2}\begin{bmatrix}1\\-j\\j\\-1\end{bmatrix}$	$\frac{1}{2}\begin{bmatrix}1\\-j\\-1\\j\end{bmatrix}$	$\frac{1}{2}\begin{bmatrix}1\\-j\\-j\\1\end{bmatrix}$
Index 16 to 23	$\frac{1}{2}\begin{bmatrix}1\\0\\1\\0\end{bmatrix}$	$\frac{1}{2}\begin{bmatrix}1\\0\\-1\\0\end{bmatrix}$	$\frac{1}{2}\begin{bmatrix}1\\0\\j\\0\end{bmatrix}$	$\frac{1}{2}\begin{bmatrix}1\\0\\-j\\0\end{bmatrix}$	$\frac{1}{2}\begin{bmatrix}0\\1\\0\\1\end{bmatrix}$	$\frac{1}{2}\begin{bmatrix}0\\1\\0\\-1\end{bmatrix}$	$\frac{1}{2}\begin{bmatrix}0\\1\\0\\j\end{bmatrix}$	$\frac{1}{2}\begin{bmatrix}0\\1\\0\\-j\end{bmatrix}$

Table 6.1-3: 6-bit precoding codebook for uplink spatial multiplexing with four transmit antennas: precoding matrices for 2-layer transmission.

	Codebook							
Index 0 to 7	$\frac{1}{2}\begin{bmatrix}1&0\\1&0\\0&1\\0&-j\end{bmatrix}$	$\frac{1}{2}\begin{bmatrix}1&0\\1&0\\0&1\\0&j\end{bmatrix}$	$\frac{1}{2}\begin{bmatrix}1&0\\-j&0\\0&1\\0&1\end{bmatrix}$	$\frac{1}{2}\begin{bmatrix}1&0\\-j&0\\0&1\\0&-1\end{bmatrix}$	$\frac{1}{2}\begin{bmatrix}1&0\\-1&0\\0&1\\0&-j\end{bmatrix}$	$\frac{1}{2}\begin{bmatrix}1&0\\-1&0\\0&1\\0&j\end{bmatrix}$	$\frac{1}{2}\begin{bmatrix}1&0\\j&0\\0&1\\0&1\end{bmatrix}$	$\frac{1}{2}\begin{bmatrix}1&0\\j&0\\0&1\\0&-1\end{bmatrix}$
Index 8 to 15	$\frac{1}{2}\begin{bmatrix}1&0\\0&1\\1&0\\0&1\end{bmatrix}$	$\frac{1}{2}\begin{bmatrix}1&0\\0&1\\1&0\\0&-1\end{bmatrix}$	$\frac{1}{2}\begin{bmatrix}1&0\\0&1\\-1&0\\0&1\end{bmatrix}$	$\frac{1}{2}\begin{bmatrix}1&0\\0&1\\-1&0\\0&-1\end{bmatrix}$	$\frac{1}{2}\begin{bmatrix}1&0\\0&1\\0&1\\1&0\end{bmatrix}$	$\frac{1}{2}\begin{bmatrix}1&0\\0&1\\0&-1\\1&0\end{bmatrix}$	$\frac{1}{2}\begin{bmatrix}1&0\\0&1\\0&1\\-1&0\end{bmatrix}$	$\frac{1}{2}\begin{bmatrix}1&0\\0&1\\0&-1\\-1&0\end{bmatrix}$

6.2 Uplink transmit diversity

For UEs with multiple transmit antennas, an uplink Single Antenna Port Mode is defined, where the UE behaviour is same as the one with single antenna from eNodeB's perspective. For a given UE, the uplink Single Antenna Port Mode can be independently configured for its PUCCH, PUSCH and SRS transmissions.

The uplink Single Antenna Port Mode is the default mode before eNodeB is aware of the UE transmit antenna configuration.

6.2.1 Transmit Diversity for Uplink Control Channel

For uplink control channels with Rel-8 PUCCH format 1/1a/1b, the spatial orthogonal-resource transmit diversity (SORTD) scheme is supported for transmissions with two antenna ports. In this transmit diversity scheme, the same modulation symbol from the uplink channel is transmitted from two antenna ports, on two separate orthogonal resources.

For the UE with four transmit antennas, the 2-tx transmit diversity scheme is applied.

6.3 Uplink multiple access

DFT-precoded OFDM is the transmission scheme used for PUSCH both in absence and presence of spatial multiplexing. In case of multiple component carriers, there is one DFT per component carrier. Both frequency-contiguous and frequency-non-contiguous resource allocation is supported on each component carrier.

Simultaneous transmission of uplink L1/L2 control signalling and data is supported through two mechanisms

- Control signalling is multiplexed with data on PUSCH according to the same principle as in Rel-8
- Control signalling is transmitted on PUCCH simultaneously with data on PUSCH

6.4 Uplink reference signals

Similar to LTE, two types of uplink reference signals are supported by LTE-Advanced:

- Demodulation reference signal
- Sounding reference signal

The precoding applied for the demodulation reference signal is the same as the one applied for the PUSCH. Cyclic shift separation is the primary multiplexing scheme of the demodulation reference signals.

The baseline for sounding reference signal in LTE-Advanced operation is non-precoded and antenna-specific. For multiplexing of the sounding reference signals, Rel-8 principles are reused.

6.5 Uplink power control

Scope of uplink power control in LTE-Advanced is similar to Rel'8:

- UL power control mainly compensates for slow-varying channel conditions while reducing the interference generated towards neighboring cells
- Fractional path-loss compensation or full path-loss compensation is used on PUSCH and full path-loss compensation on PUCCH

LTE-Advanced supports component carrier specific UL power control for both contiguous and non-contiguous carrier aggregation for closed-loop case, and for open loop at least for the cases that the number of downlink component carriers is more than or equal to that of uplink component carriers.

7 Downlink transmission scheme

7.1 Physical channel mapping

LTE-Advanced supports the PDSCH to be mapped also to MBSFN (non-control) region of MBSFN subframes that are not used for MBMS

- In case of PDSCH mapping to MBSFN subframes, both normal and extended cyclic prefix can be used for control and data region, same CP length is used for control and data
- Relation between CP length of normal and MBSFN subframes in the control region is the same as in Rel-8

7.2 Downlink spatial multiplexing

Downlink spatial multiplexing of up to eight layers is supported byLTE-Advanced.

In the downlink 8-by-X single user spatial multiplexing, up to two transport blocks can be transmitted to a scheduled UE in a subframe per downlink component carrier. Each transport block is assigned its own modulation and coding scheme. For HARQ ACK/NAK feedback on uplink, one bit is used for each transport block.

A transport block is associated with a codeword. For up to four layers, the codeword-to-layer mapping is according to section 6.3.3.2 of TS 36.211. For above four layers as well as the case of mapping one codeword to three or four layers, which is for retransmission of one out of two codewords that were initially transmitted with more than four layers, the layer mapping shall be done according to Table 7.2-1.. Complex-valued modulation symbols $d^{(q)}(0),\ldots,d^{(q)}(M_{\text{symb}}^{(q)}-1)$ for code word q shall be mapped onto the layers $x(i)=\left[x^{(0)}(i) \quad \ldots \quad x^{(\upsilon-1)}(i)\right]^T$, $i=0,1,\ldots,M_{\text{symb}}^{\text{layer}}-1$ where υ is the number of layers and $M_{\text{symb}}^{\text{layer}}$ is the number of modulation symbols per layer.

Table 7.2-1: Codeword-to-layer mapping for above four layers and the case of mapping one codeword to three or four layers

Number of layers	Number of code words	Codeword-to-layer mapping $i=0,1,\ldots,M_{\text{symb}}^{\text{layer}}-1$	
3	1	$x^{(0)}(i)=d^{(0)}(3i)$ $x^{(1)}(i)=d^{(0)}(3i+1)$ $x^{(2)}(i)=d^{(0)}(3i+2)$	$M_{\text{symb}}^{\text{layer}}=M_{\text{symb}}^{(0)}/3$
4	1	$x^{(0)}(i)=d^{(0)}(4i)$ $x^{(1)}(i)=d^{(0)}(4i+1)$ $x^{(2)}(i)=d^{(0)}(4i+2)$ $x^{(3)}(i)=d^{(0)}(4i+3)$	$M_{\text{symb}}^{\text{layer}}=M_{\text{symb}}^{(0)}/4$
5	2	$x^{(0)}(i)=d^{(0)}(2i)$ $x^{(1)}(i)=d^{(0)}(2i+1)$ $x^{(2)}(i)=d^{(1)}(3i)$ $x^{(3)}(i)=d^{(1)}(3i+1)$ $x^{(4)}(i)=d^{(1)}(3i+2)$	$M_{\text{symb}}^{\text{layer}}=M_{\text{symb}}^{(0)}/2=M_{\text{symb}}^{(1)}/3$
6	2	$x^{(0)}(i)=d^{(0)}(3i)$ $x^{(1)}(i)=d^{(0)}(3i+1)$ $x^{(2)}(i)=d^{(0)}(3i+2)$ $x^{(3)}(i)=d^{(1)}(3i)$ $x^{(4)}(i)=d^{(1)}(3i+1)$ $x^{(5)}(i)=d^{(1)}(3i+2)$	$M_{\text{symb}}^{\text{layer}}=M_{\text{symb}}^{(0)}/3=M_{\text{symb}}^{(1)}/3$
7	2	$x^{(0)}(i)=d^{(0)}(3i)$ $x^{(1)}(i)=d^{(0)}(3i+1)$ $x^{(2)}(i)=d^{(0)}(3i+2)$ $x^{(3)}(i)=d^{(1)}(4i)$ $x^{(4)}(i)=d^{(1)}(4i+1)$ $x^{(5)}(i)=d^{(1)}(4i+2)$ $x^{(6)}(i)=d^{(1)}(4i+3)$	$M_{\text{symb}}^{\text{layer}}=M_{\text{symb}}^{(0)}/3=M_{\text{symb}}^{(1)}/4$
8	2	$x^{(0)}(i)=d^{(0)}(4i)$ $x^{(1)}(i)=d^{(0)}(4i+1)$ $x^{(2)}(i)=d^{(0)}(4i+2)$ $x^{(3)}(i)=d^{(0)}(4i+3)$ $x^{(4)}(i)=d^{(1)}(4i)$ $x^{(5)}(i)=d^{(1)}(4i+1)$ $x^{(6)}(i)=d^{(1)}(4i+2)$ $x^{(7)}(i)=d^{(1)}(4i+3)$	$M_{\text{symb}}^{\text{layer}}=M_{\text{symb}}^{(0)}/4=M_{\text{symb}}^{(1)}/4$

7.2.1 Feedback in support of downlink spatial multiplexing

The baseline for feedback in support of downlink single-cell single-user spatial multiplexing is codebook-based precoding feedback.

7.3 Enhanced multiuser MIMO transmission

Enhanced multi-user MIMO transmission is supported in LTE-Advanced. Basic principle of MU-MIMO in LTE-Advanced is as follows:

- Switching between SU- and MU-MIMO transmission is possible without RRC reconfiguration

7.4 Downlink reference signals

Two types of downlink reference signals are considered for LTE-Advanced:

- Reference signals targeting PDSCH demodulation
- Reference signals targeting CSI estimation (for CQI/PMI/RI/etc reporting when needed)

The reference signal structure can be used to support multiple LTE-Advanced features, e.g. CoMP and spatial multiplexing.

7.4.1 Demodulation reference signal

Reference signals targeting PDSCH demodulation are:

- UE-specific, i.e, the PDSCH and the demodulation reference signals intended for a specific UE are subject to the same precoding operation.
- Present only in resource blocks and layers scheduled by the eNodeB for transmission.
- Reference signals transmitted on different layers are mutually orthogonal at the eNodeB.

The design principle for the demodulation reference signals is an extension to multiple layers of the concept of Rel-8 UE-specific reference signals used for beamforming (details on pattern, location, etc are FFS). Complementary use of Rel-8 cell-specific reference signals by the UE is not precluded.

Normal subframes with normal CP:

For rank 1and 2, the same DM-RS structure (including patterns, spreading and scrambling) as in LTE Rel-9 is used, as illustrated in Figure 7.3.1-1. For rank 2, DM-RS for 1st layer and that for 2nd layer are multiplexed by means of code division multiplexing (CDM) by using orthogonal cover code (OCC) over two consecutive resource elements (blue) in time domain.

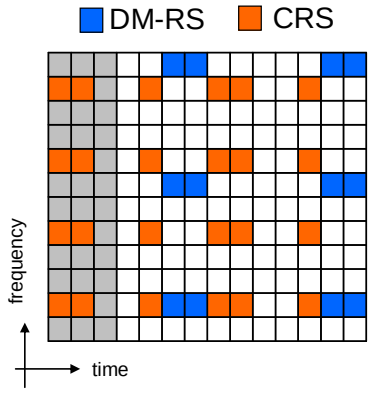

Figure 7.4.1-1: DM-RS pattern for rank 1 and 2

For rank 3 and 4, the DM-RS pattern is illustrated in Figure 7.3.1-2. DM-RS for 1st layer and that for 2nd layer are multiplexed by means of CDM by using OCC over two consecutive resource elements (blue) in time domain. DM-RS for 3rd layer and that for 4th layer are multiplexed by means of CDM by using OCC over two consecutive resource elements (green) in time domain. DM-RS for 1st and 2nd layers and that for 3rd and 4th layers are multiplexed by means of frequency division multiplexing (FDM).

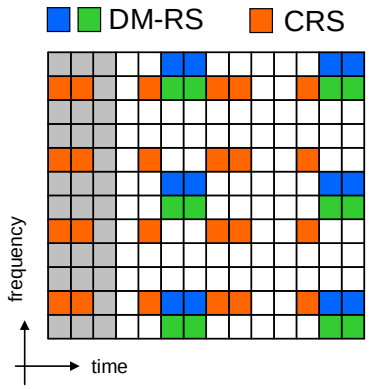

Figure 7.4.1-2: DM-RS pattern for rank 3 and 4

7.4.2 CSI reference signal

Reference signals targeting CSI estimation are

- cell specific
- sparse in frequency and time.
- punctured into the data region of normal/MBSFN subframe

7.5 Downlink transmit diversity

For the downlink transmit diversity with more than four transmit antennas applied to PDCCH, and PDSCH in non-MBSFN subframes, the Rel-8 transmit diversity scheme is used.

8 Coordinated multiple point transmission and reception

Coordinated multi-point (CoMP) transmission/reception is considered for LTE-Advanced as a tool to improve the coverage of high data rates, the cell-edge throughput and/or to increase system throughput in both high load and low load scenarios.

8.1 Downlink coordinated multi-point transmission

8.1.1 Terminology and definitions

Downlink coordinated multi-point transmission implies dynamic coordination among multiple geographically separated transmission points.

General terminology:

- Serving cell: Cell transmitting PDCCH assignments (a single cell). This is the serving cell of Rel-8 (concept that already exists)

CoMP categories:

- Joint Processing (JP): data is available at each point in CoMP cooperating set (definition below)
  - Joint Transmission: PDSCH transmission from multiple points (part of or entire CoMP cooperating set) at a time

        - data to a single UE is simultaneously transmitted from *multiple* transmission points, e.g. to (coherently or non-coherently) improve the received signal quality and/or cancel actively interference for other UEs

    - Dynamic cell selection: PDSCH transmission from one point at a time (within CoMP cooperating set)

- Coordinated Scheduling/Beamforming (CS/CB): data is only available at serving cell (data transmission from that point) but user scheduling/beamforming decisions are made with coordination among cells corresponding to the CoMP cooperating set.

CoMP sets:

- CoMP cooperating set
    - Set of (geographically separated) points directly or indirectly participating in PDSCH transmission to UE. Note that this set may or need not be transparent to the UE.
    - CoMP transmission point(s): point or set of points actively transmitting PDSCH to UE
        - CoMP transmission point(s) is a subset of the CoMP cooperating set
        - For Joint transmission, the CoMP transmission points are the points in the CoMP cooperating set
        - For Dynamic cell selection, a single point is the transmission point at every subframe. This transmission point can change dynamically within the CoMP cooperating set.
        - For Coordinated scheduling/beamforming, the CoMP transmission point corresponds to the "serving cell"
- CoMP measurement set: set of cells about which channel state/statistical information related to their link to the UE is reported as discussed in section 8.1.3
    - The CoMP measurement set may be the same as the CoMP cooperating set
    - The actual UE reports may down-select cells for which actual feedback information is transmitted (reported cells)

In addition, we have:

RRM measurement set: in support of RRM measuremets (already in Rel-8) and therefore not CoMP specific

8.1.2 Radio-interface specification areas

Downlink coordinated multi-point transmission should include the possibility of coordination between different cells. From a radio-interface perspective, there is no difference from the UE perspective if the cells belong to the same eNodeB or different eNodeBs. If inter-eNodeB coordination is supported, information needs to be signalled between eNodeBs.

Potential impact on the radio-interface specifications is foreseen in mainly three areas:

- Feedback and measurement mechanisms from the UE
    - Reporting of dynamic channel conditions between the multiple transmission points and the UE
        - For TDD, channel reciprocity may be exploited
    - Reporting to facilitate the decision on the set of participating transmission points
        - For TDD, channel reciprocity may be exploited
- Preprocessing schemes
    - Joint processing prior to transmission of the signal over the multiple transmission points
    - Downlink control signaling to support the transmission scheme
- Reference signal design

- Depending on the transmission scheme, specification of additional reference signals may be required.
    - CSI RS design should take potential needs of DL CoMP into account

New forms of feedback and signaling may be needed to support CoMP that are, for example, configured by RRC for a given UE.

- As baseline, the network need not explicitly signal to the UE the CoMP transmission point(s) and the UE reception/demodulation of CoMP transmissions (CS/CB, or JP with MBSFN subframes) is the same as that for non CoMP (SU/MU-MIMO)."

- Any additional feedback designed for CoMP shall be consistent with the feedback framework for SU/MU-MIMO.

8.1.3 Feedback in support of DL CoMP

The three main categories of CoMP feedback mechanisms have been identified to be:

- Explicit channel state/statistical information feedback
    - Channel as observed by the receiver, without assuming any transmission or receiver processing
- Implicit channel state/statistical information feedback
    - feedback mechanisms that use hypotheses of different transmission and/or reception processing, e.g., CQI/PMI/RI
- UE transmission of SRS can be used for CSI estimation at eNB exploiting channel reciprocity.

Combinations of full or subset of above three are possible.

Look at these types of feedback mechanisms for the evaluations. UL overhead (number of bits) associated with each specific feedback mechanism needs to be identified. The feedback overhead (UL) vs, DL performance tradeoff should be assessed with the goal to target minimum overhead for a given performance.

For the CoMP schemes that require feedback, individual per-cell feedback is considered as baseline. Complementary inter-cell feedback might be needed. UE CoMP feedback reports target the serving cell (on UL resources from serving cell) as baseline when X2 interface is available and is adequate for CoMP operation in terms of latency and capacity. In this case, the reception of UE reports at cells other than the serving cell is a network implementation choice.

The feedback reporting for cases with X2 interface not available or not adequate (latency and capacity), and for cases where feedback reports to the serving cell causes large interference (e.g., in heteronegenous deployment scenarios) for CoMP operation needs to be discussed and, if found needed, a solution needs to be identified.

Do not have to confine the CoMP studies to payload sizes currently supported by PUCCH operation..

Two possibilities should be studied the "container" of the DL CoMP feedback:

- Expand the supported PUCCH payload sizes
- Use periodic/a-periodic reports on PUSCH

8.1.3.1 Explicit Feedback in support of DL CoMP

This section lists different forms of explicit feedback in support of DL CoMP. They are all characterized by having a channel part and a noise-and-interference part.

Channel part:

- For each cell in the UE's measurement set that is reported in a given subframe, one or several channel properties are reported
- Channel properties include (but are not limited to) the following ('i' is the cell index):
    - Channel matrix (Hi) – short term (instantaneous)
        - The full matrix Hi, or

- main eigen component(s) of Hi

- Transmit channel covariance (Ri), where Ri = (sum{Hij†Hij})/J, j=0,1,2,…,J-1, ('j' is span over time or frequency)
  - The full matrix Ri, or
  - main eigen component(s) of Ri
- Inter-cell channel properties may also be reported

Noise-and interference part, e.g.,

- Interference outside the
  - cells reported by the UE
  - CoMP transmission points
- Total receive power (Io) or total received signal covariance matrix
- Covariance matrix of the noise-and-interference
  - the full matrix, or
  - main eigen component(s)

8.1.3.2 Implicit Feedback in support of DL CoMP

This section lists different forms of implicit feedback in support of DL CoMP.

- There are hypotheses at the UE and the feedback is based on one or a combination of two or more of the following, e.g.:
  - Single vs. Multi user MIMO
  - Single cell vs. Coordinated transmission
    - Within coordinated transmission: Single point (CB/CS) vs. multi-point (JP) transmission

      Within Joint processing CoMP:
      - Subsets of transmission points or subsets of reported cells (Joint Transmission)
      - CoMP transmission point(s) (Dynamic Cell Selection)
  - Transmit precoder (i.e. tx weights)
    - JP: multiple single-cell or multi-cell PMI capturing coherent or non-coherent channel across reported cells
    - CB/CS: Single-cell or multiple single-cell PMIs capturing channel from the reported cell(s) to the UE
      - Transmit precoder based on or derived from the PMI weight
    - Other types of feedbacks, e.g. main Multi-cell eigen-component, instead of PMI are being considered
  - Receive processing (i.e. rx weights)
  - Interference based on particular tx/rx processing

There may be a need for the UE to convey to the network the hypothesis or hypotheses used (explicit signalling of hypothesis to eNB). And/or, there may be a semi-static hypothesis configuration e.g. grouping of hypotheses (explicit signalling of hypothesis to the UE). And/or, precoded RS may be used to allow UE to generate refined CQI/RI feedback

8.1.3.3 UE transmission of SRS in support of DL CoMP

This section lists UE transmission of SRS related feedback in support of DL CoMP. UE transmission of SRS can be used for CSI estimation at multiple cells exploiting channel reciprocity. Enhanced SRS schemes may be considered.

8.1.4 Overhead in support of DL CoMP operation

DL CoMP operation overhead is very much related to the DL-RS structure (see section 7.2).

- Studies on CSI RS impact on PDSCH transmissions to Rel-8 UEs for various RS densities needed
  - There should be no impact from CSI RS transmission on transmission of PBCH/PSS/SSS

8.2 Uplink coordinated multi-point reception

Coordinated multi-point reception implies coordination among multiple, geographically separated points. Uplink coordinated multi-point reception is expected to have very limited impact on the RAN1 specifications. Uplink CoMP reception can involve joint reception (JR) of the transmitted signal at multiple reception points and/or coordinated scheduling (CS) decisions among cells to control interference and may have some RAN1 specification impact.

The need for extended CP operation in certain UL subframes should be further investigated.

9 Relaying functionality

Relaying is considered for LTE-Advanced as a tool to improve e.g. the coverage of high data rates, group mobility, temporary network deployment, the cell-edge throughput and/or to provide coverage in new areas.

The relay node is wirelessly connected to the radio-access network via a *donor cell*. With respect to the relay node's usage of spectrum, its operation can be classified into:

- *inband*, in which case the eNB -relay link shares the same carrier frequency with relay-UE links. Rel-8 UEs should be able to connect to the donor cell in this case.
- *outband*, in which case the eNB-relay link does not operate in the same carrier frequency as relay-UE links. Rel-8 UEs should be able to connect to the donor cell in this case.

For both inband and outband relaying, it shall be possible to operate the eNB-to-relay link on the same carrier frequency as eNB-to-UE links

With respect to the knowledge in the UE, relays can be classified into

- *transparent*, in which case the UE is not aware of whether or not it communicates with the network via the relay.
- *non-transparent*, in which case the UE is aware of whether or not it is communicating with the network via the relay.

Depending on the relaying strategy, a relay may

- be part of the donor cell
- control cells of its own

In the case the relay is part of the donor cell, the relay does not have a cell identity of its own (but may still have a relay ID). At least part of the RRM is controlled by the eNodeB to which the donor cell belongs, while parts of the RRM may be located in the relay. In this case, a relay should preferably support also LTE Rel-8 UEs. Smart repeaters, decode-and-forward relays, different types of L2 relays, and Type 2 relay are examples of this type of relaying.

In the case the relay is in control of cells of its own, the relay controls one or several cells and a unique physical-layer cell identity is provided in each of the cells controlled by the relay. The same RRM mechanisms are available and from a UE perspective there is no difference in accessing cells controlled by a relay and cells controlled by a "normal" eNodeB. The cells controlled by the relay should support also LTE Rel-8 UEs. Self-backhauling (L3 relay), "Type 1 relay nodes", "Type 1a relay nodes", and "Type 1b relay nodes" use this type of relaying.

At least "Type 1" and "Type 1a" relay nodes are part of LTE-Advanced.

A “Type 1” relay node is an inband relaying node characterized by the following:

- It control cells, each of which appears to a UE as a separate cell distinct from the donor cell
- The cells shall have their own Physical Cell ID (defined in LTE Rel-8) and the relay node shall transmit its own synchronization channels, reference symbols, …
- In the context of single-cell operation, the UE shall receive scheduling information and HARQ feedback directly from the relay node and send its control channels (SR/CQI/ACK) to the relay node
- It shall appear as a Rel-8 eNodeB to Rel-8 UEs (i.e. be backwards compatible)
- To LTE-Advanced UEs, it should be possible for a relay node to appear differently than Rel-8 eNodeB to allow for further performance enhancement.

“Type 1a” and “Type 1b” relay nodes are characterised by the same set of features as the “Type 1” relay node above, except “Type 1a” operates outband and “Type 1b” operates inband with adequate antenna isolation. A “Type 1a” relay node is expected to have little or no impact on RAN1 specifications.

A “Type 2” relay node is an inband relaying node characterized by the following:

- It does not have a separate Physical Cell ID and thus would not create any new cells.
- It is transparent to Rel-8 UEs; a Rel-8 UE is not aware of the presence of a Type 2 relay node.
- It can transmit PDSCH.
- At least, it does not transmit CRS and PDCCH.

9.1 Relay-eNodeB link for inband relay

9.1.1 Resource partitioning for relay-eNodeB link

In order to allow inband relaying, some resources in the time-frequency space are set aside for the backhaul link (Un) and cannot be used for the access link (Uu). At least the following scheme will be supported for this resource partitioning:

General principle for resource partitioning at the relay:

- eNB → RN and RN → UE links are time division multiplexed in a single carrier frequency (only one is active at any time)
- RN → eNB and UE → RN links are time division multiplexed in a single carrier frequency (only one is active at any time)

Multiplexing of backhaul links in FDD:

- eNB → RN transmissions are done in the DL frequency band
- RN → eNB transmissions are done in the UL frequency band

Multiplexing of backhaul links in TDD:

- eNB → RN transmissions are done in the DL subframes of the eNB and RN
- RN → eNB transmissions are done in the UL subframes of the eNB and RN

9.1.2 Backward compatible backhaul partitioning

Due to the relay transmitter causing interference to its own receiver, simultaneous eNodeB-to-relay and relay-to-UE transmissions on the same frequency resource may not be feasible unless sufficient isolation of the outgoing and incoming signals is provided e.g. by means of specific, well separated and well isolated antenna structures. Similarly, at the relay it may not be possible to receive UE transmissions simultaneously with the relay transmitting to the eNodeB.

One possibility to handle the interference problem is to operate the relay such that the relay is not transmitting to terminals when it is supposed to receive data from the donor eNodeB, i.e. to create "gaps" in the relay-to-UE transmission. These "gaps" during which terminals (including Rel-8 terminals) are not supposed to expect any relay transmission can be created by configuring MBSFN subframes as exemplified in Figure 9.1.2-1. Relay-to-eNodeB transmissions can be facilitated by not allowing any terminal-to-relay transmissions in some subframes.

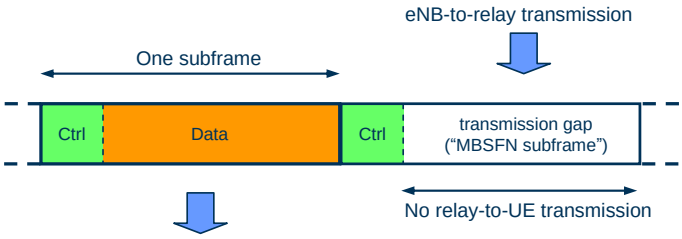

Figure 9.1.2-1: Example of relay-to-UE communication using normal subframes (left) and eNodeB-to-relay communication using MBSFN subframes (right).

9.1.3 Backhaul resource assignment

In case of downlink backhaul in downlink resources, the following is valid

- At the RN, the access link downlink subframe boundary is aligned with the backhaul link downlink subframe boundary, except for possible adjustment to allow for RN transmit/receive switching
- The set of downlink backhaul subframes, during which downlink backhaul transmission may occur, is semi-statically assigned
- The set of uplink backhaul subframes, during which uplink backhaul transmission may occur, can be semi-statically assigned, or implicitly derived from the downlink backhaul subframes using the HARQ timing relationship
- A new physical control channel (here referred to as the "R-PDCCH") is used to dynamically or "semi-persistently" assign resources, within the semi-statically assigned sub-frames, for the downlink backhaul data (corresponding to the "R-PDSCH" physical channel). The R-PDCCH may assign downlink resources in the same and/or in one or more later subframes.
- The "R-PDCCH" is also used to dynamically or "semi-persistently" assign resources for the uplink backhaul data (the "R-PUSCH" physical channel). The R-PDCCH may assign uplink resources in one or more later subframes.
- Within the PRBs semi-statically assigned for R-PDCCH transmission, a subset of the resources is used for each R-PDCCH. The actual overall set of resources used for R-PDCCH transmission within the above mentioned semi-statically assigned PRBs may vary dynamically between subframes. These resources may correspond to the full set of OFDM symbols available for the backhaul link or be constrained to a subset of these OFDM symbols. The resources that are not used for R-PDCCH within the above mentioned semi-statically assigned PRBs may be used to carry R-PDSCH or PDSCH.
- The detailed R-PDCCH transmitter processing (channel coding, interleaving, multiplexing, etc.) should reuse Rel-8 functionality to the extent possible, but allow removing some unnecessary procedure or bandwidth-wasting procedure by considering the relay property.
- If the "search space" approach of R8 is used for the backhaul link, use of common search space, which can be semi-statically configured (and potentially includes entire system bandwidth), is the baseline. If RN-specific search space is configured, it could be implicitly or explicitly known by RN.
- The R-PDCCH is transmitted starting from an OFDM symbol within the subframe that is late enough so that the relay can receive it.
- "R-PDSCH" and "R-PDCCH" can be transmitted within the same PRBs or within separated PRBs.

- No "R-PCFICH" exists for indication of backhaul control region size in time and frequency domains

9.2 Relay-eNodeB link for outband relay

If relay-eNB and relay-UE links are isolated enough in frequency (possibly with help of additional means such as antenna separation), then there is no interference issue in activating both links simultaneously. Therefore, it becomes possible for relay-eNodeB link to reuse the channels designed for UE-eNodeB link.

9.3 Relay-eNodeB link for inband relay Type 1b

If the outgoing and incoming signals at the relay are adequately isolated in the spatial domain, e.g., by appropriate arrangement of the respective antennas for the Un and Uu links, the eNB→ RN and RN→ UE (RN→ eNB and UE→ RN) links can be activated simultaneously without the need for the time division multiplexing. The operation of Type 1b relay nodes may not be supported in all deployment scenarios.

9A Heterogeneous deployments

Heterogeneous deployments consist of deployments where low power nodes are placed throughout a macro-cell layout. Different scenarios under consideration that could occur in heterogeneous deployments are discussed in Appendix A.2.1.1.2

The interference characteristics in a heterogeneous deployment can be significantly different than in a homogeneous deployment. Examples hereof are given in Figure 9A-1. In case (a), a macro user with no access to the CSG cell will be interfered by the HeNB, in case (b) a macro user causes severe interference towards the HeNB and in case (c), a CSG user is interfered by another CSG HeNB. On the right hand side, case (d), path-loss based cell association (e.g. by using biased RSRP reports) may improve the uplink but at the cost of increasing the downlink interference of non-macro users at the cell edge.

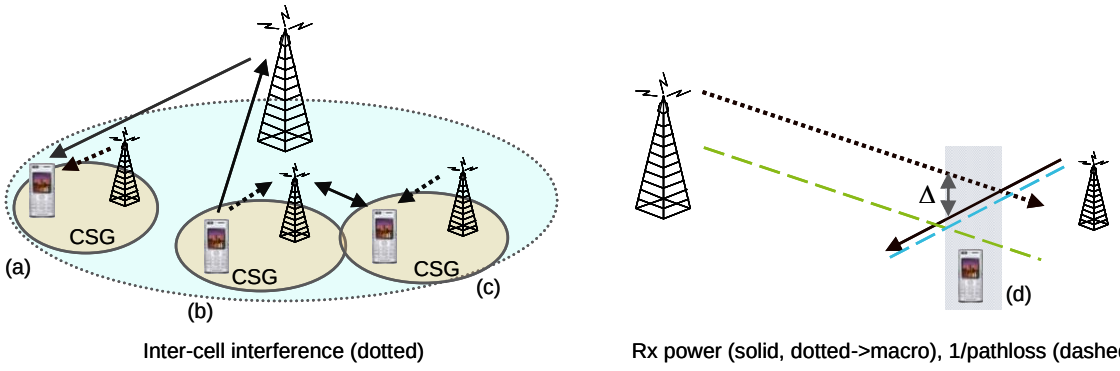

Figure 9A-1: Examples of interference scenarios in heterogeneous deployments.

In these scenarios, preliminary results indicate that methods for handling the uplink and downlink interference towards data as well as L1/L2 control signaling, synchronization signals and reference signals are important. Such methods may operate in time, frequency and/or spatial domains.

9A.1 Rel-8/9 schemes

Several methods for handling the above-mentioned interference scenarios using the functionality present in Rel-8/9 can be envisioned. Examples hereof include using different carrier frequencies for different cell layers, or, if the same carrier is used across different cell layers, by restricting the transmission power during part of the time for at least one cell layer to reduce interference to control signalling on other cell layers or through different power control schemes as discussed in [TR36.921]. Enhancements to these types of schemes can be considered in releases beyond Rel-9.

9A.2 Non-Rel-8/9 schemes

A common property of the non-Rel-8/9 schemes below is that they provide means for coordination of the control channel interference between cell layers. Examples of some mechanism that might be used for interference handling can be found in Section 8.

9A.2.1 CA-based scheme

Carrier aggregation (CA) with cross-carrier scheduling using CIF , described in Section 5.2 and agreed to be part of Rel-10, can be used for heterogeneous deployments. Downlink interference for control signaling can be handled by partitioning component carriers in each cell layer into two sets, one set used for data and control and one set used mainly for data and possibly control signaling with reduced transmission power. One example is illustrated in Figure 9A.2.1-1. For the data part, downlink interference coordination techniques can be used. Rel-8/9 terminals can be scheduled on one component carrier while Rel-10 terminal capable of carrier aggregation can be scheduled on multiple component carriers. Time synchronization between the cell layers is assumed in this example.

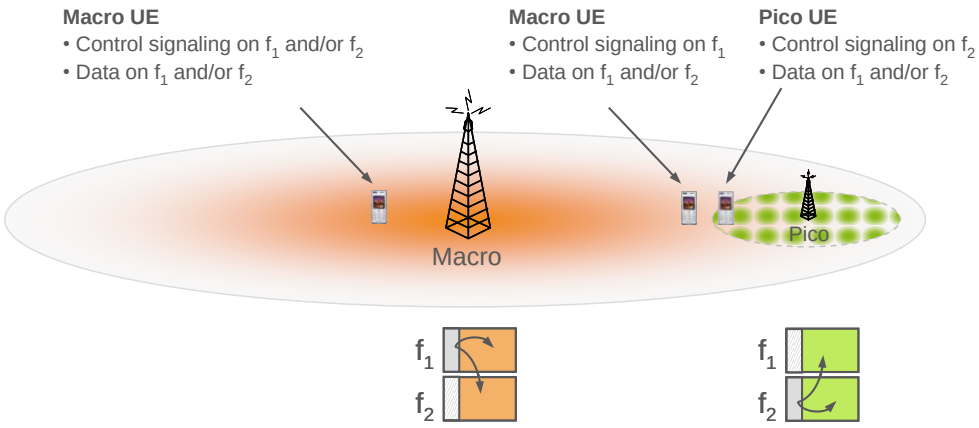

Figure 9A.2.1-1: One example of carrier aggregation applies to heterogeneous deployments.

9A.2.2 Non-CA based schemes

Several schemes for control-channel interference handling not relying on carrier aggregation can be envisioned, including, but not limited to, time-domain and frequency-domain schemes.

In a time-domain scheme, interference handling for downlink control signalling can be achieved by restricting the transmission during part of the time, possibly in combination with time shifting, for at least one cell layer to reduce interference to control signalling on other cell layers. Time synchronization between the cell layers is assumed in this approach.

In a frequency-domain scheme, the downlink control signalling is transmitted over part of the carrier bandwidth. Interference management can be achieved by using different parts of the carrier bandwidth for control signalling in different cell layers. Time synchronization between the cell layers is assumed.

10 Evaluation of techniques for Advanced E-UTRA

Section 10.1 presents the evaluation results of the techniques for advanced E-UTRA against the 3GPP targets [3]. The evaluation results in Section 10.2 are in support of the submission of the 3GPP "*LTE Release 10 & beyond (LTE-Advanced)*" to the ITU-R as a candidate technology for the IMT-Advanced.

10.1 Cell spectral efficiency and cell-edge spectral efficiency against 3GPP target

Cell spectral efficiency and cell-edge spectral efficiency are evaluated through extensive simulations conducted by a number of companies. The tables in the following subsections show the simulation results focusing on LTE-Advanced configurations, i.e., downlink and uplink MU-MIMO, downlink and uplink CoMP, and uplink SU-MIMO.

Tables 10.1-1, 2, 3, and 4 show the source specific simulation parameters that characterize the performances of downlink FDD, downlink TDD, uplink FDD, and uplink TDD, respectively. Note, however, that the performance differences among sources could also be explained by other factors such as detailed signal processing algorithms at the transmitter and the receiver.

In the tables for downlink, control channel (CCH) duration (L OFDM symbols) and the number of the MBSFN subframes are the factors that affect the overhead. In the MBSFN subframes, there are no CRS in data regions, which effectively reduce the overhead. Channel estimation and receiver types are the factors that affect the demodulation performance. CSI-assumption at eNB is the factor that characterizes the transmit signal processing at eNB for MU-MIMO and CoMP schemes. In the tables for uplink, the PUCCH bandwidth is the factor that affects the overhead.

Table 10.1-1 Simulation parameters for 3GPP targets fulfillment (DL, FDD)

	CCH duration (L symbols)	Num of MBSFN subframe	Channel estimation	Receiver type	CSI assumption at eNB
Source 1	3	6	Real	MMSE	Short-term for CS/CB-CoMP Long-term + Short-term for JP-CoMP
Source 3	3	6	Real	MMSE with IRC	Long-term
Source 4	3	6	Real	MMSE with IRC	Short-term
Source 5	3	6	Real	MMSE	Long-term + Short-term
Source 7	3	6	Ideal	MMSE	Long-term + Short-term
Source 11	3	6	Real	MMSE with IRC	Short-term
Source 15	3	6	Real	MMSE with IRC	Short-term
Source 18	3	6	Real	MMSE with IRC	Long-term

Table 10.1-2 Simulation parameters for 3GPP targets fulfillment (DL, TDD)

	CCH duration (L symbols)	Num of MBSFN subframe	Channel estimation	Receiver type	CSI assumption at eNB
Source 1	3	2	Real	MMSE	Short-term
Source 2	3	0	Real	MMSE with IRC	Short-term
Source 3	3	2	Real	MMSE with IRC	Long-term
Source 4	3	2	Real	MMSE with IRC	Short-term
Source 5	3	0	Real	MMSE	Short-term
Source 10	3	2	Real	MMSE with IRC	Short-term
Source 19	3	2	Real	MMSE with IRC	Short-term

Table 10.1-3 Simulation parameters for 3GPP targets fulfillment (UL, FDD)

	PUCCH bandwidth (RB/10 MHz)	Channel estimation	Receiver type
Source 1	6	Real	MMSE
Source 3	4	Real	MMSE with IRC
Source 4	4	Real	MMSE with IRC
Source 5	4	Real	MMSE
Source 15	4	Real	MMSE with IRC
Source 18	6	Real	MMSE with IRC

Table 10.1-4 Simulation parameters for 3GPP targets fulfillment (UL, TDD)

	PUCCH bandwidth (RB/10 MHz)	Channel estimation	Receiver type
Source 1	4	Real	MMSE
Source 2	4	Real	MMSE with IRC
Source 3	4	Real	MMSE with IRC
Source 4	4	Real	MMSE with IRC
Source 5	4	Real	MMSE with IRC
Source 10	4	Real	MMSE with IRC

Tables in the following subsections capture the spectrum efficiency results from individual sources. As performance references, the 3GPP targets and the averaged results of Rel-8 schemes (2-by-2/4-by-2/4-by-4 SU-MIMO with L=3 for downlink, and 1-by-2/1-by-4 SIMO, and 1-by-4 MU-MIMO for uplink) assuming real channel estimation.

10.1.1 3GPP Case1 (3GPP spatial channel model)

10.1.1.1 FDD, Downlink

Tables 10.1.1.1-1, 10.1.1.1-2, and 10.1.1.1-3 show the spectrum efficiency results of 2-by-2, 4-by-2, and 4-by-4 MU-MIMO schemes with eNB antenna configuration (C). Results show that the MU-MIMO schemes satisfy the 3GPP target and provide significant gain compared with the Rel-8 SU-MIMO scheme.

Table 10.1.1.1-1 Performance of DL MU-MIMO 2 x 2 (C) (3GPP Case1, FDD)

	Cell spectral efficiency (bit/sec/Hz/cell)	Cell-edge user spectral efficiency (bit/sec/Hz/user)
Source 1	2.77	0.110
Source 5	2.74	0.091
Source 15	2.56	0.070
Rel-8 SU-MIMO (2 x 2, L=3)	2.23	0.079
3GPP target	2.40	0.070

Table 10.1.1.1-2 Performance of DL MU-MIMO 4 x 2 (C) (3GPP Case1, FDD)

	Cell spectral efficiency (bit/sec/Hz/cell)	Cell-edge user spectral efficiency (bit/sec/Hz/user)
Source 1	3.55	0.120
Source 4	3.23	0.118
Source 5	3.41	0.127
Source 7	3.83	0.123
Source 11	3.15	0.104
Source 15	3.42	0.114
Rel-8 SU-MIMO (4 x 2, L=3)	2.53	0.100
3GPP target	2.60	0.090

Table 10.1.1.1-3 Performance of DL MU-MIMO 4 x 4 (C) (3GPP Case1, FDD)

	Cell spectral efficiency (bit/sec/Hz/cell)	Cell-edge user spectral efficiency (bit/sec/Hz/user)
Source 1	5.45	0.210
Source 4	4.49	0.205
Source 5	4.42	0.223
Source 11	4.63	0.196
Source 15	4.45	0.182
Rel-8 SU-MIMO (4 x 4, L=3)	3.41	0.143
3GPP target	3.70	0.120

Tables 10.1.1.1-4, 10.1.1.1-5, and 10.1.1.1-6 show the spectrum efficiency results of 2-by-2, 4-by-2, and 4-by-4 CS/CB-CoMP schemes with eNB antenna configuration (C). Results show that the CS/CB schemes satisfy the 3GPP target and achieve significant gain compared with the Rel-8 SU-MIMO scheme.

Table 10.1.1.1-4 Performance of DL CS/CB-CoMP 2 x 2 (C) (3GPP Case1, FDD)

	Cell spectral efficiency (bit/sec/Hz/cell)	Cell-edge user spectral efficiency (bit/sec/Hz/user)
Source 3	2.54	0.088
Source 15	2.58	0.070
Rel-8 SU-MIMO (2 x 2, L=3)	2.23	0.079
3GPP target	2.40	0.070

Table 10.1.1.1-5 Performance of DL CS/CB-CoMP 4 x 2 (C) (3GPP Case1, FDD)

	Cell spectral efficiency (bit/sec/Hz/cell)	Cell-edge user spectral efficiency (bit/sec/Hz/user)
Source 1	3.28	0.150
Source 3	3.34	0.144
Source 15	3.51	0.121
Source 18	3.24	0.100
Rel-8 SU-MIMO (4 x 2, L=3)	2.53	0.100
3GPP target	2.60	0.090

Table 10.1.1.1-6 Performance of DL CS/CB-CoMP 4 x 4 (C) (3GPP Case1, FDD)

	Cell spectral efficiency (bit/sec/Hz/cell)	Cell-edge user spectral efficiency (bit/sec/Hz/user)
Source 3	4.97	0.239
Source 15	4.58	0.195
Source 18	4.44	0.180
Rel-8 SU-MIMO (4 x 4, L=3)	3.41	0.143
3GPP target	3.70	0.120

Tables 10.1.1.1-7, 10.1.1.1-8, and 10.1.1.1-9 show the spectrum efficiency results of 2-by-2, 4-by-2, and 4-by-4 JP-CoMP schemes with eNB antenna configuration (C). Results show that the JP-CoMP schemes provide additional performance enhancement over MU-MIMO in Table 10.1.1-1-1, 10.1.1-1-2, and Table 10.1.1-1-3 (compared with the same source).

Table 10.1.1.1-7 Performance of DL JP-CoMP 2 x 2 (C) (3GPP Case1, FDD)

	Cell spectral efficiency (bit/sec/Hz/cell)	Cell-edge user spectral efficiency (bit/sec/Hz/user)
Source 1	2.92	0.120
Source 15	2.47	0.088
Rel-8 SU-MIMO (2 x 2, L=3)	2.23	0.079
3GPP target	2.60	0.090

Table 10.1.1.1-8 Performance of DL JP-CoMP 4 x 2 (C) (3GPP Case1, FDD)

	Cell spectral efficiency (bit/sec/Hz/cell)	Cell-edge user spectral efficiency (bit/sec/Hz/user)
Source 1	4.40	0.180
Source 15	3.34	0.143
Rel-8 SU-MIMO (4 x 2, L=3)	2.53	0.100
3GPP target	2.60	0.090

Table 10.1.1.1-9 Performance of DL JP-CoMP 4 x 4 (C) (3GPP Case1, FDD)

	Cell spectral efficiency (bit/sec/Hz/cell)	Cell-edge user spectral efficiency (bit/sec/Hz/user)
Source 1	5.89	0.31
Source 15	4.48	0.227
Rel-8 SU-MIMO (4 x 4, L=3)	3.41	0.143
3GPP target	3.70	0.120

10.1.1.2 TDD, Downlink

Tables 10.1.1.2-1, 10.1.1.2-2, and 10.1.1.2-3 show the spectrum efficiency results of 2-by-2, 4-by-2, and 4-by-4 MU-MIMO schemes with eNB antenna configuration (C). Table 10.1.1.2-4 shows the spectrum efficiency results of 4-by-2 MU-MIMO schemes with eNB antenna configuration (E). Results show that the MU-MIMO schemes satisfy the 3GPP target and provide significant gain compared with the Rel-8 SU-MIMO scheme.

Table 10.1.1.2-1 Performance of DL MU-MIMO 2 x 2 (C) (3GPP Case1, TDD)

	Cell spectral efficiency (bit/sec/Hz/cell)	Cell-edge user spectral efficiency (bit/sec/Hz/user)
Source 1	2.96	0.120
Source 5	2.80	0.106
Rel-8 SU-MIMO (2 x 2, L=3)	2.17	0.083
3GPP target	2.40	0.070

Table 10.1.1.2-2 Performance of DL MU-MIMO 4 x 2 (C) (3GPP Case1, TDD)

	Cell spectral efficiency (bit/sec/Hz/cell)	Cell-edge user spectral efficiency (bit/sec/Hz/user)
Source 1	4.23	0.160
Source 2	3.45	0.131
Source 4	4.16	0.173
Source 5	3.68	0.150
Source 10	3.52	0.172
Source 19	3.5	0.121
Rel-8 SU-MIMO (4 x 2, L=3)	2.52	0.096
3GPP target	2.60	0.090

Table 10.1.1.2-3 Performance of DL MU-MIMO 4 x 4 (C) (3GPP Case1, TDD)

	Cell spectral efficiency (bit/sec/Hz/cell)	Cell-edge user spectral efficiency (bit/sec/Hz/user)
Source 1	6.16	0.250
Source 2	4.67	0.194
Source 5	4.07	0.182
Source 19	4.70	0.160
Rel-8 SU-MIMO (4 x 4, L=3)	3.28	0.154
3GPP target	3.70	0.120

Table 10.1.1.2-4 Performance of DL MU-MIMO 4 x 2 (E) (3GPP Case1, TDD)

	Cell spectral efficiency (bit/sec/Hz/cell)	Cell-edge user spectral efficiency (bit/sec/Hz/user)
Source 10	3.35	0.150
Rel-8 SU-MIMO (4 x 2, L=3)	2.42	0.073
3GPP target	2.60	0.090

Tables 10.1.1.2-5, 10.1.1.2-6, and 10.1.1.2-7 show the spectrum efficiency results of 2-by-2, 4-by-2, and 4-by-4 CS/CB-CoMP schemes with eNB antenna configuration (C). Results show that the CS/CB schemes satisfy the 3GPP target and achieve significant gain compared with the Rel-8 SU-MIMO scheme.

Table 10.1.1.2-5 Performance of DL CS/CB-CoMP 2 x 2 (C) (3GPP Case1, TDD)

	Cell spectral efficiency (bit/sec/Hz/cell)	Cell-edge user spectral efficiency (bit/sec/Hz/user)
Source 3	2.54	0.088
Rel-8 SU-MIMO (2 x 2, L=3)	2.17	0.083
3GPP target	2.40	0.070

Table 10.1.1.2-6 Performance of DL CS/CB-CoMP 4 x 2 (C) (3GPP Case1, TDD)

	Cell spectral efficiency (bit/sec/Hz/cell)	Cell-edge user spectral efficiency (bit/sec/Hz/user)
Source 3	3.38	0.146
Rel-8 SU-MIMO (4 x 2, L=3)	2.52	0.096
3GPP target	2.60	0.090

Table 10.1.1.2-7 Performance of DL CS/CB-CoMP 4 x 4 (C) (3GPP Case1, TDD)

	Cell spectral efficiency (bit/sec/Hz/cell)	Cell-edge user spectral efficiency (bit/sec/Hz/user)
Source 3	5.06	0.244
Rel-8 SU-MIMO (4 x 4, L=3)	3.28	0.154
3GPP target	3.70	0.120

Tables 10.1.1.2-8, 10.1.1.2-9, and 10.1.1.2-10 show the spectrum efficiency results of 2-by-2, 4-by-2, and 4-by-4 JP-CoMP schemes with eNB antenna configuration (C). Table 10.1.1.2-11 shows the spectrum efficiency results of 4-by-2 JP-CoMP schemes with eNB antenna configuration (E). Results show that the JP-CoMP schemes provide additional performance enhancement over MU-MIMO in Table 10.1.1.2-1, 10.1.1.2-2, 10.1.1.2-3, and 10.1.1.2-4 (compared with the same source).

Table 10.1.1.2-8 Performance of DL JP-CoMP 2 x 2 (C) (3GPP Case1, TDD)

	Cell spectral efficiency (bit/sec/Hz/cell)	Cell-edge user spectral efficiency (bit/sec/Hz/user)
Source 1	3.15	0.130
Rel-8 SU-MIMO (2 x 2, L=3)	2.17	0.083
3GPP target	2.40	0.070

Table 10.1.1.2-9 Performance of DL JP-CoMP 4 x 2 (C) (3GPP Case1, TDD)

	Cell spectral efficiency (bit/sec/Hz/cell)	Cell-edge user spectral efficiency (bit/sec/Hz/user)
Source 1	4.89	0.210
Source 10	4.38	0.188
Rel-8 SU-MIMO (4 x 2, L=3)	2.52	0.096
3GPP target	2.60	0.090

Table 10.1.1.2-10 Performance of DL JP-CoMP 4 x 4 (C) (3GPP Case1, TDD)

	Cell spectral efficiency (bit/sec/Hz/cell)	Cell-edge user spectral efficiency (bit/sec/Hz/user)
Source 1	6.61	0.330
Rel-8 SU-MIMO (4 x 4, L=3)	3.28	0.154
3GPP target	3.70	0.120

Table 10.1.1.2-11 Performance of DL JP-CoMP 4 x 2 (E) (3GPP Case1, TDD)

	Cell spectral efficiency (bit/sec/Hz/cell)	Cell-edge user spectral efficiency (bit/sec/Hz/user)
Source 10	4.05	0.175
Rel-8 SU-MIMO (4 x 2, L=3)	2.42	0.073
3GPP target	2.60	0.090

10.1.1.3 FDD, Uplink

Tables 10.1.1.3-1 and 10.1.1.3-2 show the spectrum efficiency results of 2-by-4 SU-MIMO with eNB antenna configuration (A) and (C), respectively. Results show that the 2-by-4 SU-MIMO schemes satisfy the 3GPP target and provide significant gain compared with the Rel-8 SIMO scheme.

Table 10.1.1.3-1 Performance of UL SU-MIMO 2 x 4 (A) (3GPP Case1, FDD)

	Cell spectral efficiency (bit/sec/Hz/cell)	Cell-edge user spectral efficiency (bit/sec/Hz/user)
Source 3	2.46	0.112
Source 15	2.26	0.093
Source 18	2.36	0.086
Rel-8 SIMO (1 x 4)	1.95	0.075
3GPP target	2.00	0.070

Table 10.1.1.3-2 Performance of UL SU-MIMO 2 x 4 (C) (3GPP Case1, FDD)

	Cell spectral efficiency (bit/sec/Hz/cell)	Cell-edge user spectral efficiency (bit/sec/Hz/user)
Source 1	2.33	0.070
Source 3	2.37	0.118
Source 4	2.43	0.096
Source 5	2.34	0.080
Source 15	2.01	0.096
Source 18	2.12	0.087
Rel-8 SIMO (1 x 4)	2.00	0.075
3GPP target	2.00	0.070

Tables 10.1.1.3-3 and 10.1.1.3-4 show the spectrum efficiency results of 1-by-2 CoMP with eNB antenna configuration (A) and (C), respectively. Results show that the Rel-8 SIMO scheme satisfies the 3GPP target. Tables 10.1.1.3-5 and 10.1.1.3-6 show spectrum efficiency results of 2-by-4 CoMP with eNB antenna configuration (A) and (C), respectively. Results show that multi point reception provides additional performance enhancement compared with the Rel-8 SIMO scheme.

Table 10.1.1.3-3 Performance of UL CoMP 1 x 2 (A) (3GPP Case1, FDD)

	Cell spectral efficiency (bit/sec/Hz/cell)	Cell-edge user spectral efficiency (bit/sec/Hz/user)
Source 18	1.44	0.052
Rel-8 SIMO (1 x 2)	1.42	0.050
3GPP target	1.20	0.040

Table 10.1.1.3-4 Performance of UL CoMP 1 x 2 (C) (3GPP Case1, FDD)

	Cell spectral efficiency (bit/sec/Hz/cell)	Cell-edge user spectral efficiency (bit/sec/Hz/user)
Source 18	1.40	0.051
Rel-8 SIMO (1 x 2)	1.33	0.047
3GPP target	1.20	0.040

Table 10.1.1.3-5 Performance of UL CoMP 2 x 4 (A) (3GPP Case1, FDD)

	Cell spectral efficiency (bit/sec/Hz/cell)	Cell-edge user spectral efficiency (bit/sec/Hz/user)
Source 18	2.43	0.092
Rel-8 SIMO (1 x 4)	1.95	0.075
3GPP target	2.00	0.070

Table 10.1.1.3-6 Performance of UL CoMP 2 x 4 (C) (3GPP Case1, FDD)

	Cell spectral efficiency (bit/sec/Hz/cell)	Cell-edge user spectral efficiency (bit/sec/Hz/user)
Source 18	2.18	0.092
Rel-8 SIMO (1 x 4)	2.00	0.075
3GPP target	2.00	0.070

10.1.1.4 TDD, Uplink

Tables 10.1.1.4-1 and 10.1.1.4-2 show the spectrum efficiency results of 2-by-4 SU-MIMO with eNB antenna configuration (A) and (C), respectively. Results show that the 2-by-4 SU-MIMO schemes satisfy the 3GPP target and provide gain compared with the Rel-8 SIMO and Rel-8 MU-MIMO schemes.

Table 10.1.1.4-1 Performance of UL SU-MIMO 2 x 4 (A) (3GPP Case1, TDD)

	Cell spectral efficiency (bit/sec/Hz/cell)	Cell-edge user spectral efficiency (bit/sec/Hz/user)
Source 3	2.23	0.101
Source 5	2.33	0.080
Rel-8 MU-MIMO (1 x 4)	2.09	0.070
3GPP target	2.00	0.070

Table 10.1.1.4-2 Performance of UL SU-MIMO 2 x 4 (C) (3GPP Case1, TDD)

	Cell spectral efficiency (bit/sec/Hz/cell)	Cell-edge user spectral efficiency (bit/sec/Hz/user)
Source 1	2.16	0.080
Source 3	2.15	0.107
Source 4	2.13	0.082
Rel-8 SIMO (1 x 4)	1.83	0.064
3GPP target	2.00	0.070

Table 10.1.1.4-3 shows the spectrum efficiency results of 1-by-2 CoMP with eNB antenna configuration (C). Results show that the Rel-8 SIMO scheme satisfies the 3GPP target and multi point reception provides performance enhancement compared with the Rel-8 SIMO scheme.

Table 10.1.1.4-3 Performance of UL CoMP 1 x 2 (C) (3GPP Case1, TDD)

	Cell spectral efficiency (bit/sec/Hz/cell)	Cell-edge user spectral efficiency (bit/sec/Hz/user)
Source 10	1.51	0.051
Rel-8 SIMO (1 x 2)	1.24	0.045
3GPP target	1.20	0.040

Table 10.1.1.4-4 shows the spectrum efficiency results of 2-by-4 MU-MIMO with eNB antenna configuration (C). Result shows that MU-MIMO provides performance enhancement compared with the Rel-8 SIMO scheme.

Table 10.1.1.4-4 Performance of UL MU-MIMO 2 x 4 (C) (3GPP Case1, TDD)

	Cell spectral efficiency (bit/sec/Hz/cell)	Cell-edge user spectral efficiency (bit/sec/Hz/user)
Source 2	2.59	0.079
Rel-8 SIMO (1 x 4)	1.83	0.064
3GPP target	2.00	0.070

10.2 Cell spectral efficiency and cell-edge spectral efficiency for ITU-R requirements

Cell spectral efficiency and cell-edge spectral efficiency are evaluated through extensive simulations conducted by a number of companies. The simulation assumptions applied in the following evaluations are shown in Annex A.3.

Detailed information covering a range of possible configurations is provided in Annex A.4 and [5]. The tables in the following subsections show the simulation results focusing on LTE-Advanced configurations, i.e., downlink and uplink MU-MIMO, downlink and uplink CoMP, and uplink SU-MIMO.

Tables 10.2-1, 2, 3, and 4 show the source specific simulation parameters that characterize the performances of downlink FDD, downlink TDD, uplink FDD, and uplink TDD, respectively. Note, however, that the performance differences among sources could also be explained by other factors such as detailed signal processing algorithms at the transmitter and the receiver. More detailed assumption on each component is shown in [5].

Table 10.2-1 Simulation parameters (DL, FDD)

	CCH duration (L symbols)	Num of MBSFN subframe	Channel estimation	Receiver type	CSI assumption at eNB
Source 1	3	0	Real	MMSE	Short-term
Source 2	2	0	Real (Ideal for JP-CoMP)	MMSE	Short-term
Source 3	3	6	Real	MMSE with IRC	Long-term
Source 4	3	0	Real	MMSE	Short-term
Source 5	3	6	Real	MMSE	Short-term
Source 7	3	0	Ideal	MMSE	No
Source 8	3 (Normal subframe) 2 (MBSFN subframe)	6	Real	MMSE	Short-term
Source 9	3	0	Real	MMSE with IRC	Short-term
Source 10	2	0	Real	MMSE with IRC	Short-term
Source 11	3 (Normal subframe) 2 (MBSFN subframe)	6	Real	MMSE with IRC	Short-term and Long-term
Source 12	3	6	Real	MMSE with IRC	Short-term
Source 13	3	0	Real	MMSE with IRC	Long-term
Source 15	3	6	Real	MMSE with IRC	Long-term
Source 16	2	0	Ideal	MMSE	No
Source 18	2	6	Real	MMSE with IRC	Long-term

Table 10.2-2 Simulation parameters (DL, TDD)

	CCH duration (L symbols)	Num of MBSFN subframe	Channel estimation	Receiver type	CSI assumption at eNB
Source 1	2	0	Real	MMSE	Short-term
Source 2	2	0	Real (Ideal for JP-CoMP)	MMSE	Short-term
Source 3	3	2	Real	MMSE with IRC	Long-term
Source 4	2	0	Real	MMSE	Short-term
Source 7	3	0	Real	MMSE	No
Source 8	3 (Normal subframe) 2 (MBSFN subframe)	2	Real	MMSE	Short-term
Source 9	2	0	Real	MMSE with IRC	Short-term
Source 10	2	0	Real	MMSE with IRC	Short-term
Source 12	3	2	Real	MMSE with IRC	Short-term
Source 13	3	0	Real	MMSE with IRC	Long-term

Table 10.2-3 Simulation parameters (UL, FDD)

	PUCCH bandwidth (RB/10 MHz)	Channel estimation	Receiver type
Source 1	6	Real	MMSE
Source 2	4	Real	MMSE
Source 3	4	Real	MMSE with IRC
Source 4	4	Real	MMSE
Source 5	4	Real	MMSE
Source 7	4	Ideal	MMSE
Source 8	4	Real	MMSE
Source 9	4	Real	MMSE with IRC
Source 10	4	Real	MMSE with IRC
Source 11	4	Real	MMSE with IRC
Source 12	6	Real	MMSE with IRC
Source 14	3 (InH) 4 (Others)	Real	MMSE with IRC and MMSE with SIC for rank 2
Source 18	4	Real	MMSE with IRC

Table 10.2-4 Simulation parameters (UL, TDD)

	PUCCH bandwidth (RB/10 MHz)	Channel estimation	Receiver type
Source 1	4	Real	MMSE
Source 2	4	Real	MMSE
Source 3	4	Real	MMSE with IRC
Source 4	4	Real	MMSE
Source 8	4	Real	MMSE
Source 9	4	Real	MMSE with IRC
Source 10	4	Real	MMSE with IRC
Source 12	3	Real	MMSE with IRC

Tables in the following subsections capture the spectrum efficiency results from individual sources. As performance references, the ITU-R requirements and the averaged results of Rel-8 schemes (4-by-2 SU-MIMO with L=3 for downlink, and 1-by-4 SIMO for uplink) assuming real channel estimation.

10.2.1 Indoor (InH channel model)

10.2.1.1 FDD, Downlink (InH)

Tables 10.2.1.1-1 and 10.2.1.1-2 show the spectrum efficiency results of 4-by-2 MU-MIMO schemes with eNB antenna configuration (C) and (A), respectively. Results show that the MU-MIMO schemes satisfy the ITU-R requirements and provide significant gain compared with the 4-by-2 SU-MIMO scheme in Rel-8.

Table 10.2.1.1-1 Performance of DL MU-MIMO 4 x 2 (C) (InH, FDD)

	Cell spectral efficiency (bit/sec/Hz/cell)	Cell-edge user spectral efficiency (bit/sec/Hz/user)
Source 2	5.68	0.224
Source 8	5.39	0.210
Source 15	5.66	0.232
Rel-8 SU-MIMO (4 x 2, L=3)	4.00	0.200
ITU-R requirement	3.00	0.100

Table 10.2.1.1-2 Performance of DL MU-MIMO 4 x 2 (A) (InH, FDD)

	Cell spectral efficiency (bit/sec/Hz/cell)	Cell-edge user spectral efficiency (bit/sec/Hz/user)
Source 8	5.39	0.211
Rel-8 SU-MIMO (4 x 2, L=3)	4.14	0.198
ITU-R requirement	3.00	0.100

Table 10.2.1.1-3 shows the spectrum efficiency results of 8-by-2 MU-MIMO scheme with the eNB antenna configuration (C/E). Results show that increasing the number of eNB antennas contributes to additional performance enhancement in cell spectral efficiency.

Table 10.2.1.1-3 Performance of DL MU-MIMO 8 x 2 (C/E) (InH, FDD)

	Cell spectral efficiency (bit/sec/Hz/cell)	Cell-edge user spectral efficiency (bit/sec/Hz/user)
Source 8	5.60	0.203
Rel-8 SU-MIMO (4 x 2, L=3)	4.00	0.200
ITU-R requirement	3.00	0.100

10.2.1.2 TDD, Downlink (InH)

Table 10.2.1.2-1 shows the spectrum efficiency results of 4-by-2 MU-MIMO schemes with eNB antenna configuration (C). Results show that the MU-MIMO schemes satisfy the ITU-R requirements and provide significant gain compared with the 4-by-2 SU-MIMO scheme in Rel-8.

Table 10.2.1.2-1 Performance of DL MU-MIMO 4 x 2 (C) (InH, TDD)

	Cell spectral efficiency (bit/sec/Hz/cell)	Cell-edge user spectral efficiency (bit/sec/Hz/user)
Source 2	5.63	0.221
Source 8	5.03	0.186
Source 9	5.80	0.220
Source 10	5.91	0.180
Rel-8 SU-MIMO (4 x 2, L=3)	3.90	0.211
ITU-R requirement	3.00	0.100

Table 10.2.1.2-2 shows the spectrum efficiency results of 8-by-2 MU-MIMO scheme with the eNB antenna configuration (C/E). Results show that increasing the number of eNB antennas enhances cell spectral efficiency.

Table 10.2.1.2-2 Performance of DL MU-MIMO 8 x 2 (C/E) (InH, TDD)

	Cell spectral efficiency (bit/sec/Hz/cell)	Cell-edge user spectral efficiency (bit/sec/Hz/user)
Source 8	5.18	0.198
Rel-8 SU-MIMO (4 x 2, L=3)	3.90	0.211
ITU-R requirement	3.00	0.100

10.2.1.3 FDD, Uplink (InH)

Table 10.2.1.3-1 shows the spectrum efficiency results of 2-by-4 SU-MIMO schemes with eNB antenna configuration (A). Results show that the SU-MIMO schemes satisfy the ITU-R requirements and provide significant gain compared with the 1-by-4 SU-MIMO scheme in Rel-8. Use of advanced receiver such as IRC and SIC provides additional gains.

Table 10.2.1.3-1 Performance of UL SU-MIMO 2 x 4 (A) (InH, FDD)

	Cell spectral efficiency (bit/sec/Hz/cell)	Cell-edge user spectral efficiency (bit/sec/Hz/user)
Source 1	4.01	0.276
Source 3	4.31	0.274
Source 5	3.91	0.265
Source 12	4.39	0.139
Source 14	5.84	0.400
Source 18	4.65	0.273
Rel-8 SIMO (1 x 4)	3.25	0.226
ITU-R requirement	2.25	0.070

Table 10.2.1.3-2 shows the spectrum efficiency results of 1-by-4 CoMP schemes with eNB antenna configuration (A). Results show that multi point reception provides performance enhancement compared with the Rel-8 1-by-4 SIMO scheme.

Table 10.2.1.3-2 Performance of UL CoMP 1 x 4 (A) (InH, FDD)

	Cell spectral efficiency (bit/sec/Hz/cell)	Cell-edge user spectral efficiency (bit/sec/Hz/user)
Source 1	3.42	0.271
Source 18	3.32	0.239
Rel-8 SIMO (1 x 4)	3.25	0.226
ITU-R requirement	2.25	0.070

Table 10.2.1.3-3 shows the spectrum efficiency results of 2-by-4 CoMP schemes with eNB antenna configuration (A). Results show that additional transmit antenna provides further performance enhancement.

Table 10.2.1.3-3 Performance of UL CoMP 2 x 4 (A) (InH, FDD)

	Cell spectral efficiency (bit/sec/Hz/cell)	Cell-edge user spectral efficiency (bit/sec/Hz/user)
Source 1	4.12	0.278
Source 18	4.74	0.274
Rel-8 SIMO (1 x 4)	3.25	0.226
ITU-R requirement	2.25	0.070

10.2.1.4 TDD, Uplink (InH)

Table 10.2.1.4-1 shows the spectrum efficiency results of 2-by-4 SU-MIMO schemes with eNB antenna configuration (A). Results show that the 2-by-4 SU-MIMO schemes satisfy the ITU-R requirements. Performance improvement from the Rel-8 1-by-4 SIMO scheme is also demonstrated. Use of advanced receiver such as IRC and SIC provides additional gains.

Table 10.2.1.4-1 Performance of UL SU-MIMO 2 x 4 (A) (InH, TDD)

	Cell spectral efficiency (bit/sec/Hz/cell)	Cell-edge user spectral efficiency (bit/sec/Hz/user)
Source 1	3.78	0.243
Source 3	3.98	0.260
Source 12	4.43	0.124
Rel-8 SIMO (1 x 4)	3.04	0.206
ITU-R requirement	2.25	0.070

Table 10.2.1.4-2 shows the spectrum efficiency results of 1-by-4 CoMP schemes with eNB antenna configuration (A). Results show that multi point reception provides performance enhancement compared with the Rel-8 1-by-4 SIMO scheme.

Table 10.2.1.4-2 Performance of UL CoMP 1 x 4 (A) (InH, TDD)

	Cell spectral efficiency (bit/sec/Hz/cell)	Cell-edge user spectral efficiency (bit/sec/Hz/user)
Source 1	3.41	0.250
Rel-8 SIMO (1 x 4)	3.04	0.206
ITU-R requirement	2.25	0.070

Table 10.2.1.4-3 shows the spectrum efficiency results of 2-by-4 CoMP schemes with eNB antenna configuration (A). Results show that additional transmit antenna provides further performance enhancement in cell spectral efficiency.

Table 10.2.1.4-3 Performance of UL CoMP 2 x 4 (A) (InH, TDD)

	Cell spectral efficiency (bit/sec/Hz/cell)	Cell-edge user spectral efficiency (bit/sec/Hz/user)
Source 1	3.84	0.240
Rel-8 SIMO (1 x 4)	3.04	0.206
ITU-R requirement	2.25	0.070

10.2.2 Microcellular (UMi channel model)

10.2.2.1 FDD, Downlink (UMi)

Tables 10.2.2.1-1 and 10.2.2.1-2 show the spectrum efficiency results of 4-by-2 MU-MIMO schemes with eNB antenna configuration (C) and (A), respectively. Results show that the MU-MIMO schemes satisfy the ITU-R requirements and provide significant gain compared with the 4-by-2 SU-MIMO scheme in Rel-8 that cannot meet the requirement. Use of MBSFN subframes (overhead reduction), IRC receiver, and short-term feedback tends to improve the cell- and cell-edge spectrum efficiency performances.

Table 10.2.2.1-1 Performance of DL MU-MIMO 4 x 2 (C) (UMi, FDD)

	Cell spectral efficiency (bit/sec/Hz/cell)	Cell-edge user spectral efficiency (bit/sec/Hz/user)
Source 1	2.51	0.079
Source 2	2.86	0.083
Source 4	3.14	0.078
Source 5	2.97	0.076
Source 7	2.18	0.063
Source 8	2.88	0.105
Source 11	3.17	0.084
Source 12	2.95	0.103
Source 15	2.74	0.081
Rel-8 SU-MIMO (4 x 2, L=3)	2.14	0.068
ITU requirement	2.60	0.075

Table 10.2.2.1-2 Performance of DL MU-MIMO 4 x 2 (A) (UMi, FDD)

	Cell spectral efficiency (bit/sec/Hz/cell)	Cell-edge user spectral efficiency (bit/sec/Hz/user)
Source 5	3.15	0.103
Source 8	2.61	0.100
Source 12	2.65	0.093
Rel-8 SU-MIMO (4 x 2, L=3)	1.96	0.061
ITU requirement	2.60	0.075

Table 10.2.2.1-3 shows the spectrum efficiency results of 8-by-2 MU-MIMO schemes with the eNB antenna configuration (C/E). Obviously, increasing the number of eNB antennas contributes to further performance enhancement.

Table 10.2.2.1-3 Performance of DL MU-MIMO 8 x 2 (C/E) (UMi, FDD)

	Cell spectral efficiency (bit/sec/Hz/cell)	Cell-edge user spectral efficiency (bit/sec/Hz/user)
Source 1	3.62	0.138
Source 5	3.72	0.140
Source 8	3.03	0.130
Source 10	3.36	0.089
Rel-8 SU-MIMO (4 x 2, L=3)	2.14	0.068
ITU requirement	2.60	0.075

Tables 10.2.2.1-4 and 10.2.2.1-5 show the spectrum efficiency results of 4-by-2 CS/CB-CoMP schemes with eNB antenna configuration (C) and (A), respectively. Table 10.2.2.1-6 shows the spectrum efficiency results of 8-by-2 CS/CB-CoMP schemes with eNB antenna configuration (C/E). Results show that the CS/CB schemes satisfy the ITU requirements and achieve significant gain compared with the Rel-8 4-by-2 SU-MIMO scheme.

Table 10.2.2.1-4 Performance of DL CS/CB-CoMP 4 x 2 (C) (UMi, FDD)

	Cell spectral efficiency (bit/sec/Hz/cell)	Cell-edge user spectral efficiency (bit/sec/Hz/user)
Source 3	2.84	0.092
Source 11	3.11	0.086
Source 12	2.99	0.114
Source 13	3.21	0.084
Source 18	3.15	0.083
Rel-8 SU-MIMO (4 x 2, L=3)	2.14	0.068
ITU requirement	2.60	0.075

Table 10.2.2.1-5 Performance of DL CS/CB-CoMP 4 x 2 (A) (UMi, FDD)

	Cell spectral efficiency (bit/sec/Hz/cell)	Cell-edge user spectral efficiency (bit/sec/Hz/user)
Source 12	2.71	0.103
Rel-8 SU-MIMO (4 x 2, L=3)	1.96	0.061
ITU requirement	2.60	0.075

Table 10.2.2.1-6 Performance of DL CS/CB-CoMP 8 x 2 (C) (UMi, FDD)

	Cell spectral efficiency (bit/sec/Hz/cell)	Cell-edge user spectral efficiency (bit/sec/Hz/user)
Source 3	3.99	0.105
Source 4	3.05	0.088
Rel-8 SU-MIMO (4 x 2, L=3)	2.14	0.068
ITU requirement	2.60	0.075

Table 10.2.2.1-7 shows the spectrum efficiency results of 4-by-2 JP-CoMP schemes with eNB antenna configuration (C). Results show that the JP-CoMP schemes provide additional performance enhancement over MU-MIMO in Table 10.2.2-1-1 (compared with the same source).

Table 10.2.2.1-7 Performance of DL JP-CoMP 4 x 2 (C) (UMi, FDD)

	Cell spectral efficiency (bit/sec/Hz/cell)	Cell-edge user spectral efficiency (bit/sec/Hz/user)
Source 1	3.45	0.108
Source 2	3.06	0.097
Rel-8 SU-MIMO (4 x 2, L=3)	2.14	0.068
ITU requirement	2.60	0.075

Tables 10.2.2.1-8 and 10.2.2.1-9 show the spectrum efficiency results of 8-by-2 SU-MIMO scheme with eNB antenna configuration (A) and (C), respectively. Results show that use of 8 transmit antenna gives additional degrees of freedom, resulting in enhanced performance.

Table 10.2.2.1-8 Performance of DL SU-MIMO 8 x 2 (A) (UMi, FDD)

	Cell spectral efficiency (bit/sec/Hz/cell)	Cell-edge user spectral efficiency (bit/sec/Hz/user)
Source 16	3.65	0.140
Rel-8 SU-MIMO (4 x 2, L=3)	1.96	0.061
ITU requirement	2.60	0.075

Table 10.2.2.1-9 Performance of DL SU-MIMO 8 x 2 (C) (UMi, FDD)

	Cell spectral efficiency (bit/sec/Hz/cell)	Cell-edge user spectral efficiency (bit/sec/Hz/user)
Source 16	3.74	0.153
Rel-8 SU-MIMO (4 x 2, L=3)	2.14	0.068
ITU requirement	2.60	0.075

10.2.2.2 TDD, Downlink (UMi)

Tables 10.2.2.2-1 and 10.2.2.2-2 show the spectrum efficiency results of 4-by-2 MU-MIMO schemes with eNB antenna configuration (C) and (A), respectively. Results show that the MU-MIMO schemes satisfy the ITU-R requirements and provide significant gain compared with the 4-by-2 SU-MIMO scheme in Rel-8 that cannot meet the requirement. Use of MBSFN subframes (overhead reduction), IRC receiver, and short-term feedback tends to improve the cell- and cell-edge spectrum efficiency performances.

Table 10.2.2.2-1 Performance of DL MU-MIMO 4 x 2 (C) (UMi, FDD)

	Cell spectral efficiency (bit/sec/Hz/cell)	Cell-edge user spectral efficiency (bit/sec/Hz/user)
Source 1	2.85	0.087
Source 2	3.07	0.084
Source 4	3.07	0.076
Source 7	3.33	0.090
Source 8	2.71	0.103
Source 9	3.22	0.095
Source 10	2.94	0.084
Source 12	2.90	0.105
Rel-8 SU-MIMO (4 x 2, L=3)	2.20	0.076
ITU-R requirement	2.60	0.075

Table 10.2.2.2-2 Performance of DL MU-MIMO 4 x 2 (A) (UMi, TDD)

	Cell spectral efficiency (bit/sec/Hz/cell)	Cell-edge user spectral efficiency (bit/sec/Hz/user)
Source 12	2.65	0.092
Rel-8 SU-MIMO (4 x 2, L=3)	1.99	0.067
ITU-R requirement	2.60	0.075

Table 10.2.2.2-3 shows the spectrum efficiency results of 8-by-2 MU-MIMO schemes with the eNB antenna configuration (C/E). Obviously, increasing the number of eNB antennas contributes to further performance enhancement.

Table 10.2.2.2-3 Performance of DL MU-MIMO 8 x 2 (C/E) (UMi, TDD)

	Cell spectral efficiency (bit/sec/Hz/cell)	Cell-edge user spectral efficiency (bit/sec/Hz/user)
Source 1	3.85	0.106
Source 2	3.46	0.089
Source 9	3.33	0.099
Source 10	3.47	0.096
Rel-8 SU-MIMO (4 x 2, L=3)	2.20	0.076
ITU-R requirement	2.60	0.075

Tables 10.2.2.2-4 and 10.2.2.2-5 show the spectrum efficiency results of 4-by-2 CS/CB-CoMP schemes with eNB antenna configuration (C), and 8-by-2 CS/CB-CoMP schemes with eNB antenna configuration (C), respectively. Table 10.2.2.1-6 shows the spectrum efficiency results of 4-by-2 JP-CoMP schemes with eNB antenna configuration (C). Results show that the CoMP schemes satisfy the ITU requirements and achieve significant gain compared with the Rel-8 4-by-2 SU-MIMO scheme.

Table 10.2.2.2-4 Performance of DL CS/CB-CoMP 4 x 2 (C) (UMi, TDD)

	Cell spectral efficiency (bit/sec/Hz/cell)	Cell-edge user spectral efficiency (bit/sec/Hz/user)
Source 2	3.28	0.087
Source 3	2.78	0.089
Source 13	3.20	0.083
Rel-8 SU-MIMO (4 x 2, L=3)	2.20	0.076
ITU-R requirement	2.60	0.075

Table 10.2.2.2-5 Performance of DL CS/CB-CoMP 8 x 2 (C) (UMi, TDD)

	Cell spectral efficiency (bit/sec/Hz/cell)	Cell-edge user spectral efficiency (bit/sec/Hz/user)
Source 2	3.83	0.096
Source 4	3.20	0.096
Rel-8 SU-MIMO (4 x 2, L=3)	2.20	0.076
ITU-R requirement	2.60	0.075

Table 10.2.2.2-6 Performance of DL JP-CoMP 4 x 2 (C) (UMi, TDD)

	Cell spectral efficiency (bit/sec/Hz/cell)	Cell-edge user spectral efficiency (bit/sec/Hz/user)
Source 1	3.76	0.082
Source 2	3.03	0.096
Rel-8 SU-MIMO (4 x 2, L=3)	2.20	0.076
ITU-R requirement	2.20	0.060

10.2.2.3 FDD, Uplink (UMi)

Table 10.2.2.3-1 shows the spectrum efficiency results of 2-by-4 SU-MIMO schemes with eNB antenna configuration (A). Results show that the SU-MIMO schemes satisfy the ITU-R requirements and provide significant gain compared with the 1-by-4 SU-MIMO scheme in Rel-8. Use of advanced receiver such as IRC and SIC provides additional gains.

Table 10.2.2.3-1 Performance of UL SU-MIMO 2 x 4 (A) (UMi, FDD)

	Cell spectral efficiency (bit/sec/Hz/cell)	Cell-edge user spectral efficiency (bit/sec/Hz/user)
Source 1	2.23	0.087
Source 3	2.52	0.112
Source 5	2.24	0.088
Source 11	1.93	0.075
Source 12	1.98	0.051
Source 14	2.45	0.071
Source 18	2.08	0.092
Rel-8 SIMO (1 x 4)	1.93	0.074
ITU-R requirement	1.80	0.050

Tables 10.2.2.3-2 and 10.2.2.3-3 show the spectrum efficiency results of 1-by-4 CoMP schemes with eNB antenna configuration (A) and 2-by-4 CoMP schemes with eNB antenna configuration (A), respectively. Results show that multi point reception provides performance enhancement compared with the Rel-8 1-by-4 SIMO scheme.

Table 10.2.2.3-2 Performance of UL CoMP 1 x 4 (A) (UMi, FDD)

	Cell spectral efficiency (bit/sec/Hz/cell)	Cell-edge user spectral efficiency (bit/sec/Hz/user)
Source 1	2.22	0.093
Source 18	2.03	0.089
Rel-8 SIMO (1 x 4)	1.93	0.074
ITU-R requirement	1.80	0.050

Table 10.2.2.3-3 Performance of UL CoMP 2 x 4 (A) (UMi, FDD)

	Cell spectral efficiency (bit/sec/Hz/cell)	Cell-edge user spectral efficiency (bit/sec/Hz/user)
Source 1	2.45	0.102
Source 18	2.18	0.102
Rel-8 SIMO (1 x 4)	1.93	0.074
ITU-R requirement	1.80	0.050

Table 10.2.2.3-4 shows the spectrum efficiency results of 2-by-4 MU-MIMO schemes with eNB antenna configuration (A). Results show that MU-MIMO provides performance enhancement compared with SU-MIMO shown in Table 10.2.2.3-1 (compared with the same source).

Table 10.2.2.3-4 Performance of UL MU-MIMO 2 x 4 (A) (UMi, FDD)

	Cell spectral efficiency (bit/sec/Hz/cell)	Cell-edge user spectral efficiency (bit/sec/Hz/user)
Source 12	2.51	0.086
Rel-8 SIMO (1 x 4)	1.93	0.074
ITU-R requirement	1.80	0.050

10.2.2.4 TDD, Uplink (UMi)

Table 10.2.2.4-1 shows the spectrum efficiency results of 2-by-4 SU-MIMO schemes with eNB antenna configuration (A). Results show that the SU-MIMO schemes satisfy the ITU-R requirements and provide significant gain compared with the 1-by-4 SU-MIMO scheme in Rel-8.

Table 10.2.2.4-1 Performance of UL SU-MIMO 2 x 4 (A) (UMi, TDD)

	Cell spectral efficiency (bit/sec/Hz/cell)	Cell-edge user spectral efficiency (bit/sec/Hz/user)
Source 1	2.12	0.081
Source 3	2.29	0.100
Source 12	1.90	0.058
Rel-8 SIMO (1 x 4)	1.87	0.072
ITU-R requirement	1.80	0.050

Tables 10.2.2.4-2 and 10.2.2.4-3 show the spectrum efficiency results of 1-by-4 CoMP schemes with eNB antenna configuration (A) and 2-by-4 CoMP schemes with eNB antenna configuration (A), respectively. Results show that multi point reception provides performance enhancement compared with the Rel-8 1-by-4 SIMO scheme.

Table 10.2.2.4-2 Performance of UL CoMP 1 x 4 (A) (UMi, TDD)

	Cell spectral efficiency (bit/sec/Hz/cell)	Cell-edge user spectral efficiency (bit/sec/Hz/user)
Source 1	2.15	0.083
Rel-8 SIMO (1 x 4)	1.87	0.072
ITU-R requirement	1.80	0.050

Table 10.2.2.4-3 Performance of UL CoMP 2 x 4 (A) (UMi, TDD)

	Cell spectral efficiency (bit/sec/Hz/cell)	Cell-edge user spectral efficiency (bit/sec/Hz/user)
Source 1	2.35	0.097
Rel-8 SIMO (1 x 4)	1.87	0.072
ITU-R requirement	1.80	0.050

Table 10.2.2.4-4 shows the spectrum efficiency results of 2-by-4 MU-MIMO schemes with eNB antenna configuration (A). Results show that MU-MIMO provides performance enhancement compared with SU-MIMO shown in Table 10.2.2.4-1 (compared with the same source).

Table 10.2.2.4-4 Performance of UL MU-MIMO 2 x 4 (A) (UMi, TDD)

	Cell spectral efficiency (bit/sec/Hz/cell)	Cell-edge user spectral efficiency (bit/sec/Hz/user)
Source 12	2.79	0.068
Rel-8 SIMO (1 x 4)	1.87	0.072
ITU-R requirement	1.80	0.050

Table 10.2.2.4-5 shows the spectrum efficiency results of 1-by-8 MU-MIMO schemes with eNB antenna configuration (C/E). Results show that additional eNB receive antennas contributes to additional performance enhancement.

Table 10.2.2.4-5 Performance of UL MU-MIMO 1 x 8 (C/E) (UMi, TDD)

	Cell spectral efficiency (bit/sec/Hz/cell)	Cell-edge user spectral efficiency (bit/sec/Hz/user)
Source 2	2.97	0.079
Rel-8 SIMO (1 x 4)	1.82	0.067
ITU-R requirement	1.80	0.050

10.2.3 Base coverage urban (UMa channel model)

10.2.3.1 FDD, Downlink (UMa)

Tables 10.2.3.1-1 and 10.2.3.1-2 show the spectrum efficiency results of 4-by-2 MU-MIMO schemes with eNB antenna configuration (C) and (A), respectively. Results show that the MU-MIMO schemes satisfy the ITU-R requirements and provide significant gain compared with the 4-by-2 SU-MIMO scheme in Rel-8 that cannot meet the requirement. Use of MBSFN subframes (overhead reduction), IRC receiver, and short-term feedback tends to improve the cell- and cell-edge spectrum efficiency performances.

Table 10.2.3.1-1 Performance of DL MU-MIMO 4 x 2 (C) (UMa, FDD)

	Cell spectral efficiency (bit/sec/Hz/cell)	Cell-edge user spectral efficiency (bit/sec/Hz/user)
Source 1	2.14	0.056
Source 5	2.22	0.060
Source 7	2.06	0.060
Source 8	2.48	0.063
Source 11	2.66	0.070
Source 12	2.36	0.076
Source 15	2.22	0.062
Rel-8 SU-MIMO (4 x 2, L=3)	1.61	0.050
ITU-R requirement	2.20	0.060

Table 10.2.3.1-2 Performance of DL MU-MIMO 4 x 2 (A) (UMa, FDD)

	Cell spectral efficiency (bit/sec/Hz/cell)	Cell-edge user spectral efficiency (bit/sec/Hz/user)
Source 1	1.75	0.047
Source 5	2.33	0.064
Rel-8 SU-MIMO (4 x 2, L=3)	1.45	0.043
ITU-R requirement	2.20	0.060

Table 10.2.3.1-3 shows the spectrum efficiency results of 8-by-2 MU-MIMO schemes with the eNB antenna configuration (C/E). Obviously, increasing the number of eNB antennas contributes to further performance enhancement.

Table 10.2.3.1-3 Performance of DL MU-MIMO 8 x 2 (C/E) (UMa, FDD)

	Cell spectral efficiency (bit/sec/Hz/cell)	Cell-edge user spectral efficiency (bit/sec/Hz/user)
Source 1	2.77	0.091
Source 5	2.80	0.104
Source 10	2.55	0.070
Rel-8 SU-MIMO (4 x 2, L=3)	1.61	0.050
ITU-R requirement	2.20	0.060

Tables 10.2.3.1-4 and 10.2.3.1-5 show the spectrum efficiency results of 4-by-2 CS/CB-CoMP schemes with eNB antenna configuration (C) and 8-by-2 CS/CB-CoMP schemes with eNB antenna configuration (C), respectively. Results show that the CS/CB-CoMP schemes satisfy the ITU requirements and achieve significant gain compared with the Rel-8 4-by-2 SU-MIMO scheme.

Table 10.2.3.1-4 Performance of DL CS/CB-CoMP 4 x 2 (C) (UMa, FDD)

	Cell spectral efficiency (bit/sec/Hz/cell)	Cell-edge user spectral efficiency (bit/sec/Hz/user)
Source 2	2.68	0.067
Source 3	2.38	0.073
Source 11	2.44	0.067
Source 12	2.33	0.083
Source 13	2.30	0.063
Source 18	2.45	0.060
Rel-8 SU-MIMO (4 x 2, L=3)	1.61	0.050
ITU-R requirement	2.20	0.060

Table 10.2.3.1-5 Performance of DL CS/CB-CoMP 8 x 2 (C) (UMa, FDD)

	Cell spectral efficiency (bit/sec/Hz/cell)	Cell-edge user spectral efficiency (bit/sec/Hz/user)
Source 3	3.34	0.088
Source 4	2.70	0.085
Source 13	3.22	0.073
Rel-8 SU-MIMO (4 x 2, L=3)	1.61	0.050
ITU-R requirement	2.20	0.060

Tables 10.2.3.1-6 and 10.2.3.1-7 show the spectrum efficiency results of 4-by-2 JP-CoMP schemes with eNB antenna configuration (C) and (A), respectively. Tables show that the JP CoMP schemes provide additional performance enhancement over MU-MIMO in Table 10.2.3.1-1 (compared with the same source).

Table 10.2.3.1-6 Performance of DL JP-CoMP 4 x 2 (C) (UMa, FDD)

	Cell spectral efficiency (bit/sec/Hz/cell)	Cell-edge user spectral efficiency (bit/sec/Hz/user)
Source 1	2.41	0.064
Source 2	2.32	0.069
Rel-8 SU-MIMO (4 x 2, L=3)	1.61	0.050
ITU-R requirement	2.20	0.060

Table10.2.3.1-7 Performance of DL JP-CoMP 4 x 2 (A) (UMa, FDD)

	Cell spectral efficiency (bit/sec/Hz/cell)	Cell-edge user spectral efficiency (bit/sec/Hz/user)
Source 5	2.41	0.065
Rel-8 SU-MIMO (4 x 2, L=3)	1.45	0.043
ITU-R requirement	2.20	0.060

Tables 10.2.3.1-8 and 10.2.3.1-9 show the spectrum efficiency results of 8-by-2 SU-MIMO schemes with eNB antenna configuration (A) and (C), respectively. Results show that the use of 8 antenna elements gives additional degrees of freedom, which leads to improved performance.

Table 10.2.3.1-8 Performance of DL SU-MIMO 8 x 2 (A) (UMa, FDD)

	Cell spectral efficiency (bit/sec/Hz/cell)	Cell-edge user spectral efficiency (bit/sec/Hz/user)
Source 16	3.53	0.150
Rel-8 SU-MIMO (4 x 2, L=3)	1.45	0.043
ITU-R requirement	2.20	0.060

Table 10.2.3.1-9 Performance of DL SU-MIMO 8 x 2 (C) (UMa, FDD)

	Cell spectral efficiency (bit/sec/Hz/cell)	Cell-edge user spectral efficiency (bit/sec/Hz/user)
Source 16	3.54	0.149
Rel-8 SU-MIMO (4 x 2, L=3)	1.61	0.050
ITU-R requirement	2.20	0.060

10.2.3.2 TDD, Downlink (UMa)

Tables 10.2.3.2-1 and 10.2.3.2-2 show the spectrum efficiency results of 4-by-2 MU-MIMO schemes with eNB antenna configuration (C) and (A), respectively. Results show that the MU-MIMO schemes satisfy the ITU-R requirements and provide significant gain compared with the 4-by-2 SU-MIMO scheme in Rel-8 that cannot meet the requirements. Use of MBSFN subframes (overhead reduction), IRC receiver, and short-term feedback tends to improve the cell- and cell-edge spectrum efficiency performances.

Table 10.2.3.2-1 Performance of DL MU-MIMO 4 x 2 (C) (UMa, TDD)

	Cell spectral efficiency (bit/sec/Hz/cell)	Cell-edge user spectral efficiency (bit/sec/Hz/user)
Source 1	2.34	0.062
Source 2	2.63	0.069
Source 7	2.27	0.062
Source 8	2.43	0.062
Source 9	2.62	0.080
Source 10	2.49	0.069
Source 12	2.32	0.071
Rel-8 SU-MIMO (4 x 2, L=3)	1.34	0.040
ITU-R requirement	2.20	0.060

Table 10.2.3.2-2 Performance of DL MU-MIMO 4 x 2 (A) (UMa, TDD)

	Cell spectral efficiency (bit/sec/Hz/cell)	Cell-edge user spectral efficiency (bit/sec/Hz/user)
Source 1	1.85	0.056
Rel-8 SU-MIMO (4 x 2, L=3)	1.36	0.036
ITU-R requirement	2.20	0.060

Table 10.2.3.2-3 shows the spectrum efficiency results of 8-by-2 MU-MIMO schemes with the eNB antenna configuration (C/E). Obviously, increasing the number of eNB antennas contributes to further performance enhancement.

Table 10.2.3.2-3 Performance of DL MU-MIMO 8 x 2 (C/E) (UMa, TDD)

	Cell spectral efficiency (bit/sec/Hz/cell)	Cell-edge user spectral efficiency (bit/sec/Hz/user)
Source 1	3.42	0.102
Source 2	3.14	0.077
Source 9	2.92	0.075
Source 10	2.89	0.077
Rel-8 SU-MIMO (4 x 2, L=3)	1.34	0.040
ITU-R requirement	2.20	0.060

Tables 10.2.3.2-4 and 10.2.3.2-5 show the spectrum efficiency results of 4-by-2 CS/CB-CoMP schemes with eNB antenna configuration (C) and 8-by-2 CS/CB-CoMP schemes with eNB antenna configuration (C), respectively. Results show that the CS/CB-CoMP schemes satisfy the ITU requirements and achieve significant gain compared with the Rel-8 4-by-2 SU-MIMO scheme.

Table 10.2.3.2-4 Performance of DL CS/CB-CoMP 4 x 2 (C) (UMa, TDD)

	Cell spectral efficiency (bit/sec/Hz/cell)	Cell-edge user spectral efficiency (bit/sec/Hz/user)
Source 2	2.74	0.075
Source 3	2.34	0.072
Source 12	2.21	0.069
Source 13	2.34	0.065
Rel-8 SU-MIMO (4 x 2, L=3)	1.34	0.040
ITU-R requirement	2.20	0.060

Table 10.2.3.2-5 Performance of DL CS/CB-CoMP 8 x 2 (C) (UMa, TDD)

	Cell spectral efficiency (bit/sec/Hz/cell)	Cell-edge user spectral efficiency (bit/sec/Hz/user)
Source 2	3.30	0.093
Source 4	2.77	0.092
Source 13	3.24	0.076
Rel-8 SU-MIMO (4 x 2, L=3)	1.34	0.040
ITU-R requirement	2.20	0.060

Table 10.2.3.2-6 shows the spectrum efficiency results of 4-by-2 JP-CoMP schemes with eNB antenna configuration (C). Results show that the JP-CoMP schemes satisfy the ITU requirements and achieve significant gain compared with the Rel-8 4-by-2 SU-MIMO scheme.

Table 10.2.3.2-6 Performance of DL JP-CoMP 4 x 2 (C) (UMa, TDD)

	Cell spectral efficiency (bit/sec/Hz/cell)	Cell-edge user spectral efficiency (bit/sec/Hz/user)
Source 1	2.95	0.073
Source 2	2.23	0.068
Rel-8 SU-MIMO (4 x 2, L=3)	1.34	0.040
ITU-R requirement	2.20	0.060

10.2.3.3 FDD, Uplink (UMa)

Table 10.2.3.3-1 shows the spectrum efficiency results of 2-by-4 SU-MIMO schemes with eNB antenna configuration (A). Results show that the 2-by-4 SU-MIMO schemes satisfy the ITU-R requirements and provide significant gain compared with the 1-by-4 SU-MIMO scheme in Rel-8.

Table 10.2.3.3-1 Performance of UL SU-MIMO 2 x 4 (A) (UMa, FDD)

	Cell spectral efficiency (bit/sec/Hz/cell)	Cell-edge user spectral efficiency (bit/sec/Hz/user)
Source 1	1.77	0.086
Source 3	1.93	0.087
Source 5	1.75	0.082
Source 12	1.62	0.046
Source 14	2.03	0.072
Source 18	1.62	0.072
Rel-8 SIMO (1 x 4)	1.55	0.067
ITU-R requirement	1.40	0.030

Tables 10.2.3.3-2 and 10.2.3.3-3 show the spectrum efficiency results of 1-by-4 CoMP schemes with eNB antenna configuration (A) and (C), respectively. Results show that the performance of CoMP schemes exceeds the ITU requirements.

Table10.2.3.3-2 Performance of UL CoMP 1 x 4 (A) (UMa, FDD)

	Cell spectral efficiency (bit/sec/Hz/cell)	Cell-edge user spectral efficiency (bit/sec/Hz/user)
Source 1	1.95	0.096
Source 18	1.51	0.075
Rel-8 SIMO (1 x 4)	1.55	0.067
ITU-R requirement	1.40	0.030

Table10.2.3.3-3 Performance of UL CoMP 1 x 4 (C) (UMa, FDD)

	Cell spectral efficiency (bit/sec/Hz/cell)	Cell-edge user spectral efficiency (bit/sec/Hz/user)
Source 1	1.89	0.095
Rel-8 SIMO (1 x 4)	1.50	0.060
ITU-R requirement	1.40	0.030

Tables 10.2.3.3-4 and 10.2.3.3-5 show the spectrum efficiency results of 2-by-4 CoMP schemes with eNB antenna configuration (A) and (C), respectively. Results show that additional transmit antenna provides further performance enhancement.

Table10.2.3.3-4 Performance of UL CoMP 2 x 4 (A) (UMa, FDD)

	Cell spectral efficiency (bit/sec/Hz/cell)	Cell-edge user spectral efficiency (bit/sec/Hz/user)
Source 1	2.11	0.102
Source 18	1.74	0.081
Rel-8 SIMO (1 x 4)	1.55	0.067
ITU-R requirement	1.40	0.030

Table 10.2.3.3-5 Performance of UL CoMP 2 x 4 (C) (UMa, FDD)

	Cell spectral efficiency (bit/sec/Hz/cell)	Cell-edge user spectral efficiency (bit/sec/Hz/user)
Source 1	2.05	0.099
Rel-8 SIMO (1 x 4)	1.50	0.060
ITU-R requirement	1.40	0.030

Table 10.2.3.3-6 shows the spectrum efficiency results of 2-by-4 MU-MIMO schemes with eNB antenna configuration (A). Results show that MU-MIMO provides performance enhancement compared with SU-MIMO shown in Table 10.2.3.3-1 (compared with the same source).

Table 10.2.3.3-6 Performance of UL MU-MIMO 2 x 4 (A) (UMa, FDD)

	Cell spectral efficiency (bit/sec/Hz/cell)	Cell-edge user spectral efficiency (bit/sec/Hz/user)
Source 12	1.91	0.069
Rel-8 SIMO (1 x 4)	1.55	0.067
ITU-R requirement	1.40	0.030

10.2.3.4 TDD, Uplink (UMa)

Table 10.2.3.4-1 shows the spectrum efficiency results of 2-by-4 SU-MIMO schemes with eNB antenna configuration (A). Results show that the 2-by-4 SU-MIMO schemes satisfy the ITU-R requirements and provide significant gain compared with the 1-by-4 SU-MIMO scheme in Rel-8.

Table 10.2.3.4-1 Performance of UL SU-MIMO 2 x 4 (A) (UMa, TDD)

	Cell spectral efficiency (bit/sec/Hz/cell)	Cell-edge user spectral efficiency (bit/sec/Hz/user)
Source 1	1.73	0.083
Source 3	1.76	0.076
Source 12	1.54	0.059
Rel-8 SIMO (1 x 4)	1.51	0.062
ITU-R requirement	1.40	0.030

Tables 10.2.3.4-2 and 10.2.3.4-3 show the spectrum efficiency results of 1-by-4 CoMP schemes with eNB antenna configuration (A) and (C), respectively. Results show that multi point reception provides performance enhancement compared with the Rel-8 1-by-4 SIMO scheme.

Table10.2.3.4-2 Performance of UL CoMP 1 x 4 (A) (UMa, TDD)

	Cell spectral efficiency (bit/sec/Hz/cell)	Cell-edge user spectral efficiency (bit/sec/Hz/user)
Source 1	1.89	0.093
Rel-8 SIMO (1 x 4)	1.51	0.062
ITU-R requirement	1.40	0.030

Table10.2.3.4-3 Performance of UL CoMP 1 x 4 (C) (UMa, TDD)

	Cell spectral efficiency (bit/sec/Hz/cell)	Cell-edge user spectral efficiency (bit/sec/Hz/user)
Source 1	1.86	0.090
Rel-8 SIMO (1 x 4)	1.45	0.059
ITU-R requirement	1.40	0.030

Tables 10.2.3.4-4 and 10.2.3.4-5 show the spectrum efficiency results of 2-by-4 CoMP schemes with eNB antenna configuration (A) and (C), respectively. Results show that additional transmit antenna provides further performance enhancement.

Table10.2.3.4-4 Performance of UL CoMP 2 x 4 (A) (UMa, TDD)

	Cell spectral efficiency (bit/sec/Hz/cell)	Cell-edge user spectral efficiency (bit/sec/Hz/user)
Source 1	2.06	0.100
Rel-8 SIMO (1 x 4)	1.51	0.062
ITU-R requirement	1.40	0.030

Table 10.2.3.4-5 Performance of UL CoMP 2 x 4 (C) (UMa, TDD)

	Cell spectral efficiency (bit/sec/Hz/cell)	Cell-edge user spectral efficiency (bit/sec/Hz/user)
Source 1	2.00	0.097
Rel-8 SIMO (1 x 4)	1.45	0.059
ITU-R requirement	1.40	0.030

Table 10.2.3.4-6 shows the spectrum efficiency results of 1-by-8 MU-MIMO schemes with eNB antenna configuration (C/E). Results show that additional eNB receive antennas contributes to further performance enhancement.

Table 10.2.3.4-6 Performance of UL MU-MIMO 1 x 8 (C/E) (UMa, TDD)

	Cell spectral efficiency (bit/sec/Hz/cell)	Cell-edge user spectral efficiency (bit/sec/Hz/user)
Source 2	2.74	0.076
Rel-8 SIMO (1 x 4)	1.45	0.059
ITU-R requirement	1.40	0.030

10.2.4 High speed (RMa channel model)

10.2.4.1 FDD, Downlink (RMa)

Tables 10.2.4.1-1 and 10.2.4.1-2 show the spectrum efficiency results of 4-by-2 MU-MIMO schemes with eNB antenna configuration (C), and 8-by-2 MU-MIMO schemes with the eNB antenna configuration (C/E), respectively. Results show that the MU-MIMO schemes satisfy the ITU-R requirements and provide significant gain compared with the 4-by-2 SU-MIMO scheme in Rel-8.

Table 10.2.4.1-1 Performance of DL MU-MIMO 4 x 2 (C) (UMa, FDD)

	Cell spectral efficiency (bit/sec/Hz/cell)	Cell-edge user spectral efficiency (bit/sec/Hz/user)
Source 3	3.47	0.112
Source 8	2.94	0.077
Source 15	3.26	0.083
Rel-8 SU-MIMO (4 x 2, L=3)	1.91	0.069
ITU requirement	1.10	0.040

Table 10.2.4.1-2 Performance of DL MU-MIMO 8 x 2 (C/E) (UMa, FDD)

	Cell spectral efficiency (bit/sec/Hz/cell)	Cell-edge user spectral efficiency (bit/sec/Hz/user)
Source 10	3.45	0.110
Rel-8 SU-MIMO (4 x 2, L=3)	1.91	0.069
ITU requirement	1.10	0.040

10.2.4.2 TDD, Downlink (RMa)

Tables 10.2.4.2-1 and 10.2.4.2-2 show the spectrum efficiency results of 4-by-2 MU-MIMO schemes with eNB antenna configuration (C), and 8-by-2 MU-MIMO schemes with the eNB antenna configuration (C/E), respectively. Results show that the MU-MIMO schemes satisfy the ITU-R requirements and provide significant gain compared with the 4-by-2 SU-MIMO scheme in Rel-8.

Table 10.2.4.2-1 Performance of DL MU-MIMO 4 x 2 (C) (RMa, TDD)

	Cell spectral efficiency (bit/sec/Hz/cell)	Cell-edge user spectral efficiency (bit/sec/Hz/user)
Source 2	2.79	0.081
Source 8	2.87	0.075
Source 9	3.34	0.087
Source 10	2.86	0.086
Rel-8 SU-MIMO (4 x 2, L=3)	1.60	0.053
ITU requirement	1.10	0.040

Table 10.2.4.2-2 Performance of DL MU-MIMO 8 x 2 (C/E) (RMa, TDD)

	Cell spectral efficiency (bit/sec/Hz/cell)	Cell-edge user spectral efficiency (bit/sec/Hz/user)
Source 2	3.36	0.092
Source 10	3.33	0.106
Rel-8 SU-MIMO (4 x 2, L=3)	1.60	0.053
ITU requirement	1.10	0.040

Table 10.2.4.2-3 shows the spectrum efficiency results of 4-by-2 CS/CB-CoMP schemes with eNB antenna configuration (C). Results show that the CS/CB-CoMP scheme satisfies the ITU-R requirements and provides significant gain compared with the 4-by-2 SU-MIMO scheme in Rel-8.

Table 10.2.4.2-3 Performance of DL CS/CB-CoMP 4 x 2 (C) (RMa, TDD)

	Cell spectral efficiency (bit/sec/Hz/cell)	Cell-edge user spectral efficiency (bit/sec/Hz/user)
Source 3	3.42	0.109
Rel-8 SU-MIMO (4 x 2, L=3)	1.60	0.053
ITU requirement	1.10	0.040

10.2.4.3 FDD, Uplink (RMa)

Table 10.2.4.3-1 shows the spectrum efficiency results of 2-by-4 SU-MIMO schemes with eNB antenna configuration (A). Results show that the 2-by-4 SU-MIMO schemes satisfy the ITU-R requirements and provide significant gain compared with the 1-by-4 SU-MIMO scheme in Rel-8.

Table 10.2.4.3-1 Performance of UL SU-MIMO 2 x 4 (A) (RMa, FDD)

	Cell spectral efficiency (bit/sec/Hz/cell)	Cell-edge user spectral efficiency (bit/sec/Hz/user)
Source 1	2.32	0.129
Source 3	2.45	0.129
Source 5	2.27	0.126
Source 12	1.90	0.062
Source 14	2.46	0.129
Source 18	1.90	0.086
Rel-8 SIMO (1 x 4)	1.80	0.089
ITU requirement	0.70	0.015

Tables 10.2.4.3-2 and 10.2.4.3-3 show the spectrum efficiency results of 1-by-4 CoMP schemes with eNB antenna configuration (A) and 2-by-4 CoMP schemes with eNB antenna configuration (A), respectively. Results show that the performance of the CoMP schemes far exceed the ITU requirements.

Table 10.2.4.3-2 Performance of UL CoMP 1 x 4 (A) (RMa, FDD)

	Cell spectral efficiency (bit/sec/Hz/cell)	Cell-edge user spectral efficiency (bit/sec/Hz/user)
Source 1	2.31	0.129
Source 18	1.75	0.086
Rel-8 SIMO (1 x 4)	1.80	0.089
ITU requirement	0.70	0.015

Table 10.2.4.3-3 Performance of UL CoMP 2 x 4 (A) (RMa, FDD)

	Cell spectral efficiency (bit/sec/Hz/cell)	Cell-edge user spectral efficiency (bit/sec/Hz/user)
Source 1	2.58	0.154
Source 18	2.02	0.098
Rel-8 SIMO (1 x 4)	1.80	0.089
ITU requirement	0.70	0.015

10.2.4.4 TDD, Uplink (RMa)

Table 10.2.4.4-1 shows the spectrum efficiency results of 2-by-4 SU-MIMO schemes with eNB antenna configuration (A). Results show that the 2-by-4 SU-MIMO schemes satisfy the ITU-R requirements and provide significant gain compared with the 1-by-4 SU-MIMO scheme in Rel-8.

Table 10.2.4.4-1 Performance of UL SU-MIMO 2 x 4 (A) (RMa, TDD)

	Cell spectral efficiency (bit/sec/Hz/cell)	Cell-edge user spectral efficiency (bit/sec/Hz/user)
Source 1	2.25	0.127
Source 3	2.27	0.118
Rel-8 SIMO (1 x 4)	1.75	0.086
ITU requirement	0.70	0.015

Tables 10.2.4.4-2 and 10.2.4.4-3 show the spectrum efficiency results of 1-by-4 CoMP schemes with eNB antenna configuration (A) and 2-by-4 CoMP schemes with eNB antenna configuration (A), respectively. Results show that multi point reception provides performance enhancement compared with the Rel-8 1-by-4 SIMO scheme.

Table 10.2.4.4-2 Performance of UL CoMP 1 x 4 (A) (RMa, TDD)

	Cell spectral efficiency (bit/sec/Hz/cell)	Cell-edge user spectral efficiency (bit/sec/Hz/user)
Source 1	2.23	0.125
Rel-8 SIMO (1 x 4)	1.75	0.086
ITU requirement	0.70	0.015

Table 10.2.4.4-3 Performance of UL CoMP 2 x 4 (A) (RMa, TDD)

	Cell spectral efficiency (bit/sec/Hz/cell)	Cell-edge user spectral efficiency (bit/sec/Hz/user)
Source 1	2.52	0.153
Rel-8 SIMO (1 x 4)	1.75	0.086
ITU requirement	0.70	0.015

Table 10.2.4.4-4 shows the spectrum efficiency results of 1-by-8 MU-MIMO schemes with eNB antenna configuration (C/E). Results show that additional eNB receive antennas contributes to the further performance enhancement.

Table 10.2.4.4-4 Performance of UL MU-MIMO 1 x 8 (C/E) (RMa, TDD)

	Cell spectral efficiency (bit/sec/Hz/cell)	Cell-edge user spectral efficiency (bit/sec/Hz/user)
Source 2	2.64	0.101
Rel-8 SIMO (1 x 4)	1.73	0.077
ITU requirement	0.70	0.015

Annex A: Simulation model

A.1 Link simulation Scenarios

Link simulation analyses with (8x8) DL MIMO configuration can be conducted in relation to studies concerning the peak data rate requirements set forth in [36.913].

A.2 System simulation Scenarios

A.2.1 System simulation assumptions

A.2.1.1 Reference system deployments

This section describes the reference system deployments to use for the different system evaluations.

A.2.1.1.1 Homogeneous deployments

The minimum set of simulation cases is given in Table A.2.1.1-1 along with additional assumptions related to carrier frequency (CF), Inter-site distance (ISD), operating bandwidth (BW), penetration loss (PLoss) and UE speed.

For 3GPP cases only, the system simulation baseline parameters for the macro-cell deployment model are as specified in [TR 25.814], with the modifications given in Table A.2.1.1-2.

For the ITU cases, simulation parameters should be aligned with the ITU guidelines in [IMT Eval], some of which are reflected in Table A.2.1.1-1. Note that [IMT.EVAL] section-8 defines different antenna horizontal and vertical pattern from those defined in Table A.2.1.1-2 which is for 3GPP case evaluation only.

Table A.2.1.1-1 – E-UTRA simulation case minimum set

Simulation Cases	CF (GHz)	ISD (meters)	BW (MHz)	PLoss (dB)	Speed (km/h)	Additional Simulation Parameters
3GPP case 1	2.0	500	FDD:10+10 TDD: 20	20	3	Table A.2.1.1-2 and 25.814
3GPP case 1 extended	2.0	500	FDD:80+40* TDD: 80*	20	3	Table A.2.1.1-2 and 25.814
3GPP case 3	2.0	1732	FDD:10+10 TDD: 20	20	3	Table A.2.1.1-2 and 25.814
ITU Indoor, Indoor hotspot scenario	3.4	60	FDD:20+20 TDD: 40*	N.A.	3	[IMT Eval] Section 8
ITU Indoor extended, Indoor hotspot scenario	3.4	60	FDD:80+40* TDD: 80*	N.A.	3	[IMT Eval] Section 8
ITU Microcellular, Urban micro-cell scenario	2.5	200	FDD:10+10 TDD: 20	See [IMT Eval] Annex.1	3	[IMT Eval] Section 8
ITU Base coverage urban, Urban macro-cell scenario	2.0	500	FDD:10+10 TDD: 20	See [IMT Eval] Annex.1	30	[IMT Eval] Section 8
ITU Base coverage urban extended, Urban macro-cell scenario	2.0	500	FDD:80+40* TDD: 80*	See [IMT Eval] Annex.1	30	[IMT Eval] Section 8
ITU High speed, Rural macro-cell scenario	0.8	1732	FDD:10+10 TDD: 20	See [IMT Eval] Annex.1	120	[IMT Eval] Section 8

(*) Pending availability of applicable channel model.

**Table A.2.1.1-2 – 3GPP Case 1 and 3 (Macro-cell)
system simulation baseline parameters modifications as compared to TR 25.814**

Parameter	Assumption
Antenna pattern (horizontal) (For 3-sector cell sites with fixed antenna patterns)	$A_H(\varphi) = -\min\left[12\left(\frac{\varphi}{\varphi_{3dB}}\right)^2, A_m\right]$ φ_{3dB} = 70 degrees, A_m = 25 dB
Antenna pattern (vertical) (For 3-sector cell sites with fixed antenna patterns)	$A_V(\theta) = -\min\left[12\left(\frac{\theta-\theta_{etilt}}{\theta_{3dB}}\right)^2, SLA_v\right]$ θ_{3dB} = 10, SLA_V = 20 dB The parameter θ_{etilt} is the electrical antenna downtilt. The value for this parameter, as well as for a potential additional mechanical tilt, is not specified here, but may be set to fit other RRM techniques used. For calibration purposes, the values θ_{etilt} = 15 degrees for 3GPP case 1 and θ_{etilt} = 6 degrees for 3GPP case 3 may be used. Antenna height at the base station is set to 32m. Antenna height at the UE is set to 1.5m.
Combining method in 3D antenna pattern	$A(\varphi,\theta) = -\min\{-[A_H(\varphi)+A_V(\theta)], A_m\}$
Channel model	3GPP Spatial Channel Model (SCM) [TR 25.996] For single transmit antenna evaluations, the Typical Urban (TU) channel model may be used
Total BS TX power (Ptotal)	43dBm – 1.25, 5MHz carrier, 46/49dBm – 10, 20MHz carrier Some evaluations to exploit carrier aggregation techniques may use wider bandwidths e.g. 60 or 80 MHz (FDD). For these evaluations [49 dBm] Total BS Tx power should be used.
UE power class	23dBm (200mW) This corresponds to the sum of PA powers in multiple Tx antenna case
In addition to the antenna bore-sight orientation in TR25.814 (center direction points to the flat side), an optional orientation as shown can be used if needed in Coordinated Multipoint study (i.e., point to corners) for 3GPP internal evaluations	

A.2.1.1.2 Heterogeneous deployments

Heterogeneous deployments consist of deployments where low power nodes are placed throughout a macro-cell layout. A subset of the macro-cell layouts described in section A.2.1.1.1 could be used for heterogeneous network deployments evaluation. For calibration purpose, the following cases should be used

- Case 1
- Case 3- Rural/high speed

To assess the benefit of adding low-power nodes to become a heterogeneous network, performance comparison should be made to homogeneous macro-cell only deployment.

The categorization of the low power nodes is as described in Table A.2.1.1.2-1.

Table A.2.1.1.2-1. Categorization of new nodes

	Backhaul	Access	Notes

Remote radio head (RRH)	Several µs latency to macro	Open to all UEs	Placed indoors or outdoors
Pico eNB (i.e. node for Hotzone cells)	X2	Open to all UEs	Placed indoors or outdoors. Typically planned deployment.
HeNB (i.e. node for Femto cells)	No X2 as baseline (*)	Closed Subscriber Group (CSG)	Placed indoors. Consumer deployed.
Relay nodes	Through air-interface with a macro-cell (for in-band RN case)	Open to all UEs	Placed indoors or outdoors

Note: The reference to new nodes in this TR and its corresponding characteristics are applicable to evaluations in this TR only.

(*): Baseline is in accordance to Rel-8/9 assumption. Evaluations with interference management for HeNBs (via X2 or other means) allowed to assess interference management benefits

Table A.2.1.1.2-2 presents the baseline deployment scenario for Heterogeneous network.

Table A.2.1.1.2-2. Heterogeneous network deployment scenario

Case	Environment	Deployment Scenario	Non-traditional node
5.1	Macro + Indoor	Macro + femtocell	femtocell
5.2		Macro + indoor relay	Indoor relay
5.3		Macro + indoor RRH/Hotzone	e.g. indoor pico
6.1	Macro + Outdoor	Macro + outdoor relay	Outdoor relay
6.2		Macro + outdoor RRH/Hotzone	e.g., outdoor pico

Note 1: Priorities are as follows:

1. Indoor HeNB clusters
2. Outdoor Hotzone cells with configuration #1 and #4 (in Table A.2.1.1.2-4)
3. Indoor Hotzone scenario (RAN4 femto or pico models could be used)
4. Other scenarios can be studied with lower priority

Note 2: Relay deployment scenario (5.2, 6.1) are studied separately.

Table A.2.1.1.2-3 presents the baseline parameters for initial evaluations in heterogeneous networks. More detailed modelling of new nodes propagation and channel model based on IMT.EVAL should be considered for performance evaluation at a later stage.

Table A.2.1.1.2-3. Heterogeneous system simulation baseline parameters

Parameter	Assumption		
	RRH / Hotzone	**Femto**	**Relay**
Nodes per macro-cell	RRH/Hotzone, and outdoor relay: 1, 2, 4 or 10 (nodes) Femto and indoor relay: 1 (cluster) Note: The number of HeNB and indoor relay nodes in each cluster is FFS.		
Distance-dependent path loss from new nodes to UE*1	For outdoor RRH/Hotzone Model 1: Macro to UE: *L= 128.1+37.6log10(R)* Pico to UE: $L=140.7+36.7\log_{10}R$ for 2GHz, *R* in km *Model 2:* *Macro to UE:* *PL_{LOS}(R)= 103.4+24.2log10(R)* *PL_{NLOS}(R)= 131.1+42.8log10(R)* For 2GHz, *R* in km. Penetration loss 20dB Case 1: *Prob(R)=min(0.018/R,1)*(1-exp(-R/0.063))+exp(-R/0.063)* Case 3 (Suburban): *Prob(R)=exp(-(R-0.01)/0.2)* Case 3 *(Rural/ Suburban)*: *Prob(R)=exp(-(R-0.01)/1.0)* *Pico to UE:* *PL_{LOS}(R)=103.8+20.9log10(R)* *PL_{NLOS}(R)=145.4+37.5log10(R)* For 2GHz, R in km Case 1: *Prob(R)=0.5-min(0.5,5exp(-0.156/R))+min(0.5, 5exp(-R/0.03))* Case 3: *Prob(R)=0.5-min(0.5,3exp(-0.3/R))+min(0.5, 3exp(-R/0.095))* For indoor RRH/Hotzone, see Table 2.1.1.5-1/2	Model 1: 5x5 Grid Femto to UEs inside the same cluster $L=127+30\log_{10}R$ Other links L= 128.1+37.6log10(R) for 2GHz, *R* in km, the number of floors in the path is assumed to be 0. Model 1: Dual strip Model *See Table A.2.1.1.2-7 and A.2.1.1.2-8* Model 2 *See Table A.2.1.1.2-7 and A.2.1.1.2-8*	Macro to UE: *PL_{LOS}(R)= 103.4+24.2log10(R)* *PL_{NLOS}(R)= 131.1+42.8log10(R)* For 2GHz, *R* in km. Case 1: *Prob(R)=min(0.018/R,1)*(1-exp(-R/0.063))+exp(-R/0.063)* Case 3 (Suburban): *Prob(R)=exp(-(R-0.01)/0.2)* Case 3 *(Rural/ Suburban)*: *Prob(R)=exp(-(R-0.01)/1.0)* Macro to relay: Relay with outdoor donor antenna: *PL_{LOS}(R)=100.7+23.5log10(R)* *PL_{NLOS}(R)= 125.2+36.3log10(R)* For 2GHz, R in km. *Prob(R)* based on ITU models: Case 1: *Prob(R)=min(0.018/R,1)*(1-exp(-R/0.072))+exp(-R/0.072)* Case 3 (Suburban): *Prob(R)=exp(-(R-0.01)/0.23)* Case 3 (Rural/ Suburban) *Prob(R)=exp(-(R-0.01)/1.15)* Note 1: Bonus for donor macro (from each of its sectors) to relay for optimized deployment by site planning optimization methodology described in [A.2.1.1.4]. Note 2: Higher probability of LOS shall be reflected in consideration of the height of RN antenna and site planning optimization. described in [A.2.1.1.4]. Note3: If link from donor Macro to optimized relay site is LOS, the links from other macros to optimized relay site could be LOS or NLOS, else all interference links from other macros are NLOS. Relay with indoor donor antenna: *PL_{LOS}(R)= 103.4+24.2log10(R)* *PL_{NLOS}(R)= 131.1+42.8log10(R)* For 2GHz, *R* in km Case 1:

			Prob(R)=min(0.018/R,1)(1-exp(-R/0.063))+exp(-R/0.063)* Case 3: *Prob(R)=exp(-(R-0.01)/1.0)* Note 4: Higher probability of LOS shall be reflected in consideration of the height of RN antenna
			Relay to UE: Relay with outdoor coverage antenna: $PL_{LOS}(R)=103.8+20.9\log10(R)$ $PL_{NLOS}(R)=145.4+37.5\log10(R)$ For 2GHz, R in km Case 1: *Prob(R)=0.5-min(0.5,5exp(-0.156/R))+min(0.5, 5exp(-R/0.03))* Case 3: *Prob(R)=0.5-min(0.5,3exp(-0.3/R))+min(0.5, 3exp(-R/0.095))* Note 1: this path loss model assumes in-band relay. Simulations for out-of-band relay should re-examine this assumption. Relay with indoor coverage antenna: Model 1: 5x5 Grid Relay to UEs inside the same cluster $L=127+30\log_{10}R$ Relay to UEs in different clusters $L= 128.1+37.6\log_{10}(R)$ for 2GHz, *R* in km, the number of floors in the path is assumed to be 0. Model 1: Dual strip Model Use the HeNB to UE model in *Table A.2.1.1.2-7 and A.2.1.1.2-8* Model 2 Use the HeNB to UE model in *Table A.2.1.1.2-7 and A.2.1.1.2-8*
Lognormal Shadowing	Similar to UMTS 30.03, B 1.41.4 [ETSI TR 101 112]		
Shadowing standard deviation*2	For outdoor RRH/Hotzone for pathloss model 1: 10 dB for pathloss model 2 : ITU-R M.2135 (i.e., according to LOS, NLOS) For indoor RRH/Hotzone, see Table 2.1.1.5-1/2	Model 1: 5x5 Grid 10dB for Link between HeNB and HeNB UE. 8dB for other links Dual strip: 4dB for Link between HeNB and HeNB UE. 8dB for other links. Model 2 : 3dB for LOS Link between HeNB and HeNB UE.	Macro to relay Relay with outdoor donor antenna: 6 dB Relay with indoor donor antenna: 8 dB Relay to UE: Relay with outdoor coverage antenna: 10 dB Relay with indoor coverage antenna: Model 1: 5x5 Grid 10 dB for link between relay and relay UE. 8dB for other links

			4dB for NLOS Link between HeNB and HeNB UE. 8dB for NLOS other links. FFS for LOS other links.	Dual strip: 4dB for link between relay and relay UE. 8dB for other links. Model 2: 3dB for LOS Link between relay and relay UE. 4dB for NLOS Link between relay and relay UE. 8dB for NLOS other links. FFS for LOS other links.
Shadowing correlation	Between cells*3	For outdoor RRH/Hotzone 0.5 For indoor RRH/Hotzone 0	0	Relay with outdoor coverage antenna:0.5 Relay with indoor coverage antenna: 0
	Between sectors	N/A	N/A	N/A
Penetration Loss		For outdoor RRH/Hotzone 20 dB for Case 1,3; See ITU.Eval for ITU Rural above for both "Macro to UE" and "RRH/Pico to UE" For indoor RRH/Hotzone, see Table 2.1.1.5-1/2	Model 1: 5x5 Grid Femto to UEs inside the same cluster: 0 dB All other links: 20 dB. Dual-strip: see Table A.2.1.1.2-7/8. Model 2: see Table A.2.1.1.2-7/8	Macro to UE Outdoor relay: 20 dB. Indoor relay Model 1: 5x5 Grid: 20 dB. Dual-strip: 20 dB if the UE is indoors, 0 dB if the UE is outdoors. Model 2: 20 dB if the UE is indoors, 0 dB if the UE is outdoors.
				Macro to relay: Relay with outdoor donor antenna: 0 dB Relay with indoor donor antenna: 5 dB
				Relay with outdoor coverage antenna to UE: 20 dB for Case 1,3; See ITU.Eval for ITU Rural Relay with indoor coverage antenna to UE: Model 1: 5x5 Grid Relay to UEs inside the same cluster:0 dB Relay to UEs in different clusters: 20 dB. Dual-strip: see the HeNB to UE model in Table A.2.1.1.2-7/8. Model 2: see the HeNB to UE model in Table A.2.1.1.2-7/8.
Antenna pattern (horizontal)		$A(\theta) = 0$ dB (omnidirectional)	$A(\theta) = 0$ dB (omnidirectional)	See Table 2.1.1.4-3
				See Table 2.1.1.4-3
Carrier Frequency		CF= 2GHz for case 1 and case 3 CF = 0.8GHz for high speed rural		
Channel model		If fast fading modelling is disabled in system level simulations for relative evaluations, the		

	impairment of frequency-selective fading channels shall be captured in the physical layer abstraction. For SIMO, the physical layer abstraction is based on TU link curves. For MIMO, the physical layer abstraction is FFS.		
UE speeds of interest	Case 1 and Case 3: 3 km/h Rural high speed: 120 km/h for UEs served by macro, RRH, hotzone or relay nodes. 3 km/h for UEs served by femto cells.		
Doppler of relay-macro link	N/A	N/A	Jakes spectrum with [5]Hz for NLOS component. LOS component [K=10dB].
Total BS TX power (Ptotal)	Case1: 24, 30 dBm – 10MHz carrier Case3: 24, 30, 37 dBm – 10MHz carrier (37dBm is outdoor only)	20 dBm – 10MHz carrier	See Table 2.1.1.4-3
			See Table 2.1.1.4-3
UE power class	23dBm (200mW) This corresponds to the sum of PA powers in multiple Tx antenna case		
Inter-cell Interference Modelling	UL: Explicit modelling (all cells occupied by UEs), DL: Explicit modelling else cell power = Ptotal		
Antenna configuration	2 tx , 2 rx antenna ports, or 4 tx , 4 rx antenna ports	2 tx , 2 rx antenna ports, or 4 tx , 4 rx antenna ports	See Table 2.1.1.4-3
			See Table 2.1.1.4-3
Antenna gain + connector loss [Motorola: reference for these values?]	5dBi	5dBi	See Table 2.1.1.4-3
			See Table 2.1.1.4-3
Placing of new nodes and Ues	See Table A.2.1.1.2-4	See Table A.2.1.1.2-6	See Table A.2.1.1.2-4
Minimum distance between new node and regular nodes	>=75m		
Minimum distance between UE and regular node	>= 35m		
Minimum distance between UE and new node (RRH/Hotzone, Femto, Relay)	For outdoor RRH/Hotzone > 10m For indoor RRH/Hotzone >= 3m	>= 3m	Outdoor relay:> 10m Indoor relay: >= 3m
Minimum distance among new nodes	40 m	40 m cluster radious	40 m

*1 Outdoor RRH/Hotzone model 1 is based on TR 25.814 and IMT.EVAL UMi NLOS model, outdoor relay and outdoor RRH/Hotzone model 2 LOS and NLOS path loss models are based on field measurements and LOS/NLOS probability functions for macro to UE and macro to relay are based on ITU models and probability functions for relay or pico to UE are based on field measurements; femto and indoor relay path loss is based on ITU-R M1225 single floor indoor office model. Outdoor relay antenna height for both access and backhaul link is 5m. Path loss models for case 3 with 10m antenna height are FFS.

*2 Shadowing fading value for relays is applicable to NLOS component of the path loss. Value for LOS component is FFS.

*3 Cells including macro cells of the overlay network and new nodes.

Fast fading may be modelled using any of the following:

- No fast fading as in current TR
- Fast fading with TU and fixed correlation matrix
- Fast fading with ITU/SCM models or possible simplifications [ref. R4-091103] could also be used. (Detailed proposals to be discussed, e.g., relevant propagation model to use with these.)

For preliminary simulation, all fast fading channel models can be applied. The baseline fast fading model to be used for final evaluation results should be discussed in future (or in WI).

Table A.2.1.1.2-4. Placing of new nodes and UEs

Configuration	UE density across macro cells*	UE distribution within a macro cell	New node distribution within a macro cell	Comments
1	Uniform 25/macro cell	Uniform	Uncorrelated	Capacity enhancement
2	Non-uniform [10 – 100]/macro cell	Uniform	Uncorrelated	Sensitivity to non-uniform UE density across macro cells
3	Non-uniform [10 – 100]/macro cell	Uniform	Correlated**	Cell edge enhancement
4a, 4b	Non-uniform***	Clusters	Correlated**	Hotspot capacity enhancement

* New node density is proportional to the UE density in each macro cell. UE density is defined as the number of UEs in the geographic area of a macro cell.

**Relay and hotzone nodes, often deployed by planning, see section A2.1.1.4.

*** Clustered UE Placement for Hotzone cells:

- Fix the total number of users, N_{users}, dropped within each macro geographical area, where N_{users} is 30 or 60 in fading scenarios and 60 in non-fading scenarios.
- Randomly and uniformly drop the configured number of low power nodes, N, within each macro geographical area (the same number N for every macro geographical area, where N may take values from {1, 2, 4, 10}).
- Randomly and uniformly drop N_{users_lpn} users within a 40 m radius of each low power node, where $N_{users\_lpn} = \lfloor P^{hotspot} \cdot N_{users}/N \rfloor$ with $P^{hotspot}$ defined in Table A.2.1.1.2-5, where $P^{hotspot}$ is the fraction of all hotspot users over the total number of users in the network.
- Randomly and uniformly drop the remaining users, $N_{users} - N_{users\_lpn}*N$, to the entire macro geographical area of the given macro cell (including the low power node user dropping area).

Table A.2.1.1.2-5. Configuration #4a and #4b parameters for clustered user dropping

Configuration	N_{users}	N	$P^{hotspot}$
Configuration #4a*	30 or 60	1	1/15
		2	2/15
		4	4/15
		10	2/3
Configuration #4b	30 or 60	1	2/3
		2*	2/3*
		4*	2/3*

* Baseline for Configurations #4a and #4b.

Table A.2.1.1.2-6. Placing of femto cells and UEs

Configuration	Macro-femto Deployment	Placing of nodes	Placing of UEs
1	Independent channel	Clustered	Random placing of UEs within X meters of the femto cell
2	Co-channel	Clustered	Random placing of UEs within X meters of the femto cell

* Femto cell with 5x5 grid or dual-strip apartment blocks
* Non-uniform macro-UE drop in a femto cluster.
  (Note that this does not preclude that one femto cluster may contain no UEs)
* Fraction of Macro UEs in Femto Cluster: 35% and/or 80%

Table A.2.1.1.2-7. Indoor femto Channel models (dual strip model): Suburban deployment

Cases		Path Loss (dB)	Fast Fading (when fast fading in both frequency and spatial domains is modeled)
UE to macro BS	(1) UE is outside: *PL(R)*	Model 1: PL (dB) =15.3 + 37.6$\log_{10}$R For 2GHz, *R* in m. Model2: $PL_{LOS}(R)= 30.8+24.2\log10(R)$ $PL_{NLOS}(R)= 2.7+42.8\log10(R)$ For 2GHz, *R* in m. $Prob(R)=\exp(-(R-10)/1000)$	RMa
	(2) UE is inside a house	Model1: PL (dB) =15.3 + 37.6$\log_{10}$R + L_{ow}, R in m Model2: $PL_{LOS}(R)= 30.8+24.2\log10(R)$ + L_{ow} $PL_{NLOS}(R)=2.7+42.8\log10(R)$ + L_{ow} For 2GHz, *R* in m. $Prob(R)=\exp(-(R-10)/1000)$	RMa
UE to HeNB	(3) *Dual-stripe model*: UE is inside the same	PL (dB) = 38.46 + 20 $\log_{10}$R + 0.7$d_{2D,indoor}$+ 18.3 $n^{((n+2)/(n+1)-0.46)}$ R and $d_{2D,indoor}$ are in m	InH, LOS or NLOS depends on whether line-of sight from UE to HeNB;

	house as HeNB	n is the number of penetrated floors In case of a single-floor house, the last term is not needed	
	(4) *Dual-stripe model*: UE is outside	Model 1: PL (dB) = max(15.3 + 37.6log$_{10}$R, 38.46 + 20log$_{10}$R) + 0.7d$_{2D,indoor}$ + 18.3 n $^{((n+2)/(n+1)-0.46)}$ + L$_{ow}$ R and d$_{2D,indoor}$ are in m Model 2: PL (dB) = max(2.7+42.8 log$_{10}$ R, 38.46 + 20log$_{10}$R) + 0.7d$_{2D,indoor}$ + 18.3 n $^{((n+2)/(n+1)-0.46)}$ + L$_{ow}$ R and d$_{2D,indoor}$ are in m	InH (NLOS)
	(5) *Dual-stripe model*: UE is inside a different house	Model 1: PL(dB) = max(15.3 + 37.6log$_{10}$R, 38.46 + 20log$_{10}$R) + 0.7d$_{2D,indoor}$ + 18.3 n $^{((n+2)/(n+1)-0.46)}$ + L$_{ow,1}$ + L$_{ow,2}$ R and d$_{2D,indoor}$ are in m Model 2: PL(dB) = max(2.7+42.8 log$_{10}$ R, 38.46 + 20log$_{10}$R) + 0.7d$_{2D,indoor}$ + 18.3 n $^{((n+2)/(n+1)-0.46)}$ + L$_{ow,1}$ + L$_{ow,2}$ R and d$_{2D,indoor}$ are in m	InH (NLOS)

R is the Tx-Rx separation

L$_{ow}$ is the penetration loss of an outdoor wall, which is 20dB.

In Case (3), the path loss is modeled by free space loss, penetration loss due to internal walls and floors. The loss due to internal walls is modeled as a log-linear value, equal to 0.7dB/m.

In Case (4), the path loss modeling takes account of case (2) and case (3). d$_{2D,indoor}$ is the distance inside the house.

In Case (5), d$_{2D,indoor}$ is the total distance inside the two houses. L$_{ow,1}$ and L$_{ow,2}$ are the penetration losses of outdoor walls for the two houses.

Table A.2.1.1.2-8. Indoor femto Channel models (dual strip model): Urban deployment

Cases		Path Loss (dB)	Fast Fading(when fast fading in both frequency and spatial domains is modeled)
UE to macro BS	(1) UE is outside *PL(R)*	Model1: PL (dB) =15.3 + 37.6$\log_{10}$R, R in m Model2: $PL_{LOS}(R)= 30.8+24.2log10(R)$ $PL_{NLOS}(R)= 2.7+42.8log10(R)$ For 2GHz, *R* in m. *Prob(R)=min(18/R,1)*(1-exp(-R/63))+exp(-R/63)*	UMa
	(2) UE is inside an apt	Model1: PL (dB) =15.3 + 37.6$\log_{10}$R + L_{ow}, R in m Model2: $PL_{LOS}(R)= 30.8+24.2log10(R)$ + L_{ow} $PL_{NLOS}(R)= 2.7+42.8log10(R)$ + L_{ow} For 2GHz, *R* in m *Prob(R)=min(18/R,1)*(1-exp(-R/63))+exp(-R/63)*	UMa
UE to HeNB	(3) *Dual-stripe model*: UE is inside the same apt stripe as HeNB	PL (dB) = 38.46 + 20 $\log_{10}$R + 0.7$d_{2D,indoor}$+ 18.3 n $^{((n+2)/(n+1)-0.46)}$ + q*L_{iw} R and $d_{2D,indoor}$ are in m n is the number of penetrated floors q is the number of walls separating apartments between UE and HeNB In case of a single-floor apt, the last term is not needed	InH, LOS or NLOS depends on whether line-of sight from UE to HeNB;
	(4) *Dual-stripe model*: UE is outside the apt stripe	Model 1: PL (dB) = max(15.3 + 37.6$\log_{10}$R, 38.46 + 20$\log_{10}$R) + 0.7$d_{2D,indoor}$ + 18.3 n $^{((n+2)/(n+1)-0.46)}$ + q*L_{iw} + L_{ow}	InH (NLOS)

		Model 2: PL (dB) = max(2.7+42.8 $\log_{10}$ R, 38.46 + 20$\log_{10}$R) + 0.7$d_{2D,indoor}$ + 18.3 $n^{((n+2)/(n+1)-0.46)}$ + q*L_{iw} + L_{ow} R and $d_{2D,indoor}$ are in m q is the number of walls separating apartments between UE and HeNB	
	(5) *Dual-stripe model*: UE is inside a different apt stripe	Model 1: PL(dB) = max(15.3 + 37.6$\log_{10}$R, 38.46 + 20$\log_{10}$R) + 0.7$d_{2D,indoor}$ + 18.3 $n^{((n+2)/(n+1)-0.46)}$ + q*L_{iw} + $L_{ow,1}$ + $L_{ow,2}$ Model 2: PL(dB) = max(2.7+42.8 $\log_{10}$ R, 38.46 + 20$\log_{10}$R) + 0.7$d_{2D,indoor}$ + 18.3 $n^{((n+2)/(n+1)-0.46)}$ + q*L_{iw} + $L_{ow,1}$ + $L_{ow,2}$ R and $d_{2D,indoor}$ are in m q is the number of walls separating apartments between UE and HeNB	InH (NLOS)

L_{iw} is the penetration loss of the wall separating apartments, which is 5dB.

The term $0.7d_{2D,indoor}$ takes account of penetration loss due to walls inside an apartment.

L_{ow} is the penetration loss of an outdoor wall, which is 20dB.

$L_{ow,1}$ and $L_{ow,2}$ are the penetration losses of outdoor walls for the two houses.

A.2.1.1.3 Assumptions for Coordinated Multi point Transmission and Reception Evaluations

Performance evaluations should at least provide details related to:

- Cooperating scheduler
  - CoMP category
- Feedback assumption and feedback impairment modelling
- Backhaul assumptions
- Time/frequency synchronization assumptions
- Transmission modes:

  - MU-MIMO and/or SU-MIMO operation in conjunction with CoMP
  - Selection of transmission mode (assumptions on how dynamic or semi-static the transmission mode can be selected)
- Creation and maintenance of CoMP sets:
  - Assumptions on CoMP sets definition and creation
  - fixed vs. adaptive clusters, size of cluster…

Geometry cdf for the CoMP UE should be provided where appropriate, compared to the geometry cdf for a non-CoMP UE.

The performance of downlink/uplink multi-point transmission and reception, and advanced ICIC techniques is sensitive to the backhaul capacity and latency. In general, the backhaul latency could be classified into the following –categories

- Minimal latency (in the order of μs) for eNB to RRH links
- Low latency (<1 ms) associated with co-located cells or cells connected with fibre links and only limited number of routers in between
- Typical inter-cell latency associated with X2 interfaces.

The X2 backhaul latency, or more generally latency between new nodes, or new nodes and eNBs, or between eNBs, is highly deployment dependent such as whether there is a dedicated X2 fibre network or a generic IP network.

The proponents should describe and justify the model assumed in particular studies.

A.2.1.1.4 Assumptions for Relay Evaluations

The evaluation scenarios for relay is summarized as two basic scenarios as follows,

Table A.2.1.1.4-1. Evaluation scenarios for relay

CASE	Scenarios	ISD[m]	Carrier[GHz]
3GPP case 1.Relay	Urban Macro	500	2.0
3GPP case 3.Relay	Rural Area	1732	2.0
3GPP case 1.Indoor relay	Urban Macro	500	2.0
3GPP case 3.Indoor relay	Rural Area	1732	2.0

For 3GPP case 1&3.Relay scenarios, the placement of relay also regarded as site planning could be taken by two major steps,

1) Virtual Relay Placement: A virtual relay is placed trying to enhance the cell edge throughput or overall cell throughput.

   [TBD]

2) Relay Site planning: Finding an optimal place among N candidate relay sites around the virtual relay which offers optimization of shadow fading, LOS probability and etc.

   Relays were placed on positions they are most needed in terms of SINR (geometry). Positions, where a relay placement would result in the highest geometry gain, were found in an exhaustive search within N candidate relay sites around the virtual relay.

   The site planning procedure provides benefit on backhaul SINR (geometry). TWO alternatives to show this benefit in simulation are considered with respect to

   Alternative 1: Adding bonus to path loss formula.

   This process offers optimization of shadow fading, LOS probability and etc.

   The corrections of site planning with respect to macro-relay pathloss, LOS probability and shadowing standard deviation are listed in Table 2.1.1.4-2.

Table A.2.1.1.4-2. Corrections of site planning (alternative 1)

	No site planning	Correction after site planning
Macro-relay Path Loss	For LOS: $PL_{LOS}(R)$ For NLOS: $PL_{NLOS}(R)$	For LOS: $PL_{LOS}(R)$ For NLOS: $PL_{NLOS}(R)-B$ Where B=5dB, for donor macro (from each of its sectors) to relay, otherwise, for non-donor cell and non optimized deployment B=0dB.
Macro-relay LOS probability	Prob(R)	*1-(1- Prob(R))^N* Where *N=3*, for donor macro (from each of its sectors) to relay, otherwise, for non-donor cell and non optimized deployment *N*=1.

Alternative 2: Initialized in a system-level simulation by selecting best N relays according to a proposed site planning optimization approach.

The site planning optimization should be taken into consideration in a relay placement procedure in step 2. It is a process of finding an optimal place among N candidate relay sites around the virtual relay which offers benefit to the performance.

The site planning optimization approach are described as follows,

- N=5 candidate relay sites are considered within a searching area of 50m radius around the virtual relay.
- For simplicity, the candidate relays are randomly placed in the searching area.
- The best relay site is selected based on SINR criteria on the backhaul link.

For 3GPP case 1&3.Indoor relay scenarios, 2 cases are distinguished, depending on the relay node configuration:

- if the relay donor antenna is outdoors, no planning is performed.
- if the relay node is made up of a donor module and a coverage module, both being placed indoors, the donor module has to be placed near a window to optimize the backhaul link quality. This optimization is reflected by a penetration loss of 5 dB in Table A.2.1.1.2-3. The coverage module has to be placed in the center of the house to provide maximum coverage.

For a typical system level simulation, the following configurations are taken into consideration,

Table A.2.1.1.4-3. Typical configuration for simulation

Parameter	Description	Case 1	Case 3	Case 1/3 Indoor
P_{RN}	Max Tx power	30 dBm @ 10 MHz bandwidth	30 or 37 dBm @ 10 MHz bandwidth	Downlink: 20 dBm @ 10 MHz bandwidth Uplink: Indoor donor antenna: 23 dBm @ 10 MHz bandwidth Outdoor donor antenna: 30 dBm @ 10 MHz bandwidth
H_{RN}	RS antenna height	5m	5m, 10m	Outdoor antenna: case 1: 5 m case 3: 5 m, 10 m Indoor antenna: N/A
Antenna Configuration	One antenna set	5dBi antenna gain, Omni 2 tx , 2 rx antenna ports, or 4 tx , 4 rx antenna ports Use of antenna downtilt and vertical antenna FFS	5dBi, Omni 2 tx , 2 rx antenna ports, or 4 tx , 4 rx antenna ports Use of antenna downtilt and vertical antenna FFS	N/A
	Two antenna sets	<u>Relay-UE link:</u> 5dBi antenna gain, Omni $A(\theta) = 0$ dB 2 tx , 2 rx antenna ports, <u>Macro-Relay link</u> 7dBi, directional $A(\theta) = -\min\left[12\left(\frac{\theta}{\theta_{3dB}}\right)^2, A_m\right]$ θ_{3dB} = 70 degrees, Am = 20 dB. 2 tx , 2 rx antenna ports, or 4 tx , 4 rx antenna ports Use of antenna downtilt and vertical antenna FFS	<u>Relay-UE link:</u> 5dBi antenna gain, Omni $A(\theta) = 0$ dB or directional pointing away from the donor cell $A(\theta) = -\min\left[12\left(\frac{\theta}{\theta_{3dB}}\right)^2, A_m\right]$ θ_{3dB} = 70 degrees, Am = 20 dB. 2 tx , 2 rx antenna ports, <u>Macro-Relay link</u> <u>7</u>dBi, directional $A(\theta) = -\min\left[12\left(\frac{\theta}{\theta_{3dB}}\right)^2, A_m\right]$ θ_{3dB} = 70 degrees, Am = 20dB. 2 tx , 2 rx antenna ports, or 4 tx , 4 rx antenna ports Use of antenna downtilt and vertical antenna FFS	<u>Relay-UE link:</u> 5dBi antenna gain, Omni $A(\theta) = 0$ dB 2 tx , 2 rx antenna ports, or 4 tx , 4 rx antenna ports <u>Macro-Relay link</u> Indoor donor antenna: 5dBi, directional Outdoor donor antenna: 7dBi, directional $A(\theta) = -\min\left[12\left(\frac{\theta}{\theta_{3dB}}\right)^2, A_m\right]$ θ_{3dB} = 70 degrees, Am = 20 dB. 2 tx , 2 rx antenna ports, or 4 tx , 4 rx antenna ports
NF_{RN}	Noise figure	5 dB	5 dB	5 dB
HW_{RN}	Hardware loss/cable loss	0 dB	0 dB	Outdoor donor antenna: 2 dB Indoor donor antenna: 0 dB

A.2.1.1.5 Assumptions for indoor RRH/Hotzone Evaluations

The indoor hotspot scenario consists of single floor of a building as Figure.2.1.1.5-1 which is same with ITU sketch. The height of the floor is 6 m. The floor contains 16 rooms of 15 m x 15 m and a long hall of 120 m x 20m. Two sites are placed in the middle of the hall at 30m and 90m with respect to the left side of the building.

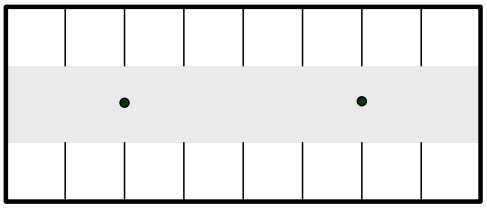

Figure.2.1.1.5-1. Sketch of indoor hotspot environment

The following two channel models are for evaluation purpose. Channel model 2 is a simplified channel model which assumes all users are allocated within buildings.

Table A.2.1.1.5-1. Channel model 1 of indoor RRH/Hotzone

Cases		Path Loss (dB)	Shadowing standard deviation	Penetration Loss	Fast Fading (when fast fading in both frequency and spatial domains is modelled)*
UE to macro BS	(1) UE is outside	$PL_{LOS}(R)= 103.4+24.2\log10(R)$ $PL_{NLOS}(R)= 131.1+42.8\log10(R)$ For 2GHz, *R* in km. Case 1: $Prob(R)=\min(0.018/R,1)*(1-\exp(-R/0.063))+\exp(-R/0.063)$ Case 3: $Prob(R)=\exp(-(R-0.01)/1.0)$	10dB	0dB	ITU UMa
	(2) UE is inside			20dB	
UE to RRH/Hotzone	(1) UE is inside a different building as the indoor hotzone	$PL(dB) =\max(131.1+42.8\log10(R), 147.4+43.3\log10(R))$ For 2GHz, *R* in km	10dB	40dB	ITU InH (NLOS)
	(2) UE is outside			20dB	
	(3) UE is inside the same building as the indoor hotzone	$PL_{LOS}(R)= 89.5 + 16.9\log10(R)$ $PL_{NLOS}(R)= 147.4+43.3\log10(R)$ For 2GHz, *R* in km $Prob(R)=\begin{cases} 1 & R \le 0.018 \\ \exp(-(R-0.018)/0.027), & 0.018 < R < 0.037 \\ 0.5 & R \ge 0.037 \end{cases}$	LOS: 3dB NLOS: 4dB	0dB	ITU InH

* No Fast Fading or TU and fixed correlation matrix can also be used.

Table A.2.1.1.5-2. Channel model 2 of indoor RRH/Hotzone

Cases		Path Loss (dB)	Shadowing standard deviation	Penetration Loss	Fast Fading (when fast fading in both frequency and spatial domains is modelled)*
UE to macro BS		$PL_{LOS}(R)= 103.4+24.2\log10(R)$ $PL_{NLOS}(R)= 131.1+42.8\log10(R)$ For 2GHz, *R* in km. Case 1: $Prob(R)=\min(0.018/R,1)*(1-\exp(-R/0.063))+\exp(-R/0.063)$ Case 3: $Prob(R)=\exp(-(R-0.01)/1.0)$	10dB	20dB	ITU UMa
UE to RRH/Hotzone	(1) UE is outside the same building as the indoor hotzone**	$PL(dB) =\max(131.1+42.8\log10(R), 147.4+43.3\log10(R))$ For 2GHz, *R* in km	10dB	20dB	ITU InH (NLOS)
	(2) UE is inside the same building as the indoor hotzone	$PL_{LOS}(R)= 89.5 + 16.9\log10(R)$ $PL_{NLOS}(R)= 147.4+43.3\log10(R)$ For 2GHz, *R* in km $Prob(R)=\begin{cases} 1 & R \le 0.018 \\ \exp(-(R-0.018)/0.027), & 0.018 < R < 0.037 \\ 0.5 & R \ge 0.037 \end{cases}$	LOS: 3dB NLOS: 4dB	0dB	ITU InH

* No Fast Fading orTU and fixed correlation matrix can also be used.

* * For UE is outside the same building as the indoor hotzone, UE are allocated within buildings which either indoor hotzone nodes are deployed or not.

A.2.1.2 Channel models

Annex B describes the IMT-Advanced Channel Models, which are specified in the IMT.EVAL of ITU-R[15].

A.2.1.3 Traffic models

Traffic models for system performance evaluations are given in Table A.2.1.3-1. System throughput studies shall be assessed using full-buffer traffic model capturing continuous traffic and non-varying interference. Additionally, evaluations with time-varying interference shall be carried out using bursty traffic models. Table A.2.1.3-1 proposes FTP traffic models to exercise system performance studies in bursty traffic.

Table A.2.1.3-1. Traffic Models

Traffic Models	Model Applies to
Full buffer	DL and UL. Continuous traffic.
Non-full buffer FTP models	DL and UL. Bursty traffic.
VoIP	DL and UL Real time services

A.2.1.3.1 FTP traffic models

Two FTP traffic models are considered as non-full buffer traffic models. Tables A.2.1.3-2 and A.2.1.3-3 show the parameters for FTP traffic model 1 and model 2, respectively. Figure A.2.1.3.1-1 and A.2.1.3.1-2 illustrate the user arrival of traffic model 1 and 2, respectively. Baseline model is Model 1 with file size of 2 Mbytes, however Model 1 with file size of 0.5 Mbytes and Model 2 with file size of 0.5 Mbytes can be also evaluated.

Table A.2.1.3.1-1. FTP Traffic Model 1

Parameter	Statistical Characterization
File size, S	2 Mbytes (0.5 Mbytes optional) (one user downloads a single file)
User arrival rate λ	Poisson distributed with arrival rate λ

- Small file size of 0.5 Mbytes can be chosen to speed-up the simulation.
- Simulations are run for various λ to find performance metrics covering at least the range of HM-NCT (See A.2.1.3.2) that leads to [10%, 50%] of RU (See A.2.1.3.2) in non-CoMP SU-MIMO.
- Possible range of λ: [0.5, 1, 1.5, 2, 2.5] for 0.5 Mbytes, [0.12, 0.25, 0.37, 0.5, 0.625] for 2 Mbytes (See A.2.1.3.4 for more details). Range of λ can further be adjusted.
- The same traffic should be simulated for CoMP and non-CoMP schemes. The above range of λ will cover RU from 10% to 50% for non-CoMP SU-MIMO

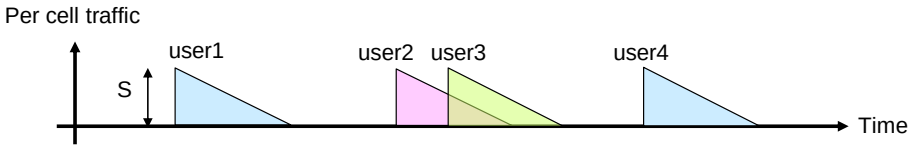

Figure A.2.1.3.1-1: Traffic generation of FTP Model 1

Table A.2.1.3.1-2. FTP Traffic Model 2

Parameter	Statistical Characterization
File Size, *S*	0.5 Mbytes
Reading Time, *D*	Exponential Distribution, Mean= 5 seconds PDF: $f_D = \lambda e^{-\lambda D}, D \geq 0 \quad \lambda = 0.2$
Number of users, K	Fixed

- Simulations are run for various K to find performance metrics covering at least the range of HM-NCT that leads to [10%, 50%] of RU in non-CoMP SU-MIMO.
- Possible range of K: [2, 5, 8, 10, 14] (See A.2.1.3.4 for more details). Range of K can further be adjusted.
- The reading time D is the time interval between end of download of previous file and the user request for the next file.

- The same traffic should be simulated for evaluating CoMP and non-CoMP schemes. The above range of K will cover RU from 10% to 50% for non-CoMP SU-MIMO.

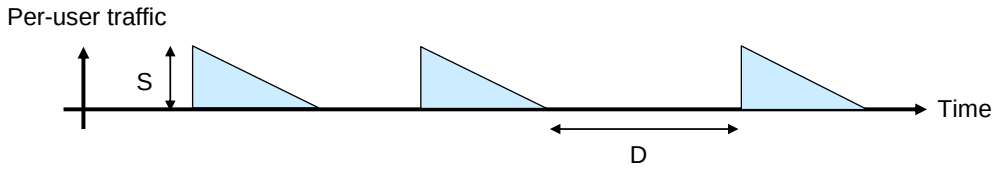

Figure A.2.1.3.1-2: Traffic generation of FTP Model 2

A.2.1.3.2 Performance metrics

The following performance metrics are considered for non-full buffer traffic models.

- Mean, 5, 50, 95 % user throughput
  - User throughput = amount of data (file size) / time needed to download data
    - time needed to download data starts when the packet is received in the transmit buffer, and ends when the last bit of the packet is correctly delivered to the receiver
- Served cell throughput
  - Served cell throughput = total amount of data for all users / total amount of observation time / number of cells
- Harmonic mean normalized cell throughput (HM-NCT)
  - Harmonic mean normalized cell throughput = served cell throughput / harmonic mean of the full buffer cell throughput
  - Harmonic mean of the full buffer cell throughput = average number of full buffer users per cell / mean(1 / full buffer user throughputs)
    - The 2% worst and 2% best users are excluded from the harmonic mean
    - Full buffer simulations are run with 10 UEs / cell
- Normalized cell throughput (NCT)
  - Normalized cell throughput = served cell throughput / full buffer served cell throughput
- Resource utilization (RU)
  - Resource utilization = Number of RB per cell used by traffic during observation time / Total number of RB per cell available for traffic over observation time
    - In case of MU-MIMO, one RB allocated to N users within a cell is counted as used N times

A.2.1.3.2.1 Reference points

Possible reference points to compare CoMP, non-CoMP, SU-MIMO and MU-MIMO techniques:

- R1: X% HM-NCT value that leads to 50% RU for SU-MIMO (i.e. X value is derived from the SU-MIMO case, and is then the same for all techniques)
- R2: Traffic load that gives 50% RU for SU-MIMO
- R3: 45% NCT

Reference point R1 may be a baseline point. However, the results should be obtained at the other reference points to gain understanding about how these new metrics relate to each other. R1 and R3 capture both the user throughput and cell capacity gains in a reasonably well utilized network. R2 captures the user throughput gain at a given offered load. Further refinement of adequate reference points can be considered.

A.2.1.3.3 File dropping criteria

A guideline of modelling file dropping for non-full buffer traffic simulation is given as follows.

- Files may be dropped from the simulation either to preserve stability at high loads, or because the radio conditions are insufficient for reliable communication.
- Method for ensuring queue stability in high load conditions:
  - drop a file if its transfer is not completed within a maximum transfer time T_drop
    - T_drop = 8s for S = 0.5 Mbyte
    - T_drop = 32s for S = 2 Mbyte
- Methods for handling HARQ retransmission failure:
  - model RLC ACK
  - if RLC ARQ is not modeled, drop the file after the maximum number of HARQ retransmissions is reached.
- Method to restrict the impact of users in very poor radio conditions:
  - if RLC is modelled: Remove from the system the users who experiment a MAC error rate higher than 3%
    - a MAC error is defined as a transport block being not correctly received after the maximum number of retransmissions.
    - do not include removed users' throughput nor contribution to the served cell throughput in the simulation results.
  - if RLC is not modeled: user outage is implicitly approximated by file dropping when the maximum number of HARQ retransmissions is reached.
- Dropping a file means:
  - the file is given zero user throughput
  - the data in the dropped file is not included in the served cell throughput
- The amount of data dropped or not transmitted shall be recorded separately according to whether it arises from users removed due to high MAC error rate or other causes, and the corresponding file dropping rates shall be indicated in the simulation results.

Alternatives methods can be considered, and should be then described.

A.2.1.3.4 Estimation of range of λ and K

For FTP Model 1

$$\text{offered traffic} = \lambda * S.$$

For LTE 2x2 10MHz, the [10%, 50%] range of resource utilization could be covered by the range of offered traffic [2 4 6 8 10] Mbps. For a file size of 500kbyte = 4 Mbit, this corresponds to:

$$\lambda = \text{offered\_traffic}/S = [2, 4, 6, 8, 10]/4 = [0.5, 1, 1.5, 2, 2.5] \text{ users/s}.$$

λ values for file size of 2Mbytes can be computed in the same way.

For model2, the inter-arrival time is given by Tt + D with Tt file transfer time. In this case $\lambda = 1/(Tt+D)$. The total offered traffic per cell is then given by

$$\text{offered traffic} = \lambda * K * S = K * S / (Tt + D)$$

Assuming download data rate of 12.5 Mbps, the file transfer (download) time Tt is 0.32 sec for file size of 500 Kbytes = 4 Mbits. By using this rough estimate, offered traffic is K*4/(0.32+5). When the range of offered loads is [2 4 6 8 10], the corresponding range of K is

$$K = [2\ 4\ 6\ 8\ 10]/4*5.32 \sim= [2\ 5\ 8\ 10\ 14] \text{ users}$$

A.2.1.4 System performance metrics

For evaluations with full-buffer traffic model, the following performance metrics need to be considered:

- Mean user throughput
- Throughput CDF
- Median and 5% worst user throughput

For evaluations with bursty traffic model, the following performance metrics need to be considered:

- User perceived throughput (during active time), defined as the size of a burst divided by the time between the arrival of the first packet of a burst and the reception of the last packet of the burst
  - Average perceived throughput of a user defined as the average from all perceived throughput for all bursts intended for this user.
  - Tail perceived throughput defined as the worst 5% perceived throughput among all bursts intended for a user
- User perceived throughput CDF (average and/or tail user perceived throughput).
- Percentage of users with [1]% or more dropped packets.
- Median and 5% worst user perceived throughput (average and/or tail user perceived throughput).
- Overall average user throughput defined as average over all users perceived throughput.

For VoIP capacity evaluations, the following performance metrics need to be considered:

- VoIP system capacity in form of the maximum number of satisfied users supported per cell in downlink and uplink.
  - System capacity is defined as the number of users in the cell when more than [95%] of the users are satisfied.
  - A VoIP user is in outage (not satisfied) if [98%] radio interface tail latency of the user is greater than [50 ms]. This assumes an end-to-end delay below [200 ms] for mobile-to-mobile communications.

For heterogeneous network performance evaluation, the following performance metrics are the highest priority:

- Existing full buffer and bursty traffic performance metrics
  - Throughput CDFs are for all UEs, i.e., macro UEs and HeNB/pico UEs
- Macro cell area throughput
- Fraction of throughput over low power nodes
- Macro and low power node serving UE throughput ratio

The following table should be included along with the simulation assumptions accompanying all results:

Are Throughput Values based solely on an assumption of a number of trials of *independent* placing of UEs?	Comments
Yes/No	If "Yes," then state the number of trials, i.e., placing of a group of UEs in cells used. If "No," either state the methodology by which confidence interval is achieved as well as confidence interval and confidence level, or justify the method of user placing in different trials.

A.2.1.5 Scheduling and resource allocation

Different scheduling approaches have impacts on performance and signalling requirements.

Evaluations should include a high-level description of the scheduling and resource allocation schemes simulated, including relevant parameter values. For frequency or carrier specific scheduling, and multipoint transmission schemes, any feedback approach, delay, and feedback error assumptions should also be indicated. For uplink queue-related scheduling, similar indications should be given for any buffer status feedback.

Evaluations should include fairness, as described in section A.2.1.4 above.

A.2.1.6 Antenna gain for a given bearing and downtilt angle

A.2.1.6.1 Polarized antenna modelling

In case of polarized antennas, the polarization is modelled as angle-independent in both azimuth and elevation, in the antenna local coordinate system. For a linearly polarized antenna, the antenna element field pattern, in the horizontal polarization and in the vertical polarization, are given by

$$F_{\phi}(\phi,\theta) = F_{\phi}(\phi,\theta,\zeta) = \sqrt{A(\phi,\theta)}\cos(\zeta)$$

and

$$F_{\theta}(\phi,\theta) = F_{\theta}(\phi,\theta,\zeta) = \sqrt{A(\phi,\theta)}\sin(\zeta),$$

respectively, where ζ is the polarization slant angle[1] and $A(\phi,\theta)$ is the 3D element antenna gain pattern as a function of azimuth angle, ϕ and elevation angle, θ, which are defined in Figure A.2.1.6.1-1. Note that the vertical and horizontal field direction are defined in terms of the spherical basis vectors, $\hat{\theta}$ and $\hat{\phi}$, respectively (i.e., $F_H(\phi,\theta) = F_{\phi}(\phi,\theta)$ and $F_V(\phi,\theta) = F_{\theta}(\phi,\theta)$).

For 2D element antenna gain pattern:

$$F_{\phi}(\phi) = F_{\phi}(\phi,\zeta) = \sqrt{A(\phi)}\cos(\zeta)$$

and

$$F_{\theta}(\phi) = F_{\theta}(\phi,\zeta) = \sqrt{A(\phi)}\sin(\zeta),$$

[1] Hence, an antenna with $\zeta = 0$ degrees corresponds to a purely horizontally polarized antenna.

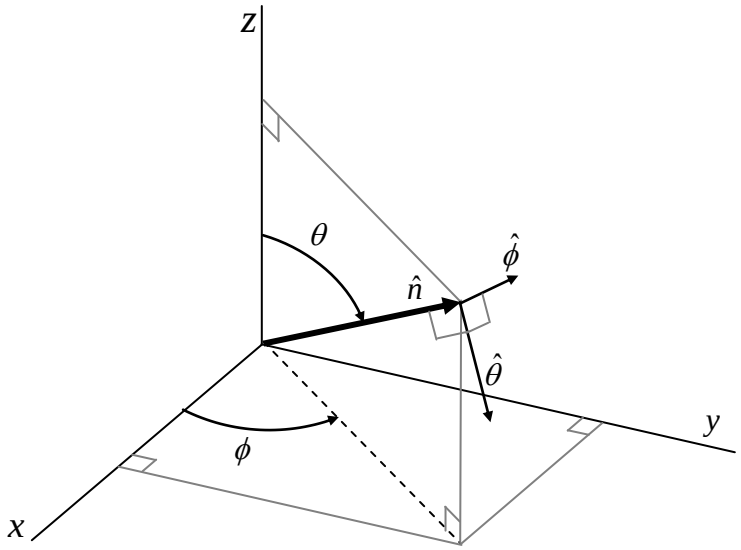

Figure A.2.1.6.1-1 Definition of spherical angles and spherical unit vectors in a Cartesian coordinate system, where $\hat{n}$ is the given direction, $\hat{\theta}$ and $\hat{\phi}$ are the spherical basis vectors.

A.2.1.6.2 Antenna gain for a given direction and mechanical tilt angle

A global coordinate system with Cartesian coordinates (*x*,*y*,*z*) and a local ("primed") coordinate system with Cartesian coordinates (*x'*,*y'*,*z'*) are defined with a common origin, with the *y'*-axis being parallel to the y-axis; that is, the x-axis of the global coordinate system, should be aligned with the pointing direction of the sector[2]. The global coordinate system is oriented with its *z*-axis along a vertical direction, thus having its *xy*-plane coinciding with a horizontal plane, and all directions in space (angles of arrival and departure) are defined in the global coordinate system angular coordinates θ and ϕ, see Figure A.2.1.6.1-1.

Assume that an antenna is installed with the antenna aperture normal direction (and antenna main beam peak for a conventional sector antenna) in the *xz*-plane and that the antenna radiation pattern is defined in terms of angles θ' and ϕ' in the local coordinate system, with the local coordinate system antenna-fixed.

Mechanical tilt is modeled as a rotation of the antenna-fixed coordinate system around the *y*-axis. For zero mechanical tilt the antenna-fixed coordinate system coincides with the global coordinate system. Conventionally, for sector antennas with cylindrical shape, the antenna radiation pattern defined in the antenna-fixed coordinate system is measured with the antenna cylinder axis installed to coincide with the *z'*-axis of the antenna-fixed coordinate system. Note that electric tilt, and hence beam pointing direction, does not in general affect the choice of antenna-fixed coordinate system.

By rotating the local coordinate system with respect to the global coordinate system the same effect as mechanical tilting is attained. Since the antenna pattern is defined in the local coordinate system, which has been rotated with respect to the global coordinate system, a transformation must be performed to allow evaluation of the tilted antenna pattern as a function of coordinates in the global coordinate system. This transformation relates the spherical angles (θ, ϕ) in the global coordinate system to spherical angles (θ', ϕ') in the local (antenna-fixed) coordinate system and is defined as follows:

$$\theta' = \arccos(\cos\phi\sin\theta\sin\beta + \cos\theta\cos\beta), \quad (1)$$

$$\phi' = \arg(\cos\phi\sin\theta\cos\beta - \cos\theta\sin\beta + j\sin\phi\sin\theta), \quad (2)$$

where β is the mechanical tilt angle around the *y*-axis as defined in Figure A.2.1.6.2-1.

[2] Note that the global coordinate system should not be interpreted as a system wide global coordinate system, but a coordinate system centered at the site antenna, with the xy-plane parallel to horizontal plane.

Having only the total gain pattern $A'(\theta',\phi')$ in the local system, the total gain in the global (θ,ϕ)-system is simply given by the relation

$$A(\theta,\phi) = A'(\theta',\phi')$$

with θ' and ϕ' given by (1) and (2).

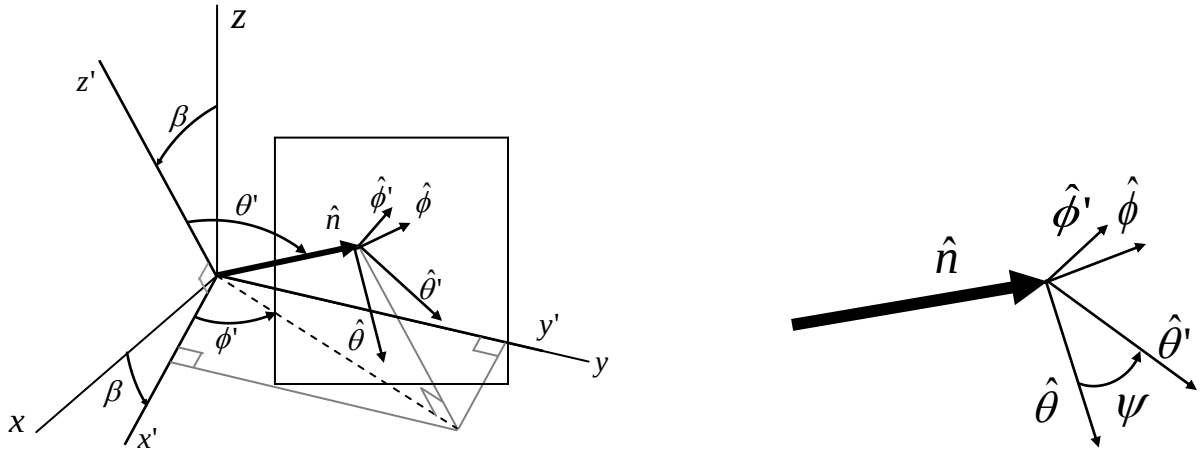

Figure A.2.1.6.2-1 Definition of angles and unit vectors when the local coordinate system has been rotated an angle β around the *y*-axis of the global coordinate system.

For polarized fields a transformation of the field components is needed, in addition to the coordinate transformation. For a mechanical tilt angle β, the global coordinate system field components $F_V(\theta,\phi)$ and $F_H(\theta,\phi)$, (defined as $F_V(\theta,\phi) = F_\theta(\theta,\phi)$ and $F_H(\theta,\phi) = F_\phi(\theta,\phi)$) are calculated from the field components $F_{\theta'}(\theta',\phi')$ and $F_{\phi'}(\theta',\phi')$ of the radiation pattern in the local (antenna-fixed) coordinate system as

$$F_V(\theta,\phi) = F_\theta(\theta,\phi) = F_{\theta'}(\theta',\phi')\cos\psi - F_{\phi'}(\theta',\phi')\sin\psi \quad (3)$$

$$F_H(\theta,\phi) = F_\phi(\theta,\phi) = F_{\theta'}(\theta',\phi')\sin\psi + F_{\phi'}(\theta',\phi')\cos\psi \quad (4)$$

where θ' and ϕ' are defined as in (1) and (2), and ψ is defined as:

$$\psi = \arg\left(\sin\theta\cos\beta - \cos\phi\cos\theta\sin\beta + j\sin\phi\sin\beta\right). \quad (5)$$

As an example, in the horizontal cut, i.e., for $\theta = 90^\circ$, equations (1), (2) and (5) become

$$\theta' = \arccos(\cos\phi\sin\beta),$$

$$\phi' = \arg(\cos\phi\cos\beta + j\sin\phi),$$

$$\psi = \arg\left(\cos\beta + j\sin\phi\sin\beta\right).$$

The notation $F_H(\phi)$ and $F_V(\phi)$, used below, should be interpreted as the field components for the specific θ that is given by the direction of the propagation; that is, the angle between the global z-axis and the line connecting the site antenna and the UE.

If $\pm 45^\circ$ polarized antennas are used, the field components $F_{\theta'}$ and $F_{\phi'}$ are related to the co-polarized and cross-polarized field components in the local (antenna-fixed) coordinate system for the -45° polarized antenna as

$$F_{\theta'} = \frac{1}{\sqrt{2}}(F_{co-45} + F_{cross-45}) \ , \tag{6}$$

$$F_{\phi'} = \frac{1}{\sqrt{2}}(-F_{co-45} + F_{cross-45}) \ , \tag{7}$$

and similarly for the $+45^{\circ}$ polarized antenna.

A.2.1.7 Advanced receivers modeling

A.2.1.7.1 Iterative soft interference cancellation receivers

Advanced receivers based on iterative soft interference cancellation receivers (e.g. Turbo SIC) are non-linear receivers whose performance improves with the reliability of the interference reconstruction as the number of iterations increases. Modeling this interference reconstruction reliability or not in system-level simulations has a significant impact on the accuracy of the performance evaluation, especially if only a small number of iterations is performed in order to limit the receiver complexity.

Therefore, for system-level simulations employing a link-to-system abstraction of iterative soft interference cancellation receivers, the interference reconstruction reliability should be modeled. In order to ease the comparison of results from different sources, the simulation conditions should briefly describe the used modeling method.

In addition, the number of iterations should be indicated, as this parameter impacts the receiver performance as well as its complexity.

A.2.1.8 Effective IoT

According to the ITU evaluation guidelines [4] an IoT (Interference over Thermal noise) measure reflecting the 'effective' interference received by the base station should be used. No definition of this measure is provided however. This section contains a simple effective IoT measure, taking the interference suppression capabilities of the receiver into account.

A linear receiver, e.g. an MRC or MMSE, with M antennas is assumed. The received signal at antenna m is

$$r_m = h_m x + e_m + n_m$$

where h_m is the channel between the (single) transmitter and receive antenna m, x is the transmitted symbol, e_m is the sum of the interfering signals (e.g. aimed at other users), and n_m is the thermal noise at antenna m. The receiver processing constitutes of estimating the transmitted symbol x by appropriately weighting the received signal at each antenna with a complex-valued weight w_m^H, and then summing the weighted signals. The sum-weighted output signal is given by

$$y = \sum_{m=1}^{M} w_m^H r_m = \sum_{m=1}^{M} w_m^H \left(h_m x + e_m + n_m\right)$$

Alternatively, using vector and matrix notation, where bold variables are column vectors spanning the antenna domain:

$$\mathbf{y} = \mathbf{w}^H \left(\mathbf{h}x + \mathbf{e} + \mathbf{n}\right)$$

The effective SINR at the receiver output is given by the ratio of the power of the desired part of the signal, $\mathbf{w}^H\mathbf{h}x$, to the power of the non-desired part of the signal, $\mathbf{w}^H(\mathbf{e}+\mathbf{n})$ which under the assumption that noise and interference is independent can be written as

$$\mathrm{SINR}_{\mathrm{eff}} = \frac{\mathbf{w}^H \mathbf{h}\mathbf{h}^H \mathbf{w}}{\mathbf{w}^H \left(\mathbf{Q} + \mathbf{N}\right)\mathbf{w}} :$$

where

$$\mathbf{Q} = E\{\mathbf{e}\mathbf{e}^H\}$$

is the covariance matrix of the interference, and

$$\mathbf{N} = E\{\mathbf{n}\mathbf{n}^H\}$$

is the covariance matrix of the noise. Note that typically $\mathbf{N}=\sigma^2\mathbf{I}$, where σ^2 is the noise variance per antenna, and $\mathbf{I}$ is the identity matrix of size *MxM*.

The denominator in the effective SINR expression now contains the effective power of the interference and thermal noise. Hence:

$$\mathrm{P}_{\mathrm{INeff}} = \mathbf{w}^H(\mathbf{Q}+\mathbf{N})\mathbf{w}.$$

The effective IoT can now be defined as the ratio between the total effective noise and interference power to the effective thermal noise power

$$\mathrm{IoT}_{eff} = \frac{\mathrm{P}_{INeff}}{\mathrm{P}_{Neff}} = \frac{\mathbf{w}^H(\mathbf{Q}+\mathbf{N})\mathbf{w}}{\mathbf{w}^H\mathbf{N}\mathbf{w}}.$$

Since receive weights typically vary over frequency and time, the effective IoT should be calculated per frequency and time instant, and then averaged (i.e. do not average $\mathrm{P}_{\mathrm{INeff}}$ and $\mathrm{P}_{\mathrm{Neff}}$ separately). The average is taken over allocated resources, non-used resources are excluded.

A.2.2 System level simulator calibration

To facilitate LTE-A evaluations simulators have been calibrated to ensure that they produce comparable results. In a first step (1a), downlink wideband SINR (also denoted 'geometry') and coupling loss distributions for the ITU scenarios and 3GPP case 1 have been evaluated and compared. In a second step (1c) downlink and uplink spectral efficiencies, user throughput distributions, and SINR distributions for a basic LTE configuration have been evaluated and compared. The parameters used are listed in Table A.2.2-1.

Table A.2.2-1. Parameters for calibration of system level simulators

Parameter	Value
General	Parameters and assumptions not explicitly stated here according to ITU guidelines M.2135 and 3GPP specifications
Duplex method	FDD
Network synchronization	Synchronized
Handover margin	1dB
Downlink transmission scheme	1x2 SIMO
Downlink scheduler	Round robin with full bandwidth allocation
Downlink link adaptation	Wideband CQI, no PMI on PUCCH (mode 1-0) 5ms periodicity, 6ms delay total (measurement in subframe n is used in subframe n+6) CQI measurement error: None MCSs based on LTE transport formats [5]
Downlink HARQ	Maximum four transmissions
Downlink receiver type	MRC
Uplink transmission scheme	1x2 SIMO
Uplink scheduler	Frequency Domain Multiplexing – non-channel dependent, share available bandwidth between users connected to the cell, all users get resources in every uplink subframe. With M users and Nrb PRBs available, Mh=mod(Nrb,M) users get floor(Nrb/M)+1 PRBs whereas Ml=M-Mh users get floor(Nrb/M) PRBs
Uplink Power control	P0 = -106dBm, alpha = 1.0
Uplink Link adaptation	Based on delayed measurements. Ideal channel estimate from UL transmission in subframe n can be used for rate adaptation in subframe n+7 MCSs based on LTE transport formats [5]
Uplink HARQ	Maximum four transmissions Proponent to specify IR or CC
Uplink receiver type	MMSE in frequency domain, MRC over antennas (no intercell interference rejection)
Antenna configuration	Vertically polarized antennas 0.5 wavelength separation at UE, 10 wavelength separation at basestation
Channel estimation	Ideal, both demodulation and sounding
Control Channel overhead, Acknowledgements etc.	LTE: L=3 symbols for DL CCHs, M=4 resource blocks for UL CCH, overhead for demodulation reference signals,
BS antenna downtilt	ITU Indoor, indoor hotspot scenario (InH): N/A ITU Microcellular, urban micro-cell scenario (Umi): 12deg ITU Base coverage urban, Urban macro-cell scenario (Uma): 12deg ITU High speed, Rural macro-cell scenario (Rma): 6 deg Case 1 3GPP 3D: 15 deg Case 1 3GPP 2D: N/A
Feeder loss	0dB, except for the ITU scenarios in step 1a where a feeder loss of 2dB is used.
Channel model	According to ITU for ITU scenarios SCM urban macro high spread for 3GPP case 1
Intercell interference modeling	Explicit

For step 1a, a summary of the results are presented in Figure A.2.2-1 and are based on averaging independent results from 17 different simulators. For the downlink wideband SINR, the results from different simulators are typically within 0.5dB of the average SINR.

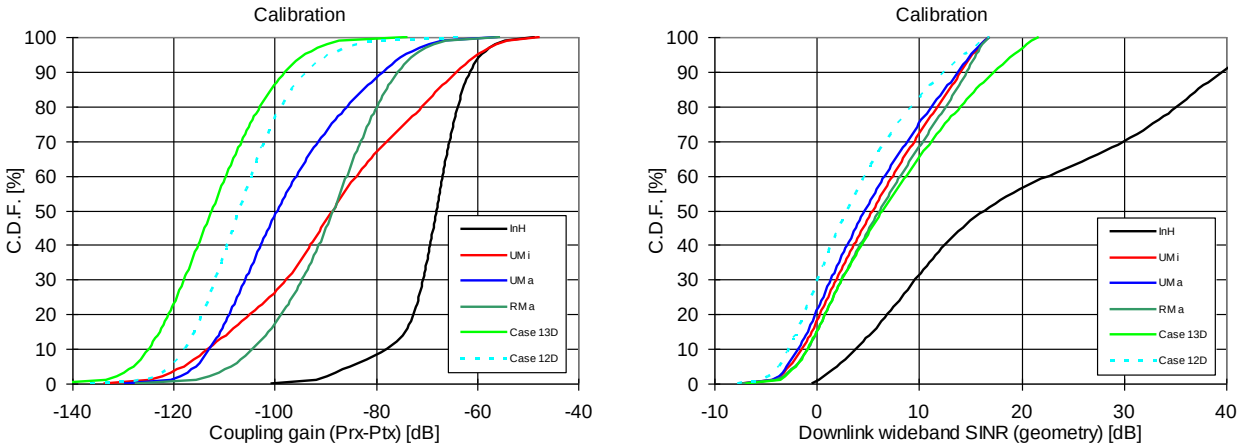

Figure A.2.2-1. Distributions of coupling gain and downlink wideband SINR (geometry).

Results for step 1c in terms of cell spectral efficiency, cell-edge user spectral efficiency, normalized user throughput distributions, and post antenna combination signal-to-noise-and-interference ratio distributions (with linear averaging over time and frequency) from 16 different simulators were available. A summary is given in Figure A.2.2-2, Figure A.2.2-3 and Table A.2.2-2, where the results have been obtained by averaging the results of the different simulators.

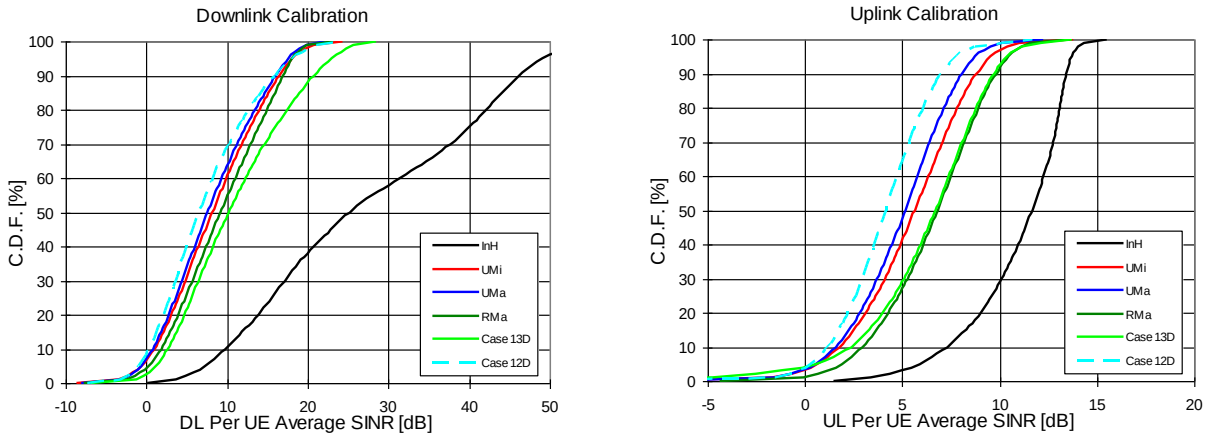

Figure A.2.2-2. Distributions of downlink and uplink SINR after antenna combination.

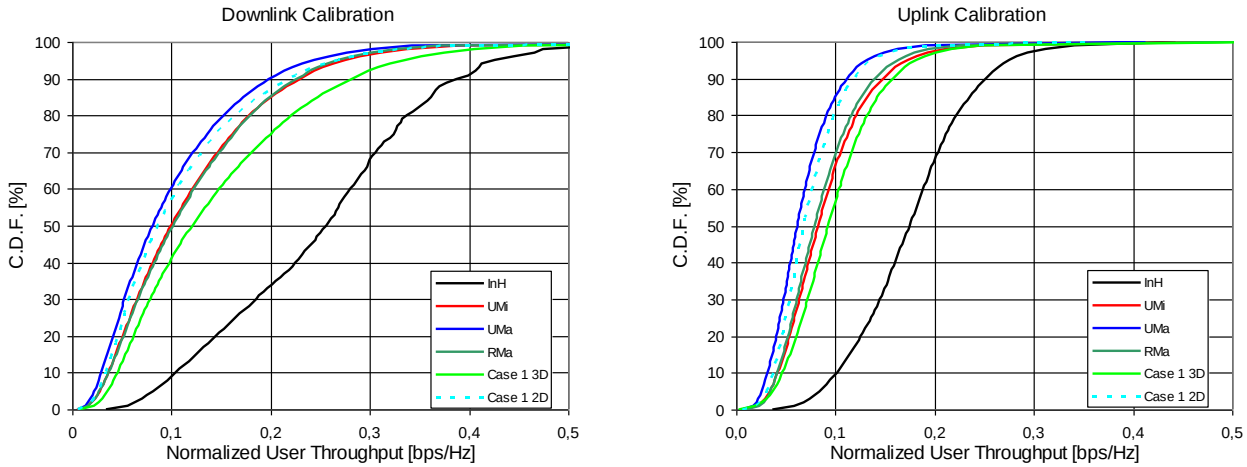

Figure A.2.2-3. Distributions of downlink and uplink normalized user throughput.

Table A.2.2-2. Spectral efficiencies for calibration in the different environments

Direction	Metric	InH	UMi	UMa	RMa	Case 1 3D	Case 1 2D
Downlink	Cell spectral efficiency	2.3	1.2	1.0	1.2	1.5	1.1
	Cell-edge user spectral efficiency	0.082	0.028	0.022	0.027	0.035	0.026
Uplink	Cell spectral efficiency	1.77	0.91	0.68	0.86	0.99	0.74
	Cell-edge user spectral efficiency	0.084	0.033	0.026	0.034	0.036	0.031

A certain spread of the results exists. The magnitude of this is summarized in Table A.2.2-3, in terms of coefficients of variation (standard deviation divided by average) for the spectral efficiencies.

Table A.2.2-3. Coefficients of variation for the different environments, directions and metrics.

Direction	Metric	InH	UMi	UMa	RMa	Case 1 3D	Case 1 2D
Downlink	Cell spectral efficiency	3%	9%	8%	6%	5%	5%
	Cell-edge user spectral efficiency	9%	19%	17%	14%	15%	15%
Uplink	Cell spectral efficiency	5%	7%	5%	5%	5%	4%
	Cell-edge user spectral efficiency	13%	16%	15%	11%	7%	9%

A.2.3 Downlink CoMP evaluation assumptions for intra-NodeB CoMP

The objectives of downlink CoMP evaluation for intra-eNodeB CoMP is to clarify the performance gain of CoMP schemes over single-cell schemes, and clarify the need of enhanced feedback or SRS.

The intra-site CoMP with up to 3 coordinated co-located cells is the baseline scenario for performance evaluation, as shown in Figure A.2.3-1, with both 2 transmit antennas per cell and 4 transmit antenna per cell. For full buffer traffic model, the evaluations include 2 users per cell and 10 users per cell. Alternative scenario (without X2 interface) can be evaluated, e.g. Intra-eNodeB CoMP with distributed Radio Remote Heads.

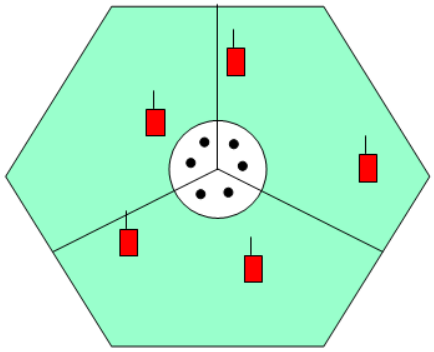

Figure A.2.3-1: Baseline evaluation scenario: 3 cell co-located Intra-site CoMP

Table A.2.3-1-system simulation parameters for downlink intra-site CoMP Evaluation

Parameter	Values used for evaluation
Deployment scenarios	Homogeneous deployments
Simulation case	3GPP-case1 SCM-UMa (high spread)
System bandwidth	10 MHz (FDD), 20MHz (TDD)
Possible transmission schemes	● SU-MIMO ● MU-MIMO ● SU-MIMO with intra-eNB CS/CB ● MU-MIMO with intra-eNB CS/CB ● SU-MIMO with intra-eNB JP-CoMP ● MU-MIMO with intra-eNB JP-CoMP - Model the impairments of JP-CoMP - Collision between CRS and PDSCH - Different control regions - Describe the way to handle the impairments
Network synchronization	Synchronized
Antenna configuration	Following priority: Config.1 eNB: Cross-polarized (0.5 l spacing) UE: Cross-polarized antennas Config.2 eNB: Grouped co-polarized (0.5 l within group, 10 l between group) UE: co-polarized antennas Config.3 eNB: co-polarized (0.5 l spacing) UE: co-polarized antennas
Antenna pattern	Follow Annex A 2.1.1.1 Table A.2.1.1-2
eNB Antenna tilt	Follow Annex A 2.1.1.1 Table A.2.1.1-2 3D as baseline 2D as additional
Channel estimation	Non-ideal. Clarify in detail the following on CoMP evaluation: - CSI knowledge of eNB - Feedback scheme and/or UL sounding scheme - Accuracy of CSI . Quantization error . Channel estimation error based on CRS/CSI-RS - Channel estimation error based on DMRS
DL overhead assumption	Should be clarified for each transmission scheme (e.g., follow ITU evaluation)
Placing of UEs	Uniform distribution
Traffic model	Full buffer and Non-full-buffer

A.3 Evaluation assumptions for IMT-A

The discussions during the study item phase have raised a lot of different choices. In order to have a meaningful set of evaluation results for ITU-R submission, a common baseline of the key L1 parameters was proposed; in order that the results from different parties would not deviate too much so that forming any common view of the expected benefits of LTE-A is less difficult. These parameters are not exclusive or restrictive to additional results.

Table A.3-1 Simulation assumption for Cell/cell-edge spectrum efficiency

Parameter	Values used for evaluation
Deployment scenario	• Indoor hotspot • Urban micro-cell • Urban macro-cell • Rural macro-cell Parameters and assumptions not shown here for each scenario are shown in ITU guidelines [ITU-R Report M.2135].
Duplex method and bandwidths	FDD: 10+10 MHz except Indoor hotspot with 20+20 MHz TDD: 20 MHz Baseline asymmetry during 5 subframes period: 2 full DL subframes, Special subframe: DwPTS 11symbol, GP 1 symbol, UpPTS 2 symbol, 2 full UL subframes Alternative special subframe configurations may be used if stated.
Network synchronization	Synchronized
Handover margin	1.0 dB
Downlink transmission scheme	Baseline transmission scheme (LTE Rel.8) • MIMO closed loop precoded spatial multiplexing (transmission mode 4 [36.213]): Baseline: 4x2 MIMO • MIMO single stream beamforming (transmission mode 7 [36.213]) Advanced scheme (LTE-A) • MU-MIMO without coordination • MU-MIMO with intercell coordination • Joint processing CoMP (SU-MIMO is possible for all cases.)
Downlink scheduler	For baseline transmission scheme (LTE Rel.8): Proportional fair in time and frequency For advanced transmission scheme (LTE-A) Aligned with transmission scheme
Downlink link adaptation	Non-ideal based on non-ideal CQI/PMI/RI reports and/or non-ideal sounding transmission, reporting mode: and period selected according to scheduler and MIMO transmission schemes; reporting delay and MCS based on LTE transport formats according to [36.213]. Baseline (LTE Rel.8): A) Non-frequency selective PMI and frequency selective CQI report with 5ms periodicity, subband CQI with measurement error: N(0,1) per PRB B) Sounding-based precoding, frequency selective CQI report with 5ms periodicity, subband CQI with measurement error: N(0,1) per PRB *Advanced transmission scheme (LTE-A)* *Following scheme(s) is assumed for the base station(s) to access the channel state information, to all UEs served by the CoMP cooperating set, which can range from a single base station, to multiple base stations.* • *The long-term, wideband, spatial channel information such as transmit channel covariance matrices or angular information can be obtained, for example, from uplink measurements (based on e.g., SRS) or by feedback with an average feedback overhead similar to that in Rel-8.* • *The short-term and/or narrowband channel state information (PMI, transmit covariance matrix, channel transfer function, etc.) can be obtained, for example, from uplink measurements (based on e.g., SRS), and/or by feedback with the average feedback overhead to be described in the evaluation results.*
Downlink HARQ scheme	Incremental redundancy or Chase combining
Downlink receiver type	Baseline scheme MMSE Advanced scheme MMSE-SIC, MLD based receiver Each company should report a description on interference rejection and cancellation capabilities.
Uplink transmission scheme	Baseline transmission scheme (LTE Rel.8) • SIMO with and without MU-MIMO Baseline: 1 x 4 SIMO Advanced transmission scheme (LTE-A)

	• SU-MIMO • UL CoMP
Uplink scheduler	Channel dependent
Uplink Power control	Baseline: Fractional power control. Alternative: Other Rel.8 specified Power control parameters (P0 and alpha) are chosen according to the deployment scenario. (IoT reported with simulation results.)
Uplink link adaptation	Non-ideal based on delayed SRS-based measurements: MCS based on LTE transport formats and SRS period and bandwidths according to [36.213].
Uplink HARQ scheme	Incremental redundancy or Chase combining
Uplink receiver type	MMSE or MMSE-SIC (MU-MIMO)
Antenna configuration base station	Baseline: 4 or 8 Tx antennas with the following configurations: A) Uncorrelated co-polarized: Co-polarized antennas separated 4 wavelengths (illustration for 4 Tx: | | | |) B) Grouped co-polarized: Two groups of co-polarized antennas. 10 wavelengths between center of each group. 0.5 wavelength separation within each group (illustration for 4 Tx: || ||) C) Correlated: co-polarized: 0.5 wavelengths between antennas (illustration for 4 Tx: ||||) D) Uncorrelated cross-polarized: Columns with +-45deg linearly polarized antennas Columns separated 4 wavelengths (illustration for 4 Tx: X X) E) Correlated cross-polarized Columns with +-45deg linearly polarized antennas Columns separated 0.5 wavelengths (illustration for 8Tx: XXXX) Baseline mappings between deployment scenario and antenna configurations: For downlink: • Indoor Hotspot: A (Rel.8) • Urban Micro: C or E (MU-MIMO), B or E (CoMP, Rel.8) • Urban Macro: C or E (MU-MIMO), C or E (CoMP) • Rural Macro: C or E (MU-MIMO, Rel.8) Note: MU-MIMO = MU-MIMO with / without coordination CoMP = Joint processing CoMP For uplink: • Indoor Hotspot: A • Urban Micro: A or B or C or E • Urban Macro: A or C or E • Rural Macro: A or C or E
Antenna configuration UE	Baseline: Vertically polarized antennas with 0.5 wavelengths separation at UE Alternative: Columns with linearly polarized orthogonal antennas with 0.5 wavelengths spacing between columns
Channel estimation (Uplink and downlink)	Recommended: Non-ideal (For non-ideal case, consider both estimation errors both for demodulation reference signals and sounding reference signals)

Control channel and reference signal overhead, Acknowledgements etc.	For baseline transmission (LTE) schemes: • Overhead for CRS and antenna port 5 according to DL transmission schemes • SRS overhead according to UL (and DL) scheduler and transmission scheme • Overhead for UL CCH according to CQI/PMI reporting mode and periodicity used for DL simulation for the same scenario • Overhead for DL CCH of [1-3] OFDM symbols For advanced transmission schemes (LTE-A) • UL overhead for CSI feedback and SRS transmission according to transmission scheme factored into the uplink results for the same scenarios. • DL overhead for additional DRS if used.
Feedback and control channel errors	None

Table A.3-2. Mobility parameters and recommended baseline values

Parameter	Baseline value
Power control	Fractional (α = 0.8), P_0 fitted to environment
Scheduling bandwidth	4-5 RB

Table A.3-3. VoIP parameters and recommended baseline values

Parameter	Range	Baseline value
Number of base station antennas	2-8	4
Scheduling	Dynamic, Semi-persistent	Both
PDDCH limitation	Included, excluded	Included
TDD configuration		Configuration 0 and 1, DwPTS 12, GP 1, UpPTS 1

A.4 Detailed simulation results

Detailed simulation results of cell spectral efficiency and cell edge spectral efficiency for full-buffer traffic in Section 10.2, VoIP capacity and mobility are contained in [6]. The following 18 corporate entities (listed below alphabetically) participated in these simulations:

Alcatel-Lucent/Alcatel-Lucent Shanghai Bell, CATT, CMCC, Ericsson/ST-Ericsson, Fujitsu, Hitachi, Huawei, LGE, Motorola, NEC, Nokia/Nokia Siemens Networks, NTT DOCOMO, Panasonic, Qualcomm, RITT, Samsung, Texas Instruments, ZTE

Annex B: Channel models (Informative)

The ITU-R IMT-Advanced channel model is a geometry-based stochastic model. It can also be called double directional channel model. It does not explicitly specify the locations of the scatters, but rather the directions of the rays, like the well-known spatial channel model (SCM) [B1]. Geometry-based modelling of the radio channel enables separation of propagation parameters and antennas.

The channel parameters for individual snapshots are determined stochastically based on statistical distributions extracted from channel measurements. Antenna geometries and radiation patterns can be defined properly by the user of the model. Channel realizations are generated through the application of the geometrical principle by summing contributions of rays (plane waves) with specific small-scale parameters like delay, power, angle-of-arrival (AoA) and angle-of-departure (AoD). Superposition results to correlation between antenna elements and temporal fading with geometry dependent Doppler spectrum.

A number of rays constitute a cluster. In the terminology of this document we equate the cluster with a propagation path diffused in space, either or both in delay and angle domains. Elements of the MIMO channel, e.g., antenna arrays at both link ends and propagation paths, are illustrated in Figure B-1. The generic MIMO channel model is applicable for all scenarios, e.g. indoor, urban and rural.

Figure B-1 The MIMO channel

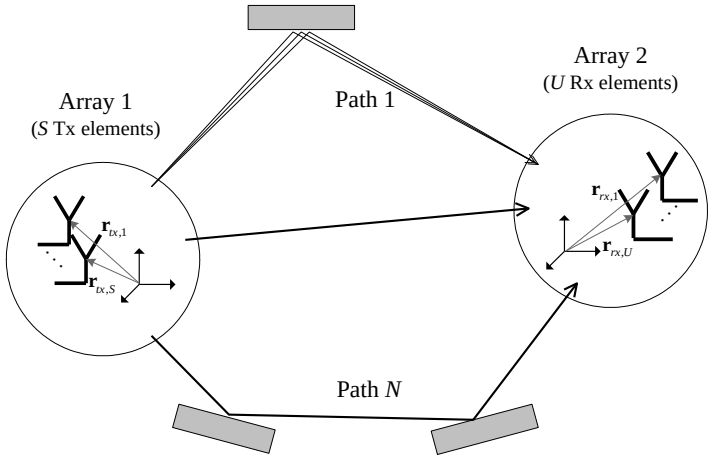

The time variant impulse response matrix of the U x S MIMO channel is given by

$$\mathbf{H}(t;\tau) = \sum_{n=1}^{N} \mathbf{H}_n(t;\tau) \ , \tag{3}$$

where t is time, τ is delay, N is the number of paths, and n is path index. It is composed of the antenna array response matrices $\mathbf{F}_{tx}$ and $\mathbf{F}_{rx}$ for the transmitter (Tx) and the receiver (Rx) respectively, and the dual-polarized propagation channel response matrix $\mathbf{h}_n$ for cluster n as follows

$$\mathbf{H}_n(t;\tau) = \iint \mathbf{F}_{rx}(\varphi)\mathbf{h}_n(t;\tau,\phi,\varphi)\mathbf{F}_{tx}^T(\phi)\, d\phi d\varphi \ . \tag{4}$$

The channel from Tx antenna element s to Rx element u for cluster n is expressed as

$$\begin{aligned} H_{u,s,n}(t;\tau) = \sum_{m=1}^{M} & \begin{bmatrix} F_{rx,u,V}(\varphi_{n,m}) \\ F_{rx,u,H}(\varphi_{n,m}) \end{bmatrix}^T \begin{bmatrix} \alpha_{n,m,VV} & \alpha_{n,m,VH} \\ \alpha_{n,m,HV} & a_{n,m,HH} \end{bmatrix} \begin{bmatrix} F_{tx,s,V}(\phi_{n,m}) \\ F_{tx,s,H}(\phi_{n,m}) \end{bmatrix} \\ & \times \exp\left(j2\pi\lambda_0^{-1}(\overline{\varphi}_{n,m} \cdot \overline{r}_{rx,u})\right) \exp\left(j2\pi\lambda_0^{-1}(\overline{\phi}_{n,m} \cdot \overline{r}_{tx,s})\right) \\ & \times \exp\left(j2\pi\upsilon_{n,m}t\right)\delta(\tau - \tau_{n,m}) \end{aligned} \tag{5}$$

where $F_{rx,u,V}$ and $F_{rx\mu,H}$ are the antenna element u field patterns for vertical and horizontal polarizations respectively, $\alpha_{n,m,VV}$ and $\alpha_{n,m,VH}$ are the complex gains of vertical-to-vertical and horizontal-to-vertical polarizations of ray n,m respectively, λ_0 is the wave length of the carrier frequency, $\overline{\phi}_{n.m}$ is the AoD unit vector, $\overline{\varphi}_{n.m}$ is the AoA unit vector, $\overline{r}_{tx,s}$ and $\overline{r}_{rx,u}$ are the location vectors of element s and u respectively, and $\upsilon_{n,m}$ is the Doppler frequency component of ray n,m. If the radio channel is modelled as dynamic, all the above mentioned small-scale parameters are time variant, i.e., they are functions of t [B8].

The IMT-Advanced channel model for the evaluation of IMT-Advanced candidate RITs consists of a Primary Module and an Extension Module. In this part, only the primary module is included, which is mandatory for IMT-Advanced evaluation. The Primary Module covers the mathematical framework, which is called *generic model*, a set of parameters as well as path loss models.

The generic channel model is a double-directional geometry-based stochastic model. It is a system level[3] model in the sense that is employed, e.g., in the SCM model [B1]. It can describe an unlimited number of propagation environment realizations for single or multiple radio links for all the defined scenarios and for arbitrary antenna configurations, with one mathematical framework by different parameter sets. The generic channel model is a stochastic model with two (or three) levels of randomness. First, large-scale (LS) parameters like shadow fading, delay, and angular spreads are drawn randomly from tabulated distribution functions. Next, small-scale (SS) parameters like delays, powers, and directions of arrival and departure are drawn randomly according to tabulated distribution functions and random LS parameters. At this stage the geometric setup is fixed and the only free variables are the random initial phases of the scatters. By picking (randomly) different initial phases, an infinite number of different realizations of the model can be generated. When the initial phases are also fixed, there is no further randomness left.

Figure B-2 shows the overview of the channel model creation. The first stage consists of two steps. First, the propagation scenario is selected. Then, the network layout and the antenna configuration are determined. In the second stage, large-scale and small-scale parameters are defined. In the third stage, channel impulse responses (ChIRs) are calculated.

The generic model is based on the drop concept. When using the generic model, the simulation of the system behaviour is carried out as a sequence of "drops", where a "drop" is defined as one simulation run over a certain time period. A drop (or snapshot or channel segment) is a simulation entity where the random properties of the channel remain constant except for the fast fading caused by the changing phases of the rays. The constant properties during a single drop are, e.g., the powers, delays, and directions of the rays. In a simulation the number and the length of drops have to be selected properly by the evaluation requirements and the deployed scenario. The generic model allows the user to simulate over several drops to get statistically representative results. Consecutive drops are independent.

Figure B-2 Channel model creation process

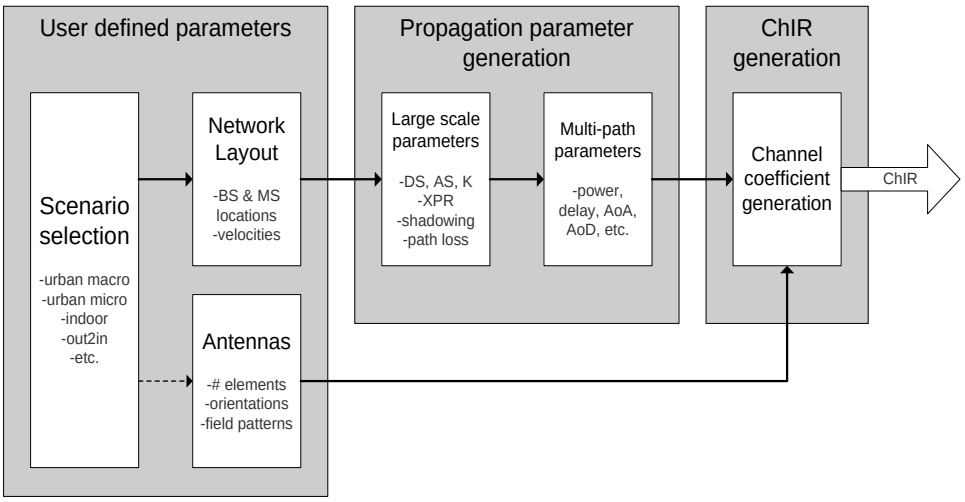

B.1 Channel models

This section provides the reference channel model for each test environment. These test environments are intended to cover the range of IMT-Advanced operating environments.

The test operating environments are considered as a basic factor in the evaluation process of the candidate RITs. The reference models are used to estimate the critical aspects, such as the spectrum, coverage and power efficiencies.

3 The term system-level means here that the model is able to cover multiple links, cells and terminals.

B.1.1 Void

B.1.2 Primary module

The following sections provide the details of the channel models, including the path loss models, for the terrestrial component. For terrestrial environments, the propagation effects are divided into three distinct types: These are the path loss, the slow variation due to shadowing and scattering, and the rapid variation in the signal due to multipath effects. The channel models are specified in the frequency range from 2 GHz to 6 GHz. For the rural macro-cell scenario (RMa), the channel model can be used for lower frequencies down to 450 MHz. The channel models also cover MIMO aspects as all desired dimensions (delay, AoA, AoD and polarisation) are considered. The channel models are targeted for up to 100 MHz RF bandwidth.

B.1.2.1 Path loss models

Path loss models for the various propagation scenarios have been developed based on measurement results carried out in [B2, B7, B9-B14], as well as results from the literature. The models can be applied in the frequency range of 2 – 6 GHz and for different antenna heights. The rural path-loss formula can be applied to the desired frequency range from 450 MHz to 6 GHz. The path loss models have been summarized in Table B.1.2.1-1. Note that the distribution of the shadow fading is log-normal, and its standard deviation for each scenario is given in the table.

Table B.1.2.1-1 Summary table of the primary module path loss models

Scenario		**Path loss [dB]** **Note: f_c is given in GHz and distance in meters!**	**Shadow fading std [dB]**	**Applicability range, antenna height default values**
Indoor Hotspot (InH)	LOS	$PL = 16.9\log_{10}(d) + 32.8 + 20\log_{10}(f_c)$	$\sigma = 3$	3 m < d < 100 m h_{BS} =3-6 m h_{UT} =1-2.5 m
	NLOS	$PL = 43.3\log_{10}(d) + 11.5 + 20\log_{10}(f_c)$	$\sigma = 4$	10 m < d < 150 m h_{BS} = 3-6 m h_{UT} = 1-2.5 m
Urban Micro (UMi)	LOS	$PL = 22.0\log_{10}(d) + 28.0 + 20\log_{10}(f_c)$ $PL = 40\log_{10}(d_1) + 7.8 - 18\log_{10}(h'_{BS}) - 18\log_{10}(h'_{UT}) + 2\log_{10}(f_c)$	$\sigma = 3$ $\sigma = 3$	10 m < d_1 < d'_{BP} [1)] d'_{BP} < d_1 < 5000 m[1)] h_{BS} = 10 m[1)], h_{UT} = 1.5 m[1)]

Urban Macro (UMa)	NLOS	**Manhattan grid layout:** $PL = \min(PL(d_1,d_2), PL(d_2,d_1))$ where $PL(d_k,d_l) =$ $PL_{LOS}(d_k) + 17.9 - 12.5n_j + 10n_j \log_{10}(d_l) +$ $3\log_{10}(f_c)$ and $n_j = \max(2.8 - 0.0024d_k, 1.84)$ and PL_{LOS} is the path loss of scenario UMi LOS and $k,l \in \{1,2\}$. **Hexagonal cell layout:** $PL = 36.7\log_{10}(d) + 22.7 + 26\log_{10}(f_c)$	σ= 4 σ= 4	10 m < $d_1 + d_2$ < 5 000 m, $w/2 < \min(d_1,d_2)$ [2] w = 20 m (street width) h_{BS} = 10 m, h_{UT} = 1.5 m When 0 < $\min(d_1,d_2)$ < $w/2$, the LOS PL is applied. 10 m < d < 2 000 m h_{BS} = 10 m h_{UT} =1-2.5 m
	O-to-I	$PL = PL_b + PL_{tw} + PL_{in}$ **Manhattan grid layout (θ known):** $\begin{cases} PL_b = PL_{B1}(d_{out} + d_{in}) \\ PL_{tw} = 14 + 15(1 - \cos(\theta))^2 \\ PL_{in} = 0.5d_{in} \end{cases}$ **For hexagonal layout (θ unknown):** PL_{tw} = 20, other values remain the same.	σ= 7	10 m < d_{out}+d_{in}< 1 000 m, 0 m < d_{in}< 25 m, h_{BS}=10m, h_{UT}=3(n_{Fl} -1)+1.5m, n_{Fl}=1, Explanations: see [3]
	LOS	PL = 22.0$\log_{10}(d)$ + 28.0 + 20$\log_{10}(fc)$ $PL = 40.0\log_{10}(d_1) + 7.8 - 18.0\log_{10}(h'_{BS})$ $-18.0\log_{10}(h'_{UT}) + 2.0\log_{10}(f_c)$	σ= 4 σ= 4	10 m < d < d'_{BP} [1] d'_{BP} < d < 5 000 m[1] h_{BS} = 25 m[1], h_{UT} = 1.5 m[1]
	NLOS	PL = 161.04 – 7.1 $\log_{10}$ (W) + 7.5 $\log_{10}$ (h) – (24.37 – 3.7(h/h_{BS})^2) $\log_{10}$ (h_{BS}) + (43.42 – 3.1 $\log_{10}$ (h_{BS})) ($\log_{10}$ (d)-3) + 20 $\log_{10}$(f_c) – (3.2 ($\log_{10}$ (11.75 h_{UT}))^2 - 4.97)	σ= 6	10 m < d < 5 000 m h = avg. building height W = street width h_{BS} = 25 m, h_{UT} = 1.5 m, W = 20 m, h = 20 m The applicability ranges: 5 m < h < 50 m 5 m < W < 50 m 10 m < h_{BS} < 150 m 1 m < h_{UT} < 10 m

Suburban Macro (SMa, optional)	LOS	$PL_1 = 20\log_{10}(40\pi d f_c/3)$ $+ \min(0.03h^{1.72},10)\log_{10}(d)$ $- \min(0.044h^{1.72},14.77)$ $+ 0.002\log_{10}(h)d$ $PL_2 = PL_1\ (d_{BP}) + 40\log_{10}(d/d_{BP})$	$\sigma = 4$ $\sigma = 6$	10 m < d < d_{BP} [4] d_{BP} < d < 5 000 m h_{BS} = 35 m, h_{UT} = 1.5 m, W = 20 m, h = 10 m (The applicability ranges of h, W, h_{BS}, h_{UT} are same as in UMa NLOS)
	NLOS	$PL = 161.04 - 7.1\log_{10}(W) + 7.5\log_{10}(h)$ $-(24.37 - 3.7(h/h_{BS})^2)\log_{10}(h_{BS})$ $+(43.42 - 3.1\log_{10}(h_{BS}))(\log_{10}(d)-3) +$ $20\log_{10}(f_c) - (3.2(\log_{10}(11.75h_{UT}))^2 - 4.97)$	$\sigma = 8$	10 m < d < 5 000 m h_{BS} = 35 m, h_{UT} = 1.5 m, W = 20 m, h = 10 m (Applicability ranges of h, W, h_{BS}, h_{UT} are same as in UMa NLOS)
Rural Macro (RMa)	LOS	$PL_1 = 20\log_{10}(40\pi d f_c/3)$ $+ \min(0.03h^{1.72},10)\log_{10}(d)$ $- \min(0.044h^{1.72},14.77)$ $+ 0.002\log_{10}(h)d$ $PL_2 = PL_1\ (d_{BP}) + 40\log_{10}(d/d_{BP})$	$\sigma = 4$ $\sigma = 6$	10 m < d < d_{BP}, [4] d_{BP} < d < 10 000 m, h_{BS} = 35 m, h_{UT} = 1.5 m, W = 20 m, h = 5 m (Applicability ranges of h, W, h_{BS}, h_{UT} are same as UMa NLOS)
	NLOS	$PL = 161.04 - 7.1\log_{10}(W) + 7.5\log_{10}(h)$ $-(24.37 - 3.7(h/h_{BS})^2)\log_{10}(h_{BS})$ $+(43.42 - 3.1\log_{10}(h_{BS}))(\log_{10}(d)-3) +$ $20\log_{10}(f_c) - (3.2(\log_{10}(11.75h_{UT}))^2 - 4.97)$	$\sigma = 8$	10 m < d < 5 000 m, h_{BS} = 35 m, h_{UT} = 1.5 m, W = 20 m, h = 5 m (The applicability ranges of h, W, h_{BS}, h_{UT} are same as UMa NLOS)

1) Break point distance $d'_{BP} = 4\,h'_{BS}\,h'_{UT}\,f_c/c$, where f_c is the centre frequency in Hz, $c = 3.0\times10^8$ m/s is the propagation velocity in free space, and h'_{BS} and h'_{UT} are the effective antenna heights at the BS and the UT, respectively. The effective antenna heights h'_{BS} and h'_{UT} are computed as follows: $h'_{BS} = h_{BS} - 1.0$ m, $h'_{UT} = h_{UT} - 1.0$ m, where h_{BS} and h_{UT} are the actual antenna heights, and the effective environment height in urban environments is assumed to be equal to 1.0 m.

2) The distances d_1 and d_2 are defined below in Figure B.1.2.1-1.

3) PL_b = basic path-loss, PL_{B1} = Loss of UMi outdoor scenario, PL_{tw} = Loss through wall, PL_{in} = Loss inside, d_{out} = distance from BS to the wall next to UT location, d_{in} = perpendicular distance from wall to UT (assumed evenly distributed between 0 and 25 m), θ = angle between LOS to the wall and a unit vector normal to the wall.

4) Break point distance $d_{BP} = 2\pi\, h_{BS}\, h_{UT}\, f_c/c$, where f_c is the centre frequency in Hz, $c = 3.0\times10^8$ m/s is the propagation velocity in free space, and h_{BS} and h_{UT} are the antenna heights at the BS and the UT, respectively.

The line-of-sight (LOS) probabilities are given in Table B.1.2.1-2. Note that probabilities are used only for system level simulations.

Table B.1.2.1-2

Scenario	LOS probability as a function of distance d [m]

InH	$P_{LOS} = \begin{cases} 1, & d \le 18 \\ \exp(-(d-18)/27), & 18 < d < 37 \\ 0.5, & d \ge 37 \end{cases}$
UMi	$P_{LOS} = \min(18/d,1)\cdot(1-\exp(-d/36))+\exp(-d/36)$ (for outdoor users only)
UMa	$P_{LOS} = \min(18/d,1)\cdot(1-\exp(-d/63))+\exp(-d/63)$
RMa	$P_{LOS} = \begin{cases} 1, & d \le 10 \\ \exp\left(-\frac{d-10}{1000}\right), & d > 10 \end{cases}$

The NLOS path loss model for scenario UMi is dependent on two distances, d_1 and d_2 in the case of the Manhattan grid. These distances are defined with respect to a rectangular street grid, as illustrated in Figure B.1.2.1-1, where the UT is shown moving along a street perpendicular to the street on which the BS is located (the LOS street). d_1 is the distance from the BS to the centre of the perpendicular street, and d_2 is the distance of the UT along the perpendicular street, measured from the centre of the LOS street.

Figure B.1.2.1-1 Geometry for d1 - d2 path-loss model

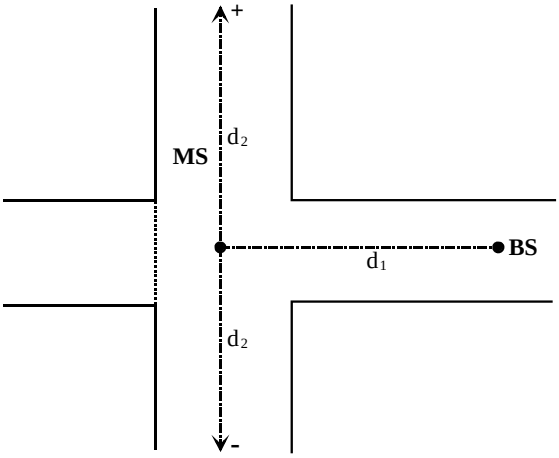

B.1.2.1.1 Autocorrelation of shadow fading

The long-term (log-normal) fading in the logarithmic scale around the mean path loss *PL* (dB) is characterized by a Gaussian distribution with zero mean and standard deviation. Due to the slow fading process versus distance Δx, adjacent fading values are correlated. Its normalized autocorrelation function $R(\Delta x)$ can be described with sufficient accuracy by the exponential function [B6]

$$R(\Delta x) = e^{-\frac{|\Delta x|}{d_{cor}}} \quad (6)$$

with the correlation length d_{cor} being dependent on the environment, see the correlation parameters for shadowing and other large scale parameters in Table B.1.2.2.1-4 (Channel model parameters).

B.1.2.2 Primary module channel model parameters

B.1.2.2.1 Generic model

The radio channels are created using the parameters listed in Table B.1.2.2.1-4. The channel realizations are obtained by a step-wise procedure [B2] illustrated in Figure B.1.2.2.1-1 and described below. It has to be noted that the geometric description covers arrival angles from the last bounce scatterers and respectively departure angles to the first scatterers interacted from the transmitting side. The propagation between the first and the last interaction is not defined. Thus, this approach can model also multiple interactions with the scattering media. This indicates also that e.g., the delay of a multipath component cannot be determined by the geometry. In the following steps, downlink is assumed. For uplink, arrival and departure parameters have to be swapped.

Figure B.1.2.2.1-1 Channel coefficient generation procedure

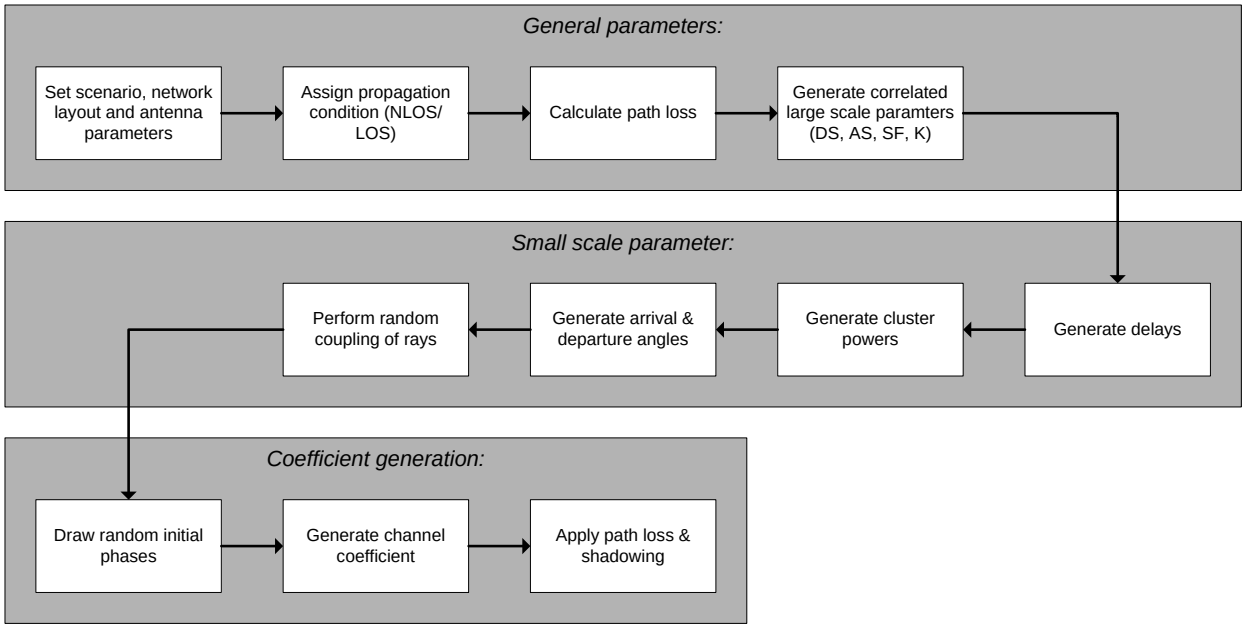

General parameters:

Step 1: Set environment, network layout, and antenna array parameters

a. Choose one of the scenarios (InH, UMi, …)
b. Give number of BS and UT
c. Give locations of BS and UT, or equally distances of each BS and UT and relative directions and ϕ_{LOS} and φ_{LOS} of each BS and UT
d. Give BS and UT antenna field patterns F_{rx} and F_{tx} and array geometries
e. Give BS and UT array orientations with respect to north (reference) direction
f. Give speed and direction of motion of UT
g. Give system centre frequency

Large scale parameters:

Step 2: Assign propagation condition (LOS/NLOS).

Step 3: Calculate path loss with formulas of Table B.1.2.1-1 for each BS-UT link to be modelled.

Step 4: Generate correlated large scale parameters, i.e. delay spread, angular spreads, Ricean K factor and shadow fading term like explained in [B2, section 3.3.1] (Correlations between large scale parameters). Limit random rms arrival and departure azimuth spread values to 104 degrees, i.e., $\sigma_\varphi = \min(\sigma_\varphi, 104°)$.

Small scale parameters:

Step 5: Generate delays τ.

Delays are drawn randomly from the delay distribution defined in Table B.1.2.2.1-4. With exponential delay distribution calculate

$$\tau_n' = -r_\tau \sigma_\tau \ln(X_n), \tag{7}$$

where r_τ is the delay distribution proportionality factor, $X_n \sim$ Uni(0,1), and cluster index $n = 1,\ldots,N$. With uniform delay distribution the delay values τ_n' are drawn from the corresponding range. Normalise the delays by subtracting the minimum delay and sort the normalised delays to descending order:

$$\tau_n = \mathrm{sort}(\tau_n' - \min(\tau_n')). \tag{8}$$

In the case of LOS condition, additional scaling of delays is required to compensate for the effect of LOS peak addition to the delay spread. The heuristically determined Ricean K-factor dependent scaling constant is

$$D = 0.7705 - 0.0433K + 0.0002K^2 + 0.000017K^3, \tag{9}$$

where K [dB] is the Ricean K-factor defined in Table B.1.2.2.1-4.. The scaled delays

$$\tau_n^{LOS} = \tau_n / D, \tag{10}$$

are **not** to be used in cluster power generation.

Step 6: Generate cluster powers P.

Cluster powers are calculated assuming a single slope exponential power delay profile. Power assignment depends on the delay distribution defined in Table B.1.2.2.1-4. With exponential delay distribution the cluster powers are determined by

$$P_n' = \exp\left(-\tau_n \frac{r_\tau - 1}{r_\tau \sigma_\tau}\right) \cdot 10^{\frac{-Z_n}{10}} \tag{11}$$

where $Z_n \sim$ N(0, ζ) is the per cluster shadowing term in [dB]. Average the power so that the sum power of all cluster powers is equal to one, i.e.,

$$P_n = \frac{P_n'}{\sum_{n=1}^{N} P_n'} \tag{12}$$

Assign the power of each ray within a cluster as P_n / M, where M is the number of rays per cluster.

Remove clusters with less than -25 dB power compared to the maximum cluster power.

Step 7: Generate arrival angles φ and departure angles ϕ.

As the composite PAS of all clusters is modelled as wrapped Gaussian (see Table B.1.2.2.1-4), except indoor hotspot scenario (InH) as Laplacian, the AoAs are determined by applying the inverse Gaussian function (13) or inverse Laplacian function (14) with input parameters P_n and RMS angle spread σ_φ

$$\varphi_n' = \frac{2\sigma_{\mathrm{AoA}}\sqrt{-\ln(P_n/\max(P_n))}}{C}. \tag{13}$$

$$\varphi_n' = -\frac{\sigma_\varphi \ln(P_n/\max(P_n))}{C} \tag{14}$$

In the equation (13) $\sigma_{\mathrm{AoA}} = \sigma_\varphi / 1.4$ is the standard deviation of the arrival angles (the factor 1.4 is the ratio of Gaussian std and the corresponding "RMS spread"). Constant C is a scaling factor related to total number of clusters and is given in the table below:

Table B.1.2.2.1-1

#	4	5	8	10	11	12	14	15	15	16	19	19	20

clusters									(InH)			(InH)	
C	0.779	0.860	1.018	1.090	1.123	1.146	1.190	1.211	1.434	1.226	1.273	1.501	1.289

In the LOS case, constant C is dependent also on the Ricean K-factor. Constant C in (13) and (14) is substituted by C^{LOS}. Additional scaling of the angles is required to compensate for the effect of LOS peak addition to the angle spread. The heuristically determined Ricean K-factor dependent scaling constant is

$$C^{LOS} = C \cdot \left(1.1035 - 0.028K - 0.002K^2 + 0.0001K^3\right), \quad (15)$$

As for indoor hotspot scenario, the scaling constant is:

$$C^{LOS} = C \cdot \left(0.9275 + 0.0439K - 0.0071K^2 + 0.0002K^3\right) \quad (16)$$

where K [dB] is the Ricean K-factor defined in Table B.1.2.2.1-4.

Assign positive or negative sign to the angles by multiplying with a random variable X_n with uniform distribution to the discrete set of {1,–1}, and add component $Y_n \sim \mathrm{N}\left(0, \sigma_\varphi / 7\right)$ to introduce random variation

$$\varphi_n = X_n \varphi_n' + Y_n + \varphi_{LOS}, \quad (17)$$

where φ_{LOS} is the LOS direction defined in the network layout description, see Step1c.

In the LOS case, substitute (17) by (18) to enforce the first cluster to the LOS direction φ_{LOS}

$$\varphi_n = \left(X_n \varphi_n' + Y_n\right) - \left(X_1 \varphi_1' + Y_1 - \varphi_{LOS}\right). \quad (18)$$

Finally add offset angles α_m from Table B.1.2.2.1-2 to the cluster angles

$$\varphi_{n,m} = \varphi_n + c_{AoA}\alpha_m, \quad (19)$$

where c_{AoA} is the cluster-wise rms azimuth spread of arrival angles (cluster ASA) in Table B.1.2.2.1-4.

Table B.1.2.2.1-2 Ray offset angles within a cluster, given for 1 rms angle spread

Ray number m	Basis vector of offset angles α_m
1,2	± 0.0447
3,4	± 0.1413
5,6	± 0.2492
7,8	± 0.3715
9,10	± 0.5129
11,12	± 0.6797
13,14	± 0.8844
15,16	± 1.1481
17,18	± 1.5195
19,20	± 2.1551

For departure angles ϕ_n the procedure is similar.

Step 8: Random coupling of rays within clusters.

Couple randomly departure ray angles $\phi_{n,m}$ to arrival ray angles $\varphi_{n,m}$ within a cluster n, or within a sub-cluster in the case of two strongest clusters (see Step 10a and Table B.1.2.2.1-2).

Coefficient generation:

Step 9: Draw random initial phase $\left\{\Phi_{n,m}^{\mathrm{vv}},\Phi_{n,m}^{\mathrm{vh}},\Phi_{n,m}^{\mathrm{hv}},\Phi_{n,m}^{\mathrm{hh}}\right\}$ for each ray *m* of each cluster *n* and for four different polarisation combinations (*vv*,*vh*,*hv*,*hh*). The distribution for initial phases is uniform within (-π, π).

In the LOS case, draw also random initial phases $\left\{\Phi_{LOS}^{\mathrm{vv}},\Phi_{LOS}^{\mathrm{hh}}\right\}$ for both VV and HH polarisations.

Step 10a: Generate channel coefficients for each cluster *n* and each receiver and transmitter element pair *u*,*s*.

For the N – 2 weakest clusters, say $n = 3,4,\ldots,N$, and uniform linear arrays (ULA), the channel coefficients are given by:

$$\mathbf{H}_{u,s,n}(t)=\sqrt{P_n}\sum_{m=1}^{M}\begin{bmatrix}F_{rx,u,V}(\varphi_{n,m})\\F_{rx,u,H}(\varphi_{n,m})\end{bmatrix}^{T}\begin{bmatrix}\exp\left(j\Phi_{n,m}^{vv}\right) & \sqrt{\kappa^{-1}}\exp\left(j\Phi_{n,m}^{vh}\right)\\\sqrt{\kappa^{-1}}\exp\left(j\Phi_{n,m}^{hv}\right) & \exp\left(j\Phi_{n,m}^{hh}\right)\end{bmatrix}\begin{bmatrix}F_{tx,s,V}(\phi_{n,m})\\F_{tx,s,H}(\phi_{n,m})\end{bmatrix} \cdot\exp\left(jd_s 2\pi\lambda_0^{-1}\sin(\phi_{n,m})\right)\exp\left(jd_u 2\pi\lambda_0^{-1}\sin(\varphi_{n,m})\right)\exp\left(j2\pi\upsilon_{n,m}t\right) \quad (20)$$

where $F_{rx,u,V}$ and $F_{rx,u,H}$ are the antenna element *u* field patterns for vertical and horizontal polarisations respectively, d_s and d_u are the uniform distances [m] between transmitter elements and receiver elements respectively, κ is the cross polarisation power ratio in linear scale, and λ_0 is the wavelength of the carrier frequency. If polarisation is not considered, the 2x2 polarisation matrix can be replaced by the scalar $\exp\left(j\Phi_{n,m}\right)$ and only vertically polarised field patterns are applied.

The Doppler frequency component is calculated from the angle of arrival (downlink), UT speed *v* and direction of travel θ_v

$$\upsilon_{n,m}=\frac{\|v\|\cos\left(\varphi_{n,m}-\theta_v\right)}{\lambda_0}, \quad (21)$$

For the two strongest clusters, say *n* = 1 and 2, rays are spread in delay to three sub-clusters (per cluster), with fixed delay offset {0,5,10 ns} (see Table B.1.2.2.1-3). The delays of the sub-clusters are

$$\begin{aligned}\tau_{n,1}&=\tau_n+0\,\mathrm{ns}\\\tau_{n,2}&=\tau_n+5\,\mathrm{ns}\\\tau_{n,3}&=\tau_n+10\,\mathrm{ns}\end{aligned} \quad (22)$$

Twenty rays of a cluster are mapped to sub-clusters as presented in Table B.1.2.2.1-3 below. The corresponding offset angles are taken from Table B.1.2.2.1-2 with mapping of Table B.1.2.2.1-3.

Table B.1.2.2.1-3 Sub-cluster information for intra cluster delay spread clusters

sub-cluster #	mapping to rays	power	delay offset
1	1,2,3,4,5,6,7,8,19,20	10/20	0 ns
2	9,10,11,12,17,18	6/20	5 ns
3	13,14,15,16	4/20	10 ns

In the LOS case, define $\mathbf{H}'_{u,s,n}=\mathbf{H}_{u,s,n}$ and determine the channel coefficients by adding a single line-of-sight ray and scaling down the other channel coefficient generated by (20). The channel coefficients are given by:

$$\mathbf{H}_{u,s,n}(t) = \sqrt{\frac{1}{K_R+1}}\mathbf{H}'_{u,s,n}(t) + \delta(n-1)\sqrt{\frac{K_R}{K_R+1}}\begin{bmatrix} F_{rx,u,V}(\varphi_{LOS}) \\ F_{rx,u,H}(\varphi_{LOS}) \end{bmatrix}^T \begin{bmatrix} \exp(j\Phi_{LOS}^{vv}) & 0 \\ 0 & \exp(j\Phi_{LOS}^{hh}) \end{bmatrix} \begin{bmatrix} F_{tx,s,V}(\phi_{LOS}) \\ F_{tx,s,H}(\phi_{LOS}) \end{bmatrix} \cdot \exp\left(jd_s 2\pi\lambda_0^{-1}\sin(\phi_{LOS})\right)\exp\left(jd_u 2\pi\lambda_0^{-1}\sin(\varphi_{LOS})\right)\exp(j2\pi\upsilon_{LOS}t) \quad (23)$$

where $\delta(\cdot)$ is the Dirac's delta function and K_R is the Ricean K-factor defined in Table B.1.2.2.1-4 converted to linear scale.

If non-ULA arrays are used, the equations must be modified. For arbitrary array configurations on the horizontal plane, see Figure B.1.2.2.1-2, the distance term d_u in equations (23) and (20) is replaced by:

$$d'_{u,n,m} = \frac{\sqrt{x_u^2 + y_u^2}\cos\left(\arctan(y_u/x_u) - \varphi_{n,m}\right)}{\sin\varphi_{n,m}}, \quad (24)$$

where (x_u,y_u) are the co-ordinates of the uth element A_u and A_0 is the reference element.

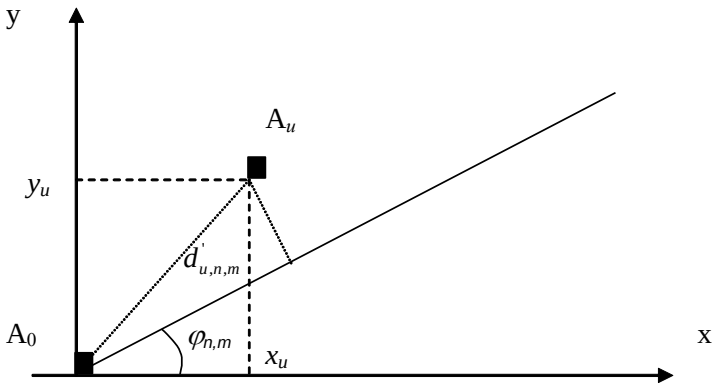

Figure B.1.2.2.1-2 Modified distance of antenna element u with non-ULA array

Step 10b: Generate channel coefficients for each cluster *n* and each receiver and transmitter element pair *u,s*. Alternatively to Step 10a channel coefficients can be generated by applying the so called correlation matrix based method. Temporal correlations (Doppler effect) are introduced either by filtering independent and identically distributed complex Gaussian sequences with a proper Doppler spectrum shaping filter or by applying some equivalent method. MIMO antenna correlations are introduced by performing a linear transformation to the temporally correlated sequences. Unique covariance matrices are determined for each drop and radio link based on the parameters defined in the previous steps. The MIMO covariance matrix can be composed of transmitter and receiver spatial correlation matrices, and by the polarization covariance matrices with the Kronecker product of matrices. Spatial correlation matrices can be derived for each cluster directly from the ChIRs of Step 10a [B3, B4]. Alternatively, spatial correlation matrices and the polarization covariance matrices can be derived from the antenna configuration and the model parameters (AoA, AoD) determined in Step7 with XPR parameter from Table B.1.2.2.1-4 [B5].

Step 11: Apply path loss and shadowing for the channel coefficients. This is valid only for system level simulations.

Table B.1.2.2.1-4 Channel model parameters

- In the table below *DS* = rms delay spread, *ASD* = rms azimuth spread of departure angles, *ASA* = rms azimuth spread of arrival angles, *SF* = shadow fading, and *K* = Ricean K-factor.
- The sign of the shadow fading is defined so that positive SF means more received power at UT than predicted by the path loss model.

Scenarios		InH		UMi			UMa		RMa	
		LOS	NLOS	LOS	NLOS	O-to-I	LOS	NLOS	LOS	NLOS
Delay spread (*DS*) $\log_{10}$([s])	μ	-7.70	-7.41	-7.19	-6.89	-6.62	-7.03	-6.44	-7.49	-7.43
	σ	0.18	0.14	0.40	0.54	0.32	0.66	0.39	0.55	0.48
AoD spread (*ASD*) $\log_{10}$([°])	μ	1.60	1.62	1.20	1.41	1.25	1.15	1.41	0.90	0.95
	σ	0.18	0.25	0.43	0.17	0.42	0.28	0.28	0.38	0.45
AoA spread (*ASA*) $\log_{10}$([°])	μ	1.62	1.77	1.75	1.84	1.76	1.81	1.87	1.52	1.52
	σ	0.22	0.16	0.19	0.15	0.16	0.20	0.11	0.24	0.13
Shadow fading (*SF*) [dB]	σ	3	4	3	4	7	4	6	4	8
K-factor (*K*) [dB]	μ	7	N/A	9	N/A	N/A	9	N/A	7	N/A
	σ	4	N/A	5	N/A	N/A	3.5	N/A	4	N/A
Cross-Correlations *	*ASD* vs *DS*	0.6	0.4	0.5	0	0.4	0.4	0.4	0	-0.4
	ASA vs *DS*	0.8	0	0.8	0.4	0.4	0.8	0.6	0	0
	ASA vs *SF*	-0.5	-0.4	-0.4	-0.4	0	-0.5	0	0	0
	ASD vs *SF*	-0.4	0	-0.5	0	0.2	-0.5	-0.6	0	0.6
	DS vs *SF*	-0.8	-0.5	-0.4	-0.7	-0.5	-0.4	-0.4	-0.5	-0.5
	ASD vs *ASA*	0.4	0	0.4	0	0	0	0.4	0	0
	ASD vs *K*	0	N/A	-0.2	N/A	N/A	0	N/A	0	N/A
	ASA vs *K*	0	N/A	-0.3	N/A	N/A	-0.2	N/A	0	N/A
	DS vs *K*	-0.5	N/A	-0.7	N/A	N/A	-0.4	N/A	0	N/A
	SF vs *K*	0.5	N/A	0.5	N/A	N/A	0	N/A	0	N/A
Delay distribution		Exp	Exp	Exp	Exp	Exp	Exp	Exp	Exp	Exp
AoD and AoA distribution		Laplacian		Wrapped Gaussian			Wrapped Gaussian		Wrapped Gaussian	
Delay scaling parameter r_τ		3.6	3	3.2	3	2.2	2.5	2.3	3.8	1.7
XPR [dB]	μ	11	10	9	8.0	9	8	7	12	7
Number of clusters		15	19	12	19	12	12	20	11	10
Number of rays per cluster		20	20	20	20	20	20	20	20	20
Cluster *ASD*		5	5	3	10	5	5	2	2	2
Cluster *ASA*		8	11	17	22	8	11	15	3	3
Per cluster shadowing std ζ [dB]		6	3	3	3	4	3	3	3	3
Correlation distance [m]	*DS*	8	5	7	10	10	30	40	50	36
	ASD	7	3	8	10	11	18	50	25	30
	ASA	5	3	8	9	17	15	50	35	40
	SF	10	6	10	13	7	37	50	37	120
	K	4	N/A	15	N/A	N/A	12	N/A	40	N/A

Table B.1.2.2.1-5 Expectation (median) output values for large scale parameters

Scenario		DS (ns)	AS at BS (º)	AS at UT (º)
InH	LOS	20	40	42
	NLOS	39	42	59
UMi	LOS	65	16	56
	NLOS	129	26	69
	O-to-I	49	18	58
UMa	LOS	93	14	65
	NLOS	365	26	74
RMa	LOS	32	8	33
	NLOS	37	9	33

B.2 References

[B1] 3GPP TR25.996 V6.1.0 (2003-09) "Spatial channel model for multiple input multiple output (MIMO) simulations" Release 6.

[B2] IST-WINNER II Deliverable 1.1.2 v.1.2, "WINNER II Channel Models", IST-WINNER2, Tech. Rep., 2007 (http://www.ist-winner.org/deliverables.html).

[B3] J. P. Kermoal, L. Schumacher, K. I. Pedersen, P. E. Mogensen, and F. Frederiksen, "A stochastic MIMO radio channel model with experimental validation," IEEE Journal on Selected Areas in Communications, vol. 20, no. 6, pp. 1211-1226, 2002.

[B4] P. J. Smith and M. Shafi, "The impact of complexity in MIMO channel models," in Proceedings of IEEE International Conference on Communications (ICC '04), vol. 5, pp. 2924-2928, Paris, France, June 2004.

[B5] WiMAX Forum, WiMAX Forum Mobile Release 1.0 Channel Model, June 2008, available at http://www.wimaxforum.org/technology/documents/wimax_forum_mobile_release_1_0_channel_model_v100.pdf.

[B6] Rec. ITU-R P.1816, " The prediction of the time and the spatial profile for broadband land mobile services using UHF and SHF bands".

[B7] T. Fujii, "Path-loss prediction formula in mobile communication -an expansion of "SAKAGAMI" path-loss prediction formula-," Trans. IEICE, Japan, J86-B, 10, pp. 2264-2267, 2003.

[B8] M. Steinbauer, A. F. Molisch, and E. Bonek, "The double-directional radio channel," IEEE Antennas and Propagation Mag., pp. 51-63, August 2001.

[B9] "Proposed Propagation Models for Evaluation Radio Transmission Technologies in IMT-Advanced," Doc. 5D/88, January 2008, Geneva, Switzerland.

[B10] Gudmundson, M. Correlation Model for Shadow Fading in Mobile Radio Systems. *Electron. Lett*, Vol. 27, 23, 2145-2146). November, 1991.

[B11] H. Omote and T. Fujii, "Empirical arrival angle profile prediction formula for mobile communication systems" Proceeding of IEEE 2007 VTC Spring, Dublin, 2007.

[B12] H. Okamoto and S, Ichitsubo "Investigations of outdoor-to-indoor propagation loss on 800MHz-8GHz at urban area," Proc. The 2005 IEICE General Conference, Japan, pp. S23-S24, March 2005 (in Japanese).

[B13] Jianhua Zhang, Di Dong, Yanping Liang, Xin Nie, Xinying Gao, Yu Zhang, Chen Huang and Guangyi Liu, "Propagation characteristics of wideband MIMO channel in urban micro- and macrocell," IEEE PIMRC 2008, Invited paper.

[B14] Dong, Weihui; Zhang, Jianhua; Gao, Xinyin; Zhang, Ping; Wu, Yufei;, "Cluster Identification and Properties of Outdoor Wideband MIMO Channel", Vehicular Technology Conference, 2007. VTC-2007 Fall. 2007 IEEE 66th, Sept. 30 2007-Oct. 3 2007 Page(s): 829 – 833.

Annex C:
Change history

Table C.1: Draft History

Change history					
Date	**TSG #**	**TSG Doc.**	**Subject/Comment**	**Old**	**New**
	R1#54bis		Draft skeleton TR TP for clause 5,6,7,8 and 9 are captured	-	0.1.0
	R1#55		TP for simulation models are captured	-	0.2.0
	R1#55bis	R1-090510	TP for winder bandwidth are captured	-	0.3.0
	R1#56	R1-091009	TP for UL scheme and channel models are captured	-	0.4.0
	R1#56	R1-091125	TP for UL/DL MIMO, DL RS, Relay are captured	-	1.0.0
18/03/10	RAN_47	RP-100357	TR36.814 ver.2.0.1 for approval by plenary	2.0.0	2.01
18/03/10	RAN_47	-	TR is put under change control as per RAN_47 decision	2.0.1	9.0.0